NTNU
Norwegian University of
Science and Technology

Site surveys at Norwegian aquaculture sites

Methodologies for wave estimation

Synnøve Risting Stemsrud

Marine Technology
Submission date: June 2018
Supervisor: Pål Lader, IMT

Norwegian University of Science and Technology
Department of Marine Technology

Sammendrag

For å sikre kostnadseffektiv produksjonsvekst i norsk havbruk finnes det per i dag to mulige løsninger: eksponert havbruk og/eller lukkede anlegg. Disse løsningene øker behovet for å evaluere kravene i dagens lokalitetsundersøkelser, hvor bølger, strøm og vindforhold dokumenteres i henhold til NYTEK-forskriften. Det er oppgavens hovedmål å identifisere potensielle forbedringspotensial i dokumentasjonskravene for bølgeforhold i lokalitetsundersøkelsen og regulering av fremtidig norsk havbruk. Relevante tekniske standarder fra andre havbaserte industrier presenteres.

Innrapporterte bølgeforhold på norske oppdrettsanlegg er analysert og årsaker til estimeringsmessige variasjoner som følge av bølgeestimeringsmetode har blitt undersøkt. De viktigste funnene er som følger:

- Strøklengdeanalyse er den mest brukte estimeringsmetoden for vindbølger (32 %), etterfulgt av SWAN, numerisk bølgemodell (18 %)
- Det er store geografiske variasjoner i anvendt estimeringsmetode for vindbølger: Trøndelag og Møre og Romsdal avviker fra de andre regionene ved at det på en stor andel av lokalitetene her har blitt benyttet SWAN
- Det tyder på at SWAN gir høyere beregnede bølgehøyder enn strøklengdeanalyse
- Numeriske bølgemodeller er hovedsakelig benyttet på lokaliteter driftet av større oppdrettsselskaper, mens strøklengdeanalyse er hovedsakelig benyttet på lokaliteter driftet av små og mellomstore oppdrettsselskaper

Funnene indikerer en mulig sammenheng mellom oppdrettsselskapenes størrelse og metode brukt for bølgeestimering. Denne observasjonen kan, hvis den blir videre underbygget, indikere et brudd på prinsippet om uavhengige inspeksjonsorganer, angitt i NYTEK §7. Funnene åpner for en videre evaluering av dokumentasjonskravene om bølgeforhold på oppdrettsanlegg og utbedring av tekniske standarder for å imøtekomme utfordringer for fremtidige havbruksanlegg.

Summary

New concepts of ocean-based fish farming are emerging in the aquaculture industry, which aim to increase production efficiency and expand usable farming space. These recent developments raise a need for evaluating present methodologies and requirements of site surveys. Legislation and regulations governing Norwegian aquaculture production are presented, with the main aim of identifying potential areas for policy improvement. In particular, the consequences of technical advances on legislative development in aquaculture are discussed. Relevant recommended practices and technical standards from other ocean engineering industries, as well as current methodologies for met-ocean estimation and design principles for marine structures are addressed.

Site surveys, including measurements of wind, waves and current, provide a basis for the estimated design levels of the environmental loads. Reported wave conditions are analyzed and the causes of deviation between estimation methods and their resulting wave conditions are investigated. The main findings are as follows:

- Fetch analysis is the most applied wind-wave estimation method (32%), followed by the numerical wave model SWAN (18%)
- There are large geographical variations in the wind-wave estimation methods applied
- SWAN analysis results in larger calculated wave heights compared to fetch length analysis
- Numerical wave models are mainly used at sites operated by large sized fish farming companies, whereas fetch length analysis is mainly used by small/ medium sized companies

The findings suggest a possible dependency of the wave estimation methodologies applied in site surveys on the fiscal strength and production capacity of fish farming companies. This observation, if further substantiated, may imply an infringement of the legal requirement for independent inspection bodies, as stipulated in NYTEK §7. The findings thus contribute to a platform for further evaluation of the legal framework governing future aquaculture installations.

Acknowledgements

This master thesis is written in conjunction with the five years integrated Master of Science degree in Marine Technology, provided by the Department of Marine Technology at the Norwegian University of Science and Technology. It is a compulsory part of the Master of Science degree, of which this thesis counts 30 credits, making up 100% of the workload of a semester.

The topic of the master thesis is self-chosen and the work has been done independently with guidance from my supervisor Pål Lader, professor in Aquaculture Technology at the Department of Marine Technology, NTNU.

I am grateful for his highly valuable advices and guidance throughout the semester. I would like to thank Gunnar Senneset and Eirik Svendsen in SINTEF Ocean for organizing and assisting full-scale measurements and post-processing. The full-scale measurements are funded by SFI Exposed Aquaculture.

Further, Daniel Landhaug, on behalf of Fiskeridirektoratet (Norwegian Directorate of Fisheries) has been of great help for questions regarding regulatory issues in Norwegian aquaculture and has provided the main set of data for the thesis. Finally, I want to thank Edmond Hansen in Multiconsult for raising question of the reliability of site surveys in Norwegian aquaculture and his guidance in developing the topic and scope for the thesis.

Contents

List of Figures

List of Tables

Chapter 1

Introduction

The technical standard NS9415 was legally implemented in 2006 to mitigate environmental risks caused by structural failures of aquaculture installations. Some measures include the introduction of a statutory site survey and technical requirements for all components used in a fish farm installation. Statutory site surveys in Norwegian aquaculture heavily emphasise wave estimation methodologies that are described in NS9415 (Standard Norway, 2016. The standard also requires documentation of the environmental conditions at fish farms including wind, wave and current phenomena, which are collectively termed *met-ocean conditions*.

Sea louse infection is the current greatest obstacle for cost-effective production growth in Norwegian aquaculture (EY, 2016). Exposed aquaculture and closed fish farms have been suggested to be the two most salient solutions to this problem (Olafsen, Winther, Olsen, and Skjermo, 2012; Samsing, Solstorm, Oppedal, Solstorm, and Dempster, 2015). The former entails movement of aquaculture facilities to more weather-exposed areas, and is important to both licensing authorities and industry stakeholders due to the scarcity and environmental challenges of current sheltered areas (Ministry of Petroleum and Energy,Ministry of Trade, Industry and Fisheries, 2017). To overcome problems of sea louse infection in exposed regions, full control of the water supply into fish farms is needed. This can be achieved by the use of closed cages, which have different dynamic behaviour than traditional cages.

Exposed aquaculture and closed caged fish farms will require drastic changes in structural design and fish farming operations. Presently, circular plastic collar fish farms are widely used in the on-growing phases in salmon production and have proven to be durable and resistant in various met-ocean conditions (Xu, Zhao, Dong, Li, and Gui, 2013). They consist of relatively cheap components, making it easy to adaptively and quickly alter their dimensions as a precautionary response to unforeseen met-ocean loads. This has led to little interest in examining the quality and precision of the wave estimation methods stipulated in NS9415. New concrete and steel structures currently being planned for exposed and closed aquaculture involve increased manufacturing costs. The large safety factors applied in design of floating

collar fish farms are not an expedient remedy for lacking knowledge about met-ocean conditions in the design of new fish farming solutions (Arntsen, Borge, Strømmesen, and Hansen, 2018).

Optimized marine structures presuppose precise met-ocean estimates are used in the design. Several fish farming concepts have been planned and designed in accordance to requirements set by NORSOK (offshore standards of the petroleum industry), which include the compulsory application of extensive met-ocean analyses. Given the increased met-ocean exposure of new fish farm solutions, it will be important to review regulations and standardizations for aquaculture site surveys to account for extreme weather conditions, by enhancing structural integrity of installations.

Wave conditions at fish farm sites depend on wind conditions and topography, proximity to open sea and bathymetry. Installations usually require areas of 2-3 sq km, and there may be variations in wave conditions within a site. Present estimation methods analyze wave conditions at one point, which may exclude important information in the overall representation of actual wave conditions.

1.1 Objectives

According to the NYTEK regulation, an independent inspection body must carry out the site survey. The standard only describes a simple method for wave estimation , although it also allows for inspection bodies to use other recognized (and more advanced) methods for wave estimations. The main objective of this thesis is therefore to investigate the variations in reported wave conditions at Norwegian aquaculture sites, which vary according to usage of different wave estimation methods. The results from this study can be used to evaluate if requirements for wave estimation in site surveys should be standardized and potentially made more stringent to ensure expedient design and operation of future aquaculture installations.

1.2 Background and results from project thesis Autumn 2017

The background for this thesis is a literature study done in Autumn 2017. A wide range of influences caused by met-ocean conditions at aquaculture sites was investigated, such as legislation, marine operations and studies of met-ocean conditions in ocean engineering. An extensive literature search also revealed a lack of studies concerning the prediction of met-ocean conditions at aquaculture sites. The findings from the project thesis relevant for further work in this master thesis is summarized as follows:

- Research publications concerning marine operations with an emphasis on met-ocean conditions in aquaculture are deficient.
- A number of studies have expressed a need for objective operational criteria for marine operations in aquaculture, however common criteria could be difficult to establish. This is mainly due to large variations of the environmental conditions at fish farm sites.
- The technical standard for aquaculture, NS9415:2009, have deficient descriptions of methodologies for estimation of met-ocean conditions when compared to standards of other marine industries.
- Aquaculture engineering research concerning met-ocean conditions have mainly focused on the structural behaviour of aquaculture installations and less on the overall performance and operability of an installation. The ongoing SFI Exposed Aquaculture program relates to this issue.

The project thesis covered a review of regulations and technical standards concerning aquaculture installations. In addition to this, methodologies for representing met-ocean conditions at aquaculture sites will addressed.

1.3 Problem statement

The objective is detailed and covered by the following problem statement:

> *What causes variations in reported wave conditions at aquaculture sites?*

The main objective is further examined by the following sub-questions:

1. What are the quantitative variances in wave estimation methods among stakeholders performing site surveys and what are the causes for these variances?
2. What is the variance in spatial wave conditions within a site? How may spatial wave energy content affect the reliability of site surveys?

1.3.1 Hypothesis

It is hypothesized that the lack of exhaustive standardized decision criteria required for estimation of met-ocean conditions at aquaculture sites influences resulting estimated wave conditions reported in site surveys. Furthermore, it is also hypothesized that an underlying cost VS benefit economic calculus influences the choice of wave estimation methodology.

1.4 Scope and quantification of data

The first sub-question is investigated by performing a quantitative study of site surveys for all Norwegian aquaculture sites. The data used is provided by the Directorate of Fisheries and originates from the mandatory NYTEK scheme. The thesis will examine the following topics:

1. Changes in aquaculture business structure through institutional and legal development.
2. Technical advances of fish farming installations and research addressing performance of fish farms in relation to wave parameters.
3. Methods for measuring and describing wave phenomena for ocean engineering applications.
4. Possible consequences of spatial variations of wave conditions within a site in relation to new fish farming structures.

1.4.1 Collaborators and resources

The objectives of the thesis were developed through conversations with Edmond Hansen in Multiconsult. Met-ocean data from site surveys reported to the Directorate of Fisheries were obtained. The data are of statutory form, and are needed to obtain and maintain aquaculture licenses granted by the Directorate of Fisheries.

The second sub-question is examined by performing full-scale wave measurements, suggested by Pål Lader, supervisor for this thesis. It was decided to focus on wave elevation at a site and evaluate the overall performance of the fish farm structure in heave. The objective is to evaluate the spatial variation of wave energy within a site. Gunnar Senneset organized full scale measurements at a fish farm site outside of Trøndelag, Norway. Eirik Svendsen assisted with calibration of the measurement devices and provided advice for post-processing of data. Both Svendsen and Senneset are employed by SINTEF Ocean and the measurement campaign is funded by SFI Exposed, where SINTEF Ocean is a managing partner.

Comments on full-scale measurements

Due to practical issues, analyses of the spatial wave conditions at the aquaculture site are not finished. Accelerometers were put out end of April 2018 and the measurement campaign finished mid May 2018. The postponements made it challenging to thoroughly analyze the results and discuss causes

of deviations. Presentation of the site, theory concerning full-scale measurements and post-processing, results and discussion are attached in the appendix A.5.4. The results serve as preliminary data for further work in increasing knowledge about the reliability of wave estimation methodologies and spatial variations of wave conditions at aquaculture sites.

Chapter 2

Managerial and legal structures in fish farming

This chapter serves as an introduction to the legal framework for ocean-based salmon production. The objective of this is to give the reader some insight into important legal factors affecting technical development of the aquaculture industry. These factors are in turn influenced by social progression, accident risk and technological innovation.

2.1 Institutional changes of the regulatory regimes in Norwegian aquaculture industry

The growing demand for sea food has led to institutional changes in aquaculture since its establishment in Norway in the 1970's. *Institutional changes* in aquaculture are defined here collectively as the changes in regulations and business structure, caused by development from small-scale, local enterprises to a large, multi-billion dollar export industry.

Causes of institutional changes in Norwegian aquaculture have been discussed by Aarset and Jakobsen, 2009. The background for this study was a switch from corporate regulation regime to monitor and control regime, which occurred in the 1990's. Characteristics of regulatory regimes can be seen in figure 2.1, directly retrieved from the article by Aarset and Jakobsen, 2009.

Characteristics	A corporative management and distribution regime (1970–91)	A control and monitoring (technocratic) regime (~2001 ⇒)
Objectives for regulations	Rural development, distributional goals	Value added, profitability, market responsiveness
Management tools	Political redistribution of resources	Neutral, technical, adaptation to international standards
Level of governance	National	Regional, national, international (multilevel system)
Source of regulation impulses	Politicians, industry actors	EU, public administration
Decision-making	Centralised	Decentralised, institutional complexity
Empowered groups	Licensed farmers	Public administration at a national level
Target for regulation	Technical capacities	Conduct of operation

Figure 2.1: Regulation regimes as given in Aarset and Jakobsen, 2009

Regulations are defined by Aarset and Jakobsen, 2009 as interventions of new laws by political institutions to achieve specific goals. The changes can occur as a transition (a step-wise adjustment) or as a wholesale replacement of regulations. The latter happens in conjunction with radical events, such as market collapse (shock) and stakeholder emigration. It can also be a consequence of technical advances, resulting in stakeholders considering the regulations as obstructive, leading to the need for institutional and radical change.

Regulatory capitalism is a term for defining the substitution of the direct provision of public and private services to expanded regulatory regimes in governance (Braithwaite, 2008). The rise of regulatory capitalism has caused a transition from corporate regulatory regimes to control and monitoring regulatory regimes in Norwegian aquaculture industry (Aarset and Jakobsen, 2009). Levi-Faur, 2005 discuss the emergence of new regulatory actors as a part of this transition, where third-party and private control bodies are mentioned as new instruments for regulation. In Norway, the use of third party accreditation was implemented as part of the EEA agreement in 1991. The use of quality control bodies and private standards in aquaculture has increased since the 1990's and is caused by a global diffusion of regulatory

capitalism (Aarset and Jakobsen, 2009).

2.1.1 Legal influences of European joint cooperation and the establishment of the EEA

The establishment of the European Economic Area (EEA) and implementation of EU legislation has resulted in decreased political control of aquaculture activities in Norway (Aarset and Jakobsen, 2009). This included less detailed political governance in the allocation and distribution of new aquaculture permits, but increased the authority of professional advisory authorities. For example, implementation of EEA legislation has led to increased limits on production license ownership, resulting in stronger oligopolistic features in the Norwegian aquaculture industry.

Depoliticizing industrial governance has led to substitutionary regulations, where authorities have established a framework to initiate self-regulation of the aquaculture industry (Aarset and Jakobsen, 2009). The fish farmer is thus obliged to monitor, control and evaluate farm-related activities, which in turn requires a stronger focus on internal control and data acquisition.

Four departments are currently directly involved in regulatory governance of the industry. They include the Directorate of Fisheries, Food Safety Authority, Directorate of Coasts and County Governor. These departments share regulatory responsibilities and further implement regulations sanctioned by the government. As a result of these new regulations, all farmers must report the technical standard of a fish farm installation and a site through the NYTEK scheme to the Directorate of Fisheries.

2.2 Regulations and standards in Norwegian aquaculture

The Norwegian aquaculture industry actively regulates environmental issues and animal welfare. The Aquaculture Act aims to avoid environmental crises, including escapes due to structural failures or collapsing production due to diseases. Regulations for the aquaculture industry are set by the Ministry of Fisheries on behalf of the Norwegian government and aims to promote sustainable growth in the Norwegian aquaculture industry. The responsibilities of regulating the salmon industry as dictated by the Aquaculture Act (e.g. surveying farms, granting production licences and approving equipment) are shared between the following Norwegian authorities (Akvakulturloven, 2006; Directorate of Fisheries, 2011; Laksetildelingsforskriften, 2015):

- *Ministry of Trade, Industry and Fisheries:* Sets policies for the aquaculture industry with authority from the Parliament of Norway
- *County Council*: Receives license applications for aquaculture activities, collects consulting statements from authorities and stakeholders relevant to the application (Regulations for aquaculture of salmon, trout and rainbow trout (the salmon license regulation, §8)
- *Directorate of Fisheries (central):* Supervisory and national managerial authority under the Act, responsible for executing political objectives for aquaculture and act as an allocation authority for licenses
- *Directorate of Fisheries (regional):* Supervisory authority under the Aquaculture Act in respective geographical regions

Salmon farming is a complex operation with many biological and technical requirements. The Norwegian Food Safety controls license compliance with relevant animal welfare regulations. They are also responsible for executing counter-measures In the event of disease outbreaks (Norwegian Food Safety Authority, 2017).

Escape of farmed salmon is another important challenge in aquaculture. Regulations aimed at reducing escapes have been made, and will be described in section 2.2.2 and further discussed in section 5.3.

2.2.1 Aquaculture licenses

Norwegian fjords and coastal areas are public spaces. If private, commercial activities in these areas are planned, permission is needed from the County Council in accordance with the Aquaculture Act. For special designs or solutions, such as new concepts for fish farming, the application is processed by the Directorate of Fisheries. The relevant County Council, in collaboration with the Directorate of Fisheries and other relevant authorities grants the number of aquaculture licenses that decides the maximum biomass of a site. The production level of a company is determined by this and further by the maximum allowance of 35% of all licences in Norway (see section 2.1.1). Each licence allows for a biomass of 780 metric tons (945 metric tons for Finnmark and Troms) where environmental considerations set by the local municipality decides the number of licences allocated per site. A company may hold numerous licenses and can, if permitted, transfer these across sites to keep the total biomass within the limits of a specific site. The total number of licences for salmon production is regulated by the Ministry of Fisheries to keep salmon production at a sustainable level. Additionally, the regulation of license numbers aims to reduce risk for diseases within an

area and control long term salmon pricing to avoid potential market collapse (Akvakulturloven, 2006; Laksetildelingsforskriften, 2015; Ministry of Petroleum and Energy,Ministry of Trade, Industry and Fisheries, 2017).

2.2.2 The NYTEK regulation, NS9415 and NS9410

The authorities, in cooperation with the aquaculture industry, have gained experience and insight in the importance of customized equipment in terms of structural strength and reliability. Through this knowledge a technical standard, NS9415, has been developed by Standard Norway. The Standard lists requirements for the design, installation and operation of fish farms. The NYTEK regulation was introduced the same year as NS9415 and requires fish farmers, equipment suppliers and other stakeholders to use certified methods and equipment in accordance with NS9415. Equipment and components can only be certified by an independent and accredited inspection body, as stated in the information leaflet *Technical requirements for fish farming installations - NYTEK* (p. 4) issued by the Ministry of Fisheries (Ministry of Trade, Industry and Fisheries, 2005). The main purpose of the law is stated in NYTEK §1 (translated from Norwegian):

> *The regulation aims to prevent the escape of fish from floating aquaculture plants by ensuring sound technical standards at the plants.*

Technical, biological and environmental factors will influence the performance of a fish farm. The plant must be built to the specifications of the environmental conditions at the site to avoid structural failures. Furthermore, animal welfare must be considered to ensure appropriate growth conditions for the fish. Environmental monitoring standards of the bottom and waters around and under a farm, as codified in NS9410, have been developed. This standard aim to control emissions from plants, maintain good water quality and bottom environment, ensure animal welfare and food safety. If requirements set by the standards are not met in accordance to current regulations and laws, aquaculture licenses cannot be granted (Akvakulturloven, 2006; Ministry of Trade, Industry and Fisheries, 2005; Norwegian Food Safety Authority, 2017).

2.2.3 Legal procedures for obtaining a facility certificate

Fish farmers granted one or multiple aquaculture licences may apply for permission to install a fish farm at a suitable location. Local authorities will determine the exact site and the extent of production allowed at the location. Along with this application the farmer must obtain information

about met-ocean conditions and give detailed descriptions of the planned fish farm installation. Ahead of installing a floating fish farm, NYTEK §9 requires that a site survey is carried out (Ministry of Trade, Industry and Fisheries, 2005). NYTEK §9 refers to NS9415:2009, where assessments of met-ocean conditions are specified. If expanding an installation, NYTEK §9 requires an update of the survey to ensure that the met-ocean parameters registered are representative for the expanded area.

The principle of independence

Total independence between decision-makers and stakeholders influencing the allowance of ocean-based aquaculture activity is an important principle stipulated in NYTEK §7 (further referring to ISO/IEC 1720:2012). Independent bodies substantiate the monitoring regimes of the authorities and are needed to provide appropriate certification and approval of the activities concerned.

The requirements for independent inspection bodies and impartiality of inspection activities are specified in *ISO/IEC 17020:2012 Conformity assessment - Requirements for the operation of various types of bodies performing inspection.* The inspector shall not have any personal, ownership, governance or financial relationship to the principal, hence there shall not be any possibilities for the client to influence the inspection body. There are three levels of independence and impartiality, as detailed in *Annex A.1 Requirements for inspection bodies* of ISO1720:2012:

- **Type A:** *The inspection body cannot be part of a legal entity or be linked to a separate legal entity that is engaged in design, manufacture, supply, installation, purchase, ownership, use or maintenance of the items inspected.* This clause prohibits ownership or other legal connection between the inspection body and the client. This is the highest level of independence.

- **Type B:** *The inspection body and its personnel shall not engage in any activities that may conflict with their independence of judgment and integrity in relation to their inspection activities. In particular, they shall not be engaged in the design, manufacture, supply, installation, use or maintenance of the items inspected.* This level of independence does not specify any requirements for separate legal entities. No separation of ownership is required if the aforementioned is fulfilled.

- **Type C:** *The design/manufacture/supply/installation/servicing/maintenance and the inspection of the same item carried out by a Type C inspection body shall not be undertaken by the same person.* This is

the lowest level of independence. The inspector and the client can be a part of the same company only if the inspector does not have any other responsibilities or stakes in the project.

NYTEK §7 and §10 require inspection activities for aquaculture to be of type A, i.e. third-party inspection body. The contractor shall have no ability to influence the outcome of an inspection.

The high level of independence and impartiality between inspector and client minimizes any risks of illicit financial gain by underestimation of met-ocean conditions motivated by reduced materials and manufacturing costs. Third party inspection bodies (in theory) guarantee objective site surveys. Potential disturbances of the principle of independence will be analyzed and discussed in section 6.2.

2.2.4 Consequences of the implementation of standards in Norwegian aquaculture industry

The NYTEK regulation and NS9415 was introduced in 2003. Since January 2006 it has been mandatory to solely sell and use components controlled and certified by accredited bodies. As a result of this, statistics from the Directorate of Fisheries given in figure 2.2 has shown a drop in the escape of farmed fish in Norwegian waters after 2006.

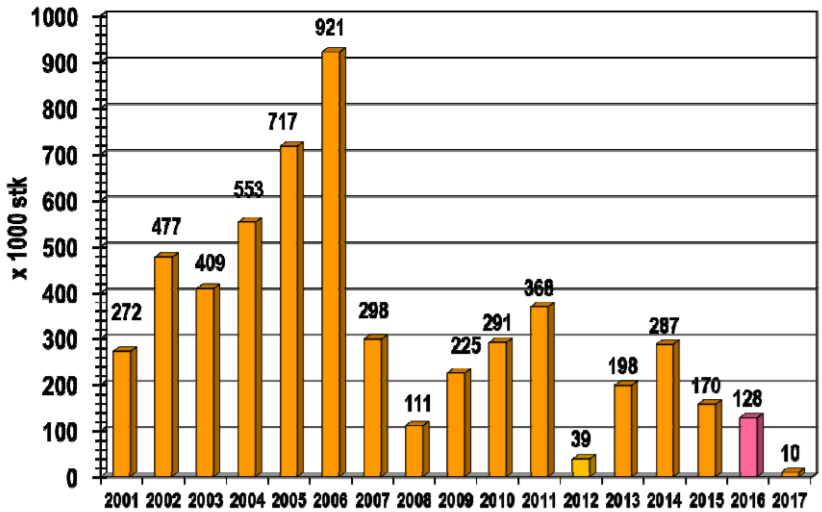

Figure 2.2: Escapes of salmon from Norwegian fish farms (*Source: Directorate of Fisheries, 2017*)

The Government commissioned the Directorate of Fisheries to establish a new strategy to prevent additional escapes from Norwegian fish farms in

2016 (Ministry of Trade, Industry and Fisheries, 2017). In 2017, a proposal for an escape prevention strategy was published by the government, including revision of NS9415. Although NS9415 was previously reviewed in 2009, recent novel design solutions have made room for improvement and adjustment of regulation compliant installations. The new edition of NS9415 will be published in 2020.

2.2.5 Other relevant technical standards and industry regulations

Aquaculture facilities in Norway are situated within the Norwegian Economic Zone, a sovereign area covered by Norwegian regulations and international conventions signed by Norway. Petroleum production has been an important activity in the waters of Norwegian Economic Zone and has led to the development of comprehensive regulations and standards. Transfers of technology and experience from offshore petroleum industry to aquaculture is relevant when exposed and potentially offshore aquaculture sites are put into service. The objective of this section is give the reader an introduction to some of the most relevant recommendations and standards used for offshore marine industries with regulation-compliant met-ocean estimations and marine operations planning. These will be relevant in terms of revision and establishment of current aquaculture regulations and standards.

NORSOK

The NORSOK standards were established by industry stakeholders and authorities due to falling profitability and uncertainty about the future competitiveness of the Norwegian offshore oil industry in the 1990s. Throughout years of expansion of the offshore oil industry, international standards had been rated to not meet the needs of the offshore oil industry. Cooperation between companies was limited with increasing use of internal company regulations. This led to increased overall costs, particularly high rig rental rates. The chaos of multiple internal regulations that offshore equipment suppliers had to deal with further raised investment costs.

One of the main aims of NORSOK, Norwegian offshore sector competitiveness, was to reduce the inefficiency caused by numerous internal regulations.

This was done by preparing a new, common set of technical standards for production and drilling facilities of offshore oil and gas. 88 standards were established, distributed within the following classes:

- *Design principles (9 standards)*
- *Common Requirements (33 standards)*
- *System Requirements (46 standards)*

Assessment of marine operations and met-ocean conditions are considered in NORSOK J-003 (marine operations) and NORSOK N-003 (action and action effects). For example, Ocean Farm 1, operated by Salmar ASA, was built and installed in compliance with relevant NORSOK and ISO standards in addition to aquaculture standards (Salmar ASA, 2017).

Simplification and standardization to function based requirements led to significant savings of time and money. It was stated in an analysis of the NORSOK project published in 2016 (Norwegian Oil and Gas, Federation of Norwegian Industries and Norwegian Shipowner's Association), that the introduction of the NORSOK standards resulted in a 40 % cost reduction. In the long term it is an aim of owners to establish international standards to replace the NORSOK standards (Nistov et al., 2016).

ISO 19901 Petroleum and natural gas industries - Specific requirements for offshore structures

The International Organization for Standardization produces and publishes international common standards known as ISO. The series *ISO 19901 Petroleum and natural gas industries - Specific requirements for offshore structures* and *ISO 19905 Petroleum and natural gas industries - Site-specific assessment of mobile offshore structures* consists of seven standards for offshore oil installations, including localization, met-ocean conditions and marine operations. Several standards in this series could provide important information for aquaculture installations and will be further introduced in the following paragraphs.

ISO 19901-1:2015 Met-ocean design and operating conditions,

The standard *ISO 19901-1 Met-ocean design and operating conditions* provides information regarding guidance and procedures for the determination of environmental conditions for both before and during the operation time of an installed production plant. Determination of design parameters for offshore structures are important and dependent on met-ocean conditions for the chosen location. Given the scarce numerical data from historic events for

offshore locations, measurement campaigns are therefore important during the planning of installations.

The scope of the ISO 19901-1:2015 is to determine oceanographic and meteorological exposure of an offshore structure in a specific location. The met-ocean parameters are applicable to numerous fields, including design, construction and operation of offshore structures. The environmental conditions presented in the standard are:

- *Extreme values with return periods of 100, 1000 and 10000 years*
- *Long term distributions of met-ocean parameters*
- *Normal, frequently expected occurring met-ocean conditions*

Site assessments for structural design may be carried out via two alternative approaches: either met-ocean parameters or the action effects caused by met-ocean phenomena. These two methods are presented as guidance in *ISO 19901-1:2013, Annex A.5.3* and will be explained in the following paragraphs. Figure 2.3 is taken from *ISO 19901-1:2013, Annex A.5.1* and provides an overview of the approach for the determination of met-ocean conditions. The input data can either be collected from (simulated) hindcast or measurements, both of which are dependent on the information available for the specific region considered.

The *Met-ocean parameters approach* is most commonly used, where met-ocean parameters (e.g. a combination of extreme met-ocean conditions) are normally determined prior to finalization of the detailed design of the structure, which results in a simplified design process. A disadvantage is that it does not provide an optimized structure or assess a risk- or reliability-based design approach.

The *Action effect method* is more radical in terms of use in design of offshore structures. This is a response-based method which requires an N-year response of the structure. When this is found (e.g. the 100-years overturning of the bending moment of a riser), met-ocean conditions resulting in the 100-years response can be determined. This provides a reliability-based approach to determine design actions and associated met-ocean parameters. The action effect method can be complex and requires close interaction between met-ocean conditions and structural models.

In summary, this standard provides detailed procedures and descriptions of assessing met-ocean data, establishment of databases and possible applications of met-ocean information (International Organization for Standardization, 2015).

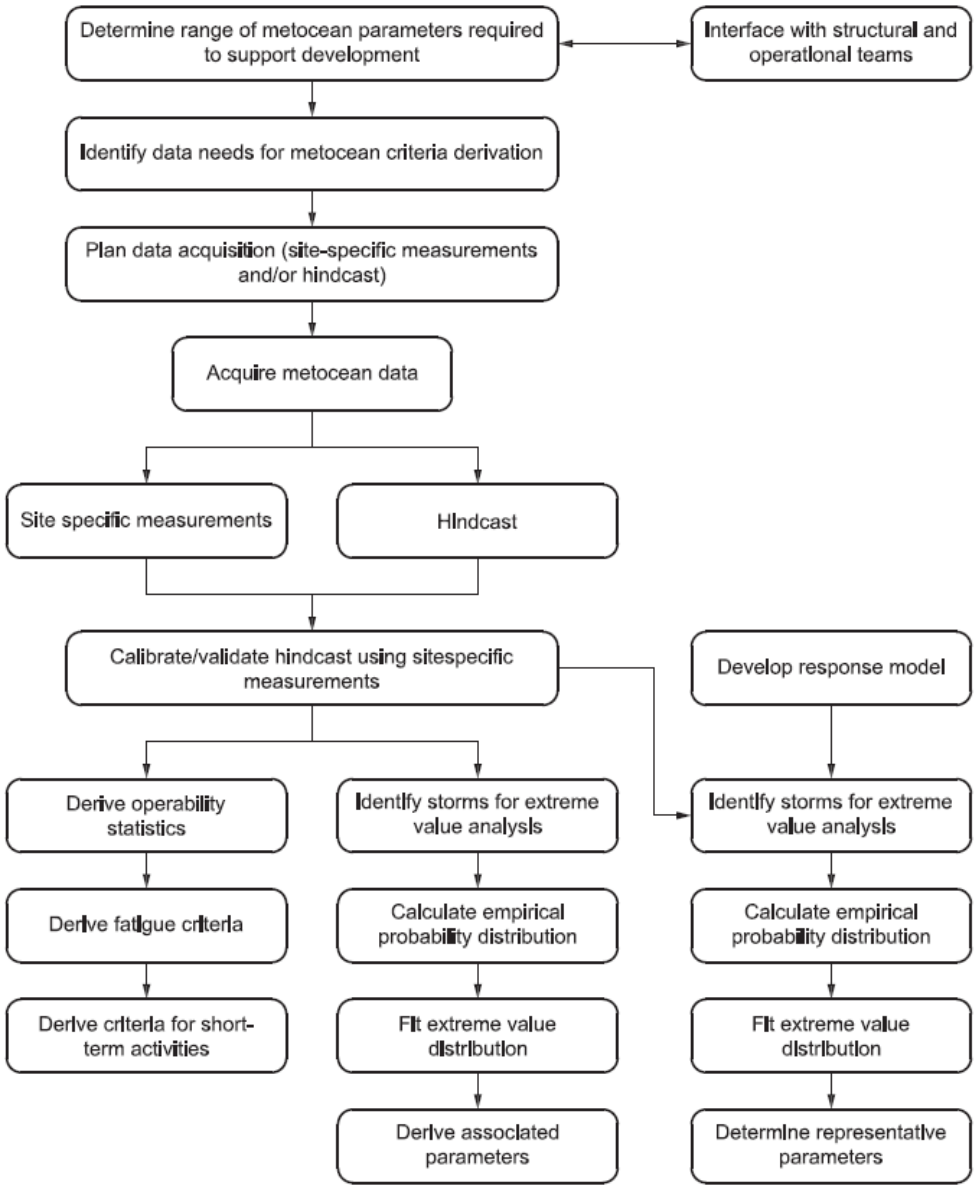

Figure 2.3: Overview of approaches for determine met-ocean parameters, ISO 19901-1:2013, Annex A.5.1, (*Source: International Organization for Standardization, 2015*)

ISO19901-6:2009 Marine Operations

This standard provides information about the planning, engineering, implementation and documentation phases for weather-restricted and weather-unrestricted operations (*ISO19901-6:2009, section 7.2*). It is applicable for floating and fixed offshore structures when the marine environment causes structural risk and covers the following topics:

- Organizational structures (such as allocation of responsibilities and HSE)
- Requirements and safety factors related to met-ocean conditions
- Special considerations regarding stability and station-keeping during operation, transportation, lifting, installation and removal of offshore structures

Met-ocean conditions for marine operations in aquaculture are not given any emphasis in NS9415:2009. The standard 19901-6:2009 can thus be used as a reference for important and/or comprehensive operations needed in the installation, operation or removal of aquaculture sites (International Organization for Standardization, 2009).

ISO19901-7:2013 Stationkeeping systems for floating offshore structures and mobile offshore units

Structural design and alignment of aquaculture installations cannot presently be directly compared to those of offshore petroleum installations. The main objective of presenting this standard is to provide some insights and comparisons to future aquaculture installations. These are expected to be situated in equivalent ocean environments similar to offshore petroleum production plants. The importance of reliable mooring systems in aquaculture facilities are discussed in the section 3.1.2. ISO19901-7:2013 covers stationkeeping of floating offshore structures and provides information about procedures for design, analysis and evaluation of mooring and dynamic positioning. Annex B provides additional requirements under the jurisdiction of *Norwegian Act no. 72* (1996). It is stated in *ISO19901-7:2013, Annex B.2.3.2* that:

> *Mooring shall be design for the combination of 100 years wave, wind and 10 years current.*

In NS9415:2009, the requirement for moorings is a loading condition consisting of 50 years wave and 10 years combined current and wind.

ISO17776 - Petroleum and natural gas industries - Offshore production installations - Major accident hazard management during the design of new installations

The main objective of NYTEK is to reduce the risk of salmon escape. Sustainable production growth and ensuring a low environmental impact of fish farming are some of the aims highlighted in *The maritime strategy of the Government of Norway* (Ministry of Petroleum and Energy,Ministry of Trade, Industry and Fisheries, 2017). These aims therefore necessitate precaution in the design of new and unproven solutions for fish farming. *ISO1776:2016* could in this context provide important guidance. *Risk* is in this standard defined as *a combination of the probability of occurrence of harm and the severity of that harm.* Management of major accident (MA) hazards during the design of offshore petroleum and natural gas installations is also described in detail. *Major accident hazards* are sources of hazardous events, if realized, resulting in accidents characterized by (retrieved from International Organization for Standardization, 2016):

1. Multiple fatalities of severe injuries
2. Extensive damage to structure, installation or plant
3. Large-scale impact on the environment

New aquaculture installations are limited by a lack of scientific and engineering standards describing structural performance in various met-ocean conditions. Further, the hazards are unknown and there is little knowledge about the risks related to exposed aquaculture (Utne, Schjølberg, Holmen, and Marie Skjøndal Bar, 2017). Figure 2.4 shows a framework for risk-related decision support in the design of marine installations. It characterizes the activity, risks, and stakeholder influences related to the activity and further describes possible design approaches for installations. Steel and concrete structures for emerging aquaculture installations comply with class C, which states that precautionary and conservative design approaches should be undertaken for risk management.

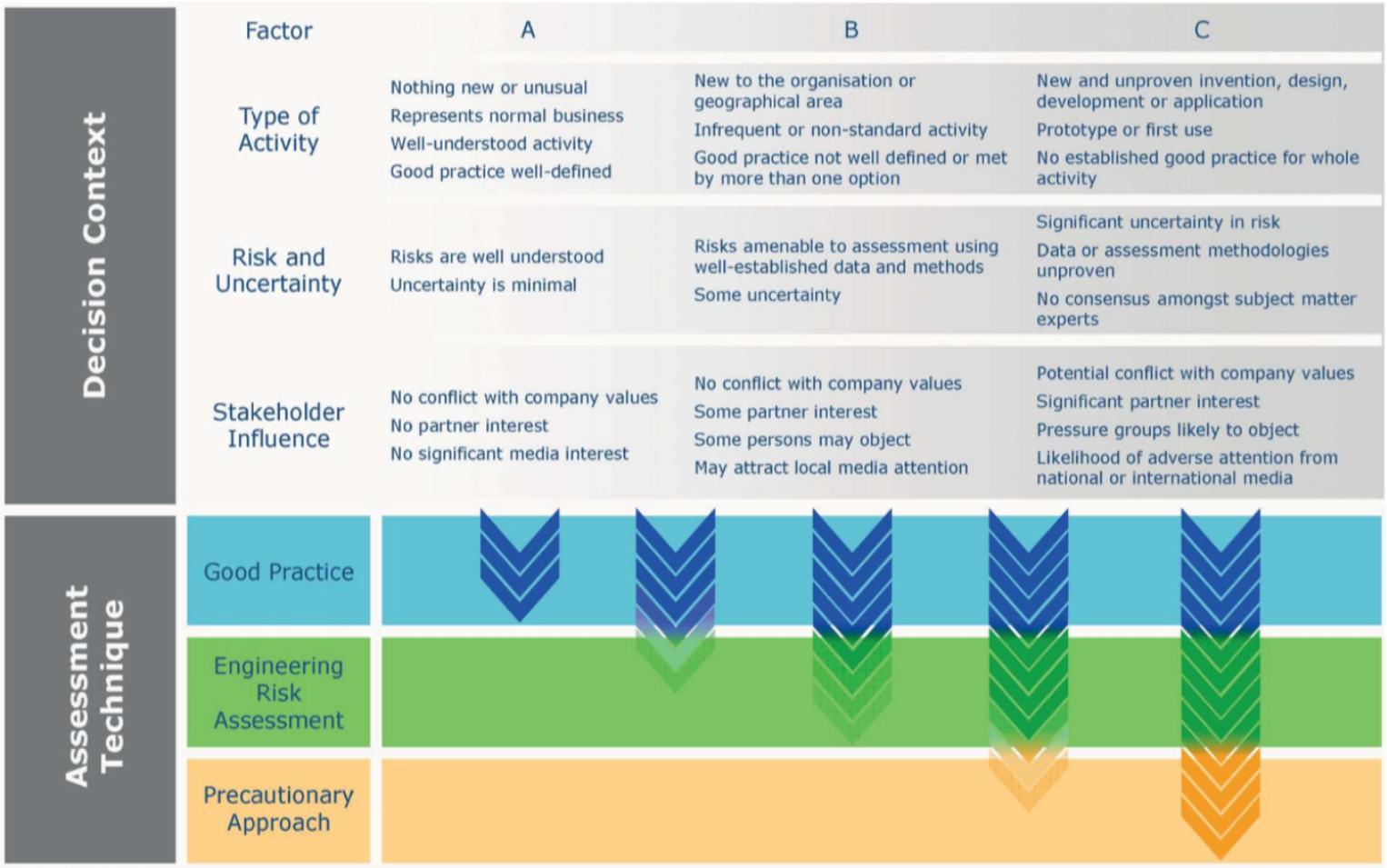

Figure 2.4: Framework for risk-related decision support. If applying to aquaculture, new structures will fall within category C (*Source: International Organization for Standardization, 2016).*

In summary, the standard outlines sound risk management practices in the development of new fish farming installations. The transfer of technology and experience from the oil and gas industry to aquaculture (EY, 2016) further validates the applicability of ISO17776 to the aquaculture industry.

DNVGL-RU-OU-0503 Offshore fish farming units and installations

In July 2017 DNV GL published their first set of rules for classification service and technical design basis for offshore fish farming plants in the DNVGLRU-OU-0503. The rules provide valuable information for the designs currently emerging in the aquaculture industry. The objective is to provide aid for designs that might not be sufficiently covered by the NS9415:2009 in terms of design procedures, performance in service and responses of the installation in an offshore environment (DNV-GL, 2017b). The rules will be more thoroughly presented in the section 3.4.1 in conjunction with new fish farming structures.

DNVGL-RP-C205 Environmental conditions and environmental loads

Evaluation of action effects at a site can be found by consultation of the *DNV GL Recommended practice C205*. It includes descriptions for analysis, modelling and prediction of environmental conditions and calculation of the corresponding loads acting on marine structures. Due to the lack of guidelines for representing collected met-ocean data in NS9415:2009, this recommended practice might be used as an extension of established aquaculture standards. The guideline complies with other standards by DNV-GL, 2017a.

Distinguishing environmental conditions, parameters and loads

Environmental loads, parameters and conditions are important terms and their differences should be noted. In DNVGL-RP-C205, the differences of the terms *environmental loads* and *environmental conditions* are given:

1.3.1 Environmental conditions

1.3.1.1 Environmental conditions cover natural phenomena, which may contribute to structural damage, operation disturbances or navigation failures. The most important phenomena for marine structures are: wind, waves, current and tides.

1.3.2 Environmental loads

1.3.2.1 Environmental loads are loads caused by environmental phenomena.

1.3.2.2 Environmental loads to be used for design shall be based on environmental data for the specific location and operation in question, and are to

be determined by use of relevant methods applicable for the location/operation taking into account type of structure, size, shape and response characteristics.

Environmental conditions are connected to environmental loads through several parameters. The parameters inducing wave loads can be described by wave length, wave number, angular frequency, wave amplitude (wave height), wave steepness, group speed and phase speed.

Preliminary summarizing words considering legal framework of aquaculture

Reulations and standards govern many technical aspects of aquaculture. These have been developed to ensure a sustainable industry, in terms of animal welfare, structural integrity and long-term production growth. The business has experienced a professionalism, where self-regulation and monitoring regimes have become important. Established practises and standards for data acquisition from other marine industries can provide as guidance in the development, design and operation of new fish farming solutions.

2.3 Status quo - Norwegian aquaculture production in numbers

Throughout the last two decades the aquaculture industry has become an important part of the maritime industry in Norway. Increasing demand for seafood products and industrial professionalism are two of the main factors for this positive development.

Over the past decade the industry has seen quadruple growth in first-hand value [1] of salmon. Values are increasing, as seen in figure 2.5 from the salmon sale statistics published by Statistics Norway, 2017. The first-hand value growth of salmon is expected to hit a turnover of 200 million NOK in 2050. This assumes that environmental obstacles (such as sea lice) are controllable and that technical development allows for the expansion of aquaculture production plants into exposed and remote areas. Aquaculture is expected to contribute 50% of the value creation in Norwegian maritime industries, a sector which petroleum industry currently dominates (Olafsen et al., 2012).

[1] First-hand value: The first-hand value corresponds to the value of sold slaughtered fish, unrefined fresh or frozen. *Source: Statistics Norway*

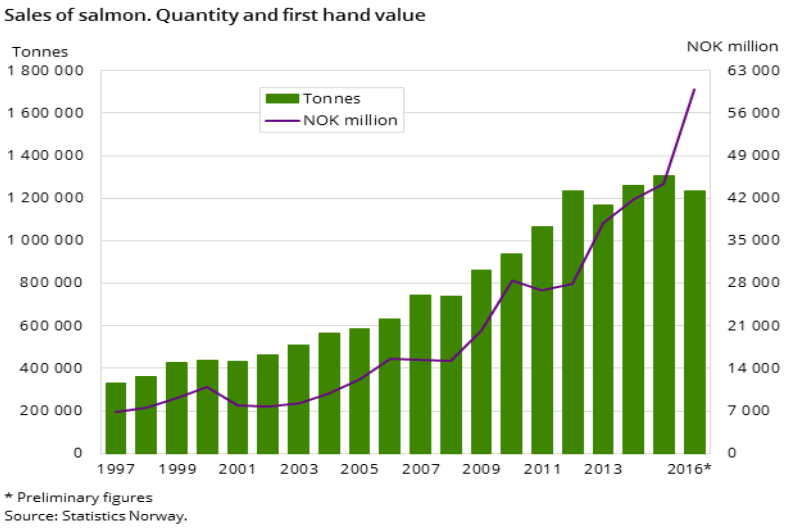

Figure 2.5: Sales of salmon. Quantity and first hand value (*Source: Statistics Norway, 2017*)

Many stakeholders are involved in salmon production and the industry has recently seen new players entering the business, transferring technology from other maritime industries. In the annual report *The Norwegian Aquaculture Analysis*, published by EY, 2016, the following supplier segment division of the value chain is presented:

- Technical solutions: *Technical solutions and equipment for all stages of production cycle, e.g. barges, feeding systems, vessels, mooring systems, cages, software*
- Biotechnology: *Fish health promoters (medicines and vaccines, fish species eating lice) and fish feed.*
- Production: *Subsegments: egg and spawn production, smolt production and sea farming subsegment. The latter is the major subsegment in the production supplier segment and includes fish farming companies.*
- Distribution: *Traders (independent or owned by salmon producers), slaughering suppliers and well boat companies and shipowners offering transport of smolt/salmon, sea lice treatment and sorting of fish.*
- Processing: *Processing suppliers, such as secondary value adding companies (fileting, smoking etc.) and packaging suppliers for fish and feed.*

The report authored by EY (2016) states that despite the increasing demand for salmon, costs are also increasing in the production cycle.

2.4 R&D investments

Keeping production costs down and meeting expected growth in the volumes produced will be a challenge for all value chain segments. Increasing investment in research and development for new solutions in the production cycle without altering operating costs has been expressed by many stakeholders, including the Government of Norway (Ministry of Petroleum and Energy,Ministry of Trade, Industry and Fisheries, 2017, p. 51-52). With the aim of preventing sea lice, diseases and area conflicts, innovation of new cage designs and moving fish farming to new locations including exposed areas have been suggested (Samsing et al., 2015). EY states in their report *The Norwegian Aquaculture Analysis 2016* that the expected effects of investments in research programs and development the recent years will only be apparent by 2020.

Fewer and larger companies have led to a decentralized and a complex structure of decision-making bodies in Norway (Aarset and Jakobsen, 2009). The aquaculture industry has a diverse value chain, often comprising a complex structure of business partners and company structures (Bostock, 2011). Private R&D investments in the Norwegian aquaculture industry has surpassed public funding in 2008, partly as a consequence of industry consolidation throughout the 90's (Asche, Roll, and Tveterås, 2012).

2.4.1 Development licenses

Over the past two years it has been possible to apply for a temporary development license. These licences were first introduced by the Ministry of Fisheries and the Directorate of Fisheries with the aim of overcoming challenges related to diseases, sea lice and area utilization in aquaculture by the introduction of innovative and commercial survivable solutions into the aquaculture industry. These temporal licenses aim to increase aquaculture companies' investment in research and technology development. Unlike the normal aquaculture license, the development licenses are granted by the Directorate of Fisheries and not the County Council. If the applicant proves to have had success with its solution, the development license can be transferred into a normal aquaculture license. The development license was first introduced in November 2015 and ended 17th November 2017. As of May 2018, 6 of 63 applications have been granted development licenses (Directorate of Fisheries, 2018a).

2.4.2 Intensified production at fewer and larger sites

Since the beginning of salmon farming the business has gone through several extensive structural changes. There has been a trend towards fewer and

larger business units for ocean-based farming of salmon, as seen in figure 2.6. The number of companies holding licences for aquaculture production has decreased and/or stabilized for the last decade, while the number of licences each company holds has increased (Directorate of Fisheries, 2018b).

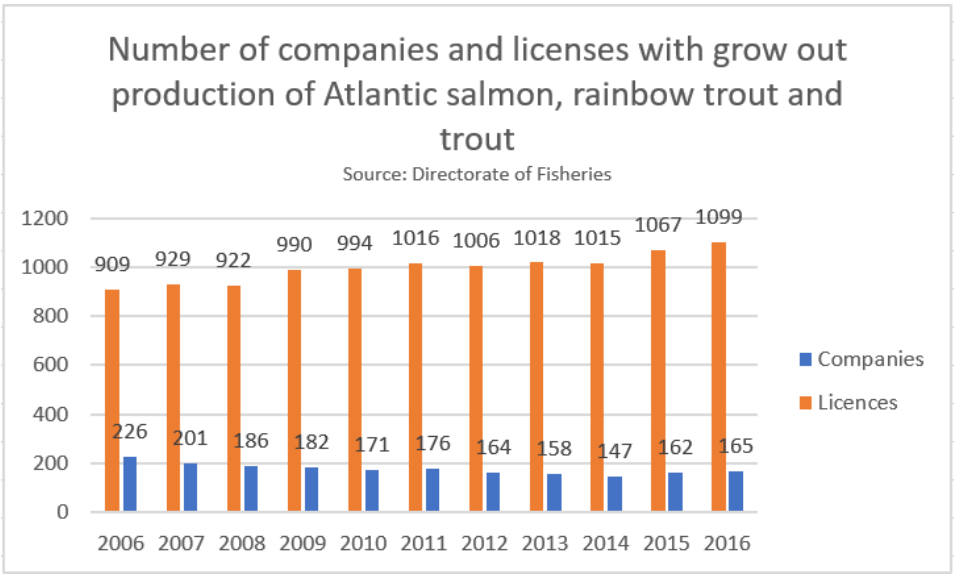

Figure 2.6: Number of companies and licences

The industry has undergone consolidation, resulting in larger, fewer and more effective production units. As seen in figure 2.7 the number sites in 2016 was 978 in Norwegian waters and there has been a slight decrease in the number of fish farms. Simultaneously production has increased by more than 50%. Thus, the productivity of each fish farm has increased by means of biomass production.

Larger production units imply larger investments and could, if not managed correctly, amplify the environmental and financial consequences of failure at the site. It is thus important to investigate the practical consequences of the regulations and the performance of fish farms under various environmental conditions.

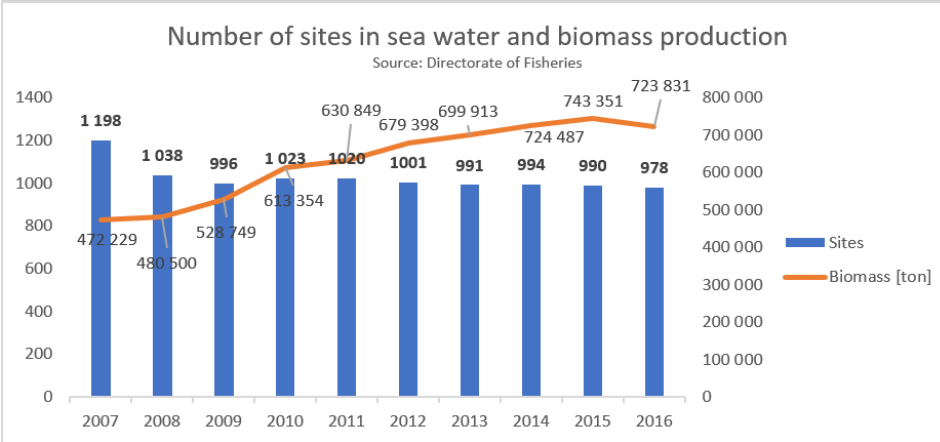

Figure 2.7: Sites in Norwegian waters

Chapter 3

Fish farms - technical aspects and dynamics

3.1 Fish farms - technical aspects

3.1.1 Classification of fish farm systems

The design solutions for fish farms vary in a large extent and choices of materials, shapes and sizes of the constructions mainly depends on the location of the site. For practical purposes, such as fatigue and structural analysis or operational planning, it is expedient to categorize the various design solutions that have been, are, or will be available in the future in relation to their designs.

In a paper by Fredheim and Langan, 2009, published in an anthology edited by Burnell and Allan (2009), two different classifications of fish farm constructions are presented; *the containment system* classification (how the fish farm maintain its volume) and *the constructional* classification (how the fish farm responds to loads). *The containment system* classification of fish farm designs was first presented by Loverich and Gace (1998), and is subdivided into five different classes:

- *Gravity fish farms:* Weights of different shapes (e.g. a ring in the bottom of the net pen) make a vertical force and maintain the shape of the net pen.
- *Anchor tension fish farms*: The shape of the net pen is provided by tension of the mooring system.
- *Semi-rigid fish farm*: A combination of ropes and rigid steel components provide the shape and keep the net pen in place.
- *Rigid steel farms*: A rigid steel or plastic structure contribute to the shape of the fish farm.
- *Other fish farm designs*: Combinations of the above mentioned designs or other solutions that do not fit into any of the categories.

Categorizing of fish farm designs based on the loads they are exposed to and their constructional properties is also common:

- Rigid structures
- Hinged connected bridges
- Flexible structures

It is common to distinguish between surface fish farms and fully or party submersible fish farms. Today almost all Norwegian Atlantic salmon farms are flexible structured, surface fish farms, however rigid and hinged structures are used in some sheltered areas.

3.1.2 Circular plastic cage fish farm solution

Design of fish farms has developed much since the first floating fish farm was introduced by the Grøntvedt brothers at the island Hitra, Norway, in 1969. Fredheim and Langan, 2009 express, at pages 915-917, the invention of the so-called Polarcirkel net pen in 1974 by the company *AKVA Group*, as an important advance in the development of the fish farm technology. This is currently the most common design solution for the sea based Atlantic salmon production and is often chosen by fish farmers due to its flexibility in various sea states and a well proven concept. A large number of global aquaculture equipment companies today offer this circular shaped plastic fish farm solution (AKVA Group AS, 2015).

The Polarcirkel cage concept consists of a circular plastic collar of high-density polyethylene (HDPE) attached to a net pen of synthetic fibers, most commonly poly-amide. The first cages had a circumference of 30 to 40 meters, and both the circumference and depth of the cages has increased since the first cages were put in service. Today circumferences from 60 meters up to 240 meters are commercially available, where a 120 meters circumference and 30 meters deep cage can keep more than 100.000 fish at once.

In addition to a HDPE floating ring, the circular plastic collar fish farm system consists of a mooring system to provide station-keeping, weights connected to the net pen to maintain the volume of the cage in different loading conditions and floaters, such as buoys. A typical Norwegian aquaculture site today consists of 6-12 plastic cages connected in a shared mooring system (Fredheim and Langan, 2009).

The flotation system

The flotation system provide buoyancy, contribute to maintain the shape of the net pen and keep the fish farm system at a water level suitable for

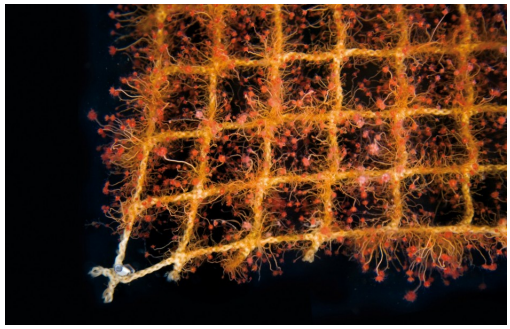

Figure 3.1: Biofouling (*Ectopleura larynx*) in net specimen (*Source: SINTEF*).

the species aquacultured. The floating collar is the main contributor to buoyancy and water level, while flotation buoys provide extra buoyancy to withstand vertical forces in the mooring system and serves as markers for mooring lines.

The net pen

The net pen is a cage-shaped net made out of synthetic fibers or a metal grid connected to the floating collar. Today nets are mainly made of Rachel knitted nylon wires, however various synthetic fibers, knitting techniques and surface treatments are common. The main purpose for the net pen is to prevent the fish from escaping. Handling of the net pen, such as change of nets, and hole in net pens were in 2015 the main cause of fish escapes, according to (Directorate of Fisheries, 2015).

Environmental loads are induced in the net and thus proper choice of material and knitting is important to prevent failures. Calculations of the structural and dynamical properties of nets are however complicated, due to the complex geometry and the large variety of loading and temperature exposure affecting both the net as a whole and the material used. Moe, Olsen, Hopperstad, Jensen, and Fredheim, 2007 presented a study where tensile strength of materials used in aquaculture nets were investigated. The authors found among other that the tensile strength of nets treated with anti-fouling paint decreased by 13% on average. Biofouling may cause higher solidity and reduced water flow through the cage, inducing larger drag forces on the net and thus be a challenge for the operator of the farm. Biofouling can be seen in figure 3.1.

Service and operation systems

The service and operation system can have larger or smaller differences depending on the size and location of a salmon production plant, where the feeding system, working areas for manning, possible storage areas for feed and equipment are most important bodies. For larger fish farms it is common to have a barge serving several cages, used for feed storage, living quarters for operators, areas for maintenance and daily operations, supervision and feeding control serving.

Mooring

The mooring system maintain the fish farm system at a fixed location and prevents large three dimensional movements due to exposure of environmental loads at a site. The mooring system is in addition an important contributor to maintain the shape of the net pen, by its brindle lines attached to each cage. The brindle lines prevent horizontal displacement, such as jaw, surge and sway movement. The mooring system can be separate for each net pen or several net pens can be connected to a larger mooring system, where the latter is more common. The brindle lines of each cage is then connected to ropes in a grid system by steel plates. The fish farm is exposed to environmental loads and the forces induced are distributed in the mooring lines and further transferred out to the anchoring system. The components of a mooring system, such as the aforementioned components and flotation buoys, which are used as markers for the system, are all joined together by steel plates or rings. Mooring lines commonly consist of a combination of ropes made of synthetic fibers and steel chains. In 2015 it was stated by the Directorate of Fisheries that contact and rubbing between mooring chains, commonly brindle lines, and net pens increase the risk tearing wholes in the net pens, thus causing escapes of salmon. This was based on investigations after a storm in the western part of Norway in 2014. Mooring systems are marked in the water surface by buoys to ease the navigation for vessels nearby the site (Directorate of Fisheries, 2015).

Anchoring system

There are several methods for anchoring a fish farm and the main purpose of anchoring is to transfer forces due to environmental loads from mooing to the ground and by this maintain the location of the fish farm. Depending on the bottom conditions and its holding power, different designs for anchoring can be utilized, where rock bolts and dead weight anchors are given special considerations in NS0415:2009. In softer sea bottom the anchor gets buried into the bottom, where the weight of the anchor is an important design

parameter. The anchoring is moreover connected to anchoring chains and ropes, joining the mooring system to the anchoring system (Li, 2017).

3.2 Sea and wind loads

Wind, wave and current loads are affecting the aquaculture plants in different aspects. Environmental loads cause difficult operational conditions and induce fatigue on various components in aquaculture installations due to excitation loads. In this section challenges in aquaculture due to the natural phenomena waves, wind and current are addressed.

3.2.1 Current loads

Water exchange in fish farms is highly dependent on the current conditions at site. The flow field will be changed dependent on design selected for the plant, current and wave exposure at site. Current loads are important in terms of fish welfare aspects; water exchange, dispersion of feed and cage volume. It is common to distinguish between regular (harmonic) and temporal (random) current components. Tidal current is an example of regular current component relevant for the whole water depth, whereas the wind-generated current components are temporal, fluctuating and only relevant for surface water columns. This complicates statistical analysis of currents.

Fredheim and Langan, 2009 state that current loads not only act on the net cage, but also on the floating collar and mooring lines. According to Li (2017), current contribute to approximately 75% of the total forces on a fish farm in medium current conditions (class c in 5.1). Current loads are in addition affecting the cage volumes of the net pens, thus increasing the biomass density in the cage by reducing the cage volume (Li, 2017).

3.2.2 Wind loads

Wind loads are relevant for the parts of fish farms above the surface, such as jumping nets, working areas for crew (walkways around the net pen) and feeding systems. Li presents in the introductory chapters of his thesis that wind loads accounts for approximately 5-10 % of the total forces on the mooring system of a farm due to the direct exposure of wind loads. Wind is affecting the upper parts of a production plant directly, while lower parts are affected indirectly by wind-induced waves and current loads.

3.2.3 Wave loads

Sea waves are the most important contributor of inducing loads on marine structures and transfer huge amounts of energy in the oceans. Wave the-

ory derived in for instance *Sea Loads on Ships and Offshore Structures* by Faltinsen, 1990, states that the displacements of fluid particles are largest in the surface and are decaying down in the water column.

Wind generated waves are caused by shear stresses in the boundary layer between the ocean surface and the atmosphere. Further pressure fluctuations in the air above the sea surface will contribute to wave motions. The size of these waves are affected by the length that the wind travels, the *fetch length*, its duration and velocity. Wind waves particularly important to take into account in sheltered areas where ocean swells are not significant.

NS9415:2009 requires that 10 and 50 years return periods of waves are found for the area where an aquaculture plant is planned installed. The return period can be described in terms of wave period or wave height, where $H_{10years}$ and $H_{50years}$ are the wave heights exceeded only once during 1 year or 50 years respectively. These return periods combined with wind and current loads form the basis for dimensioning of ocean-based aquaculture facilities. It should be noted that NORSOK, the regulations for offshore petroleum activities in Norwegian waters, requires a return period of 100 years. For new designs, such as the *Ocean Farm 1*, the offshore petroleum installation regulations have been applied to assure that the installation can withstand the environmental loads (Salmar ASA, 2017).

Waves account for approximately 20-25 % of total mooring forces and are important for both design of fish farms and operability of sites. Moreover, wave loads induce large circular shaped water particle movements which the salmon must withstand. It has currently not been found any studies concerning fish welfare in a wave load perspective.

3.3 Hydrodynamics of fish farm structures - a literature review

Structural, hydrodynamic and response analysis of aquaculture installations have been one of the main focus areas in aquaculture research the recent years. Fish farm systems are complex in terms of geometry, flow field, structural and dynamical behaviour, making it a complicated task to analyze dynamical responses in various wind, current and wave conditions. Precise predictions of the flow field inside a net cage is challenging due to the complex geometry of the netting structure and several interactions affecting the flow field, such as fish schooling[1], biofouling[2], number of cages and their spatial arrangement.

Numerical simulations, such as computational fluid dynamic analysis,

[1] An aggregation of fish swimming coordinated in the same direction

[2] Marine growth and accumulation of organisms on wet surfaces

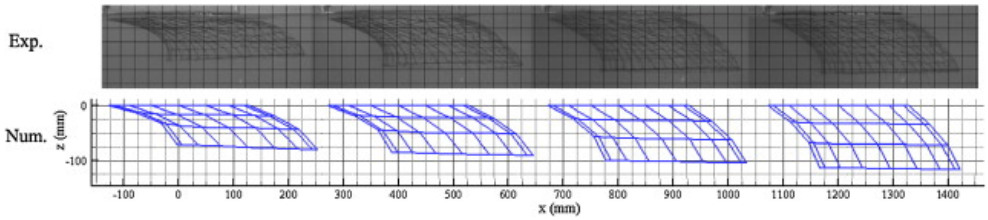

Figure 3.2: Comparison of physical model test and numerical simulation of four tandem net cages for a current velocity of 0.242 m/s (*Source: Bi, Zhao, Dong, Zheng, and Gui, 2014*)

are important tools in design and safe operation of fish farms. These studies can easily be changed to investigate single components or the system as a whole under various conditions, mostly limited to computer capacity. Several numerical simulations investigating the flow field through netting geometries have been done. One of the studies, done by Bi, Zhao, Dong, Zheng, and Gui, 2014, analyzed the impact of current velocity on the deflection on both single cage and tandem alignment of cages as well as impacts on current deflection by weights applied on the cage, which is shown in figure 3.2. Investigation of the flow field through the cage system is a complicated task mainly due to the highly detailed geometry of the net pen, making it necessary to validate the findings of CFD analysis with experimental studies.

Kristiansen and Faltinsen, 2015 did an experimental and numerical study of the mooring loads of a gravity cage with floater in current and waves. A review of hydrodynamic load models were done to determine what kind of physical effects are most important for mooring loads. The objective of this was to investigate the validity of hydrodynamic models used in analysis of gravity cages in fish farms. The authors stated that in research of fish farms, the hydrodynamic models were often over-simplified, whereas structural models sophisticated, resulting in a mismatch when analyzing the overall behaviour of the gravity cage system. Response analysis of flexible floating collars was recently presented in a PhD thesis by Li, 2017, where the wave-induced response of a circular floating ring collar was analyzed both numerically and experimentally.

Numerous numerical studies have been conducted, where a major part of the research have been on the fish farm only without presence of vessels, which is however common during marine operations. A hydrodynamic analysis of a coupled well boat-gravity cage system was done by Jia, Moan, and Jensen, 2012. They found that for small wave frequencies, the presence of a well boat can be neglected in the hydrodynamic coefficients when considering the tension of the mooring lines. Shen, Greco, and Faltinsen, 2016 investigated the presence of a well boat by an floating fish farm and how

this could affect the structural integrity of the fish farm. The study was done numerically with emphasis analyzing of forces in mooring lines during loading in extreme weather condition, with presence of waves and current. It was found that with the presence of a well boat, the forces in the mooring lines increased significantly compared to analysis of the fish farm alone. These are the only analysis of a coupled boat-fish farm system found in this literature search, however these kinds of studies can provide important results for obtaining objective decision criteria for various marine operations demanded in aquaculture, moreover be utilized to decide localization and heading of a farm.

A literature review by Klebert, Lader, Gansel, and Oppedal, 2013 provides an overview of research done on flow field in net cages. Full-scale experiments focusing on the flow field through a net cage system have been sparse, and the paper address that the focus in full-scale experiments mainly have been on investigating mooring systems rather than the responses of cage system as a whole, such as deflection of net pens. One of the few full-scale studies considering current induced deformations of two commercial sites were done by P. Lader, Dempster, Fredheim, and Jensen, 2008. It was found that current caused lifting of bottom rings, deflection of the front and back of the cage at the two sites caused as much as 40 % reduction of volume at one of the sites. The consequences of cage deflection are both negative and positive; reduction of net area exposed to the flow stream reduces the total drag forces, but significantly increases stocking density of fish. Full scale studies are important to validate numerical studies and experiments in laboratory and provide valuable insights to for instance a heading providing sufficient flow fields to increase production levels as much as possible or increase the knowledge of the operator of the dynamic behaviour of the non-visible parts of the production plant.

3.4 Emerging challenges with offshore fish farms

As a consequence of advances and incentives in aquaculture industry, new structures for ocean based aquaculture are emerging. New designs can be grouped into offshore farming solutions or closed/semi-closed farming solutions for sheltered to exposed locations. The dynamics of these structures are different compared to conventional floating collar fish farms, making it necessary to address some of the challenges related to wave loads. In this section an overview of offshore structures and challenges related to dynamic response characteristics will be given. This will be followed by a brief presentation of closed cages.

Table 3.1: DNVGL-OU-R-0503 Class notation related to structural design (*Source:DNV-GL, 2017b*).

Class notation	*Description*
Column-stabilized	A structure dependent on the buoyancy of widely spaced columns for floatation and stability in all modes of operation.
Self-elevating	A structure with hull of sufficient buoyancy for safe transport which is raised above sea surface on legs supported by the sea bed during operation.
Ship-shaped	Monohull ship and barge structures having displacement hulls with or without propulsion machinery.
Cylindrical	A cylindrical shaped displacement hull with or without machinery.
Deep draught	a SPAR, deep draught semi or other deep draught floating units. Spar can consist of multi-vertical columns, single column with or without moonpool (e.g. classic, truss and cell spar). May consist of multi-vertical columns with ring pontoon with or without a heave damping structure.

3.4.1 Offshore structures - transferring established offshore petroleum design principles into aquaculture

In July 2017 DNVGL issued a new set of Rules for classification complying offshore fish farms made of steel, *DNVGL-RU-OU-0503*. The following structures are covered by the rules.

The structures presented here are projects recently granted development licences from the authorities. The following projects, seen in table 3.2 are most probable of being put in service.

Unlike traditional floating collars having lifetimes of typically 7-10 years, new offshore aquaculture structures are estimated to have lifetimes of 20-25 years (Salmar ASA, 2017). They are designed as rigid structures and have a large weight, causing very different wave load responses than flexible, light-weight ring collars.

Possible challenges for rigid, offshore based fish farms with respect to wave conditions

Structures must be designed in accordance with typical wave periods to avoid resonance problems (see appendix A.3). This implies that swells, typically having large periods, are important to take into account when designing rigid, heavy offshore aquaculture installations. Estimation methods for swells will be discussed further in chapter 5, specifically in section 5.1.5.

As an example, the Ocean Farm 1 structure, seen in table 3.2, will have a resonance period much larger than flexible ring collars due to its weight. This is further the only new fish farm solution put into service. It is a semi-submersible, column-stabilized structure based on offshore structure design

principles, which will be shortly presented herein.

Table 3.2: Offshore fish farming projects granted development licences as of May 2018 by the Directorate of Fisheries.

Type	***Commercial example***	***Capacity/pen [tonnes]***	***Weight/pen [tonnes]***	***Design wave height, Hs [m]***	***Planned in service***
Column-stabilized	*Ocean Farm 1*, Salmar ASA	6240	7000	5	Q4, 2017
Self-elevating/Semi-closed	*Aquatraz*, Midt-Norsk Havbruk AS	3120	N/A	N/A (Exposed/ Offshore)	Q4, 2018
Colum-stabilized/self-elevating/Semi-submersible	*Arctic Offshore Farming*, NRS ASA, Aker Solutions ASA	3000	2250	5-15	Q2/Q3, 2020
Ship-shaped	*Havfarm*, Nordlaks	10000	N/A	N/A (Offshore)	Q2, 2020

3.4.2 General offshore design principles

Offshore structures need to withstand loads from harsh met-ocean conditions. Practical procedures are thoroughly explained in Næss and Moan, 2005 and in Haver, 2017. Either design wave loads, a design storm or the long-term wave conditions can be used.

The design wave approach implies establishing load conditions with a specified return period, most commonly 100 years. The design and response are evaluated by applying a wave height only exceeded by average every 100 years, equivalent to a wave height annually exceeded with a probability of 10^{-2}. The design wave is established based on available data for the site, where wave periods and directions needs to be specified.

The practical implementation of a design storm is to evaluate load effects based on a 100 year storm of duration of 3-6 hours. The most unfavourable sea state can be identified and the extreme response estimate of the structure with a probability of 10^{-2} to 10^{-4} is evaluated.

Næss and Moan, 2005 state that the most satisfactory approach is to design based on long-term statistics of the structural response. This means that characteristic long-term extreme values of the wave conditions has to be determined. They further state that this approach is not efficient in an economical and computational point, because it includes response calculations from sea states resulting in little or no load effects on the structure. However, concerning fatigue over an offshore structure's lifetime, long-term load analysis is required.

3.4.3 Closed structures and wave loads

Closed fish farming structures are developed driven by the following motivations:

- Reducing local environmental impacts of fish farming
- Reduce probability of escapes
- Get full control of inlet water quality to prohibit sea lice

Some of the concepts, such as the rigid egg-shaped cage from Hauge Aqua AS and Marine Harvest ASA and the spar buoy shaped tank from Hydra Salmon Company AS aim to utilize existing sites and infrastructure, such as mooring system, feed barges and power grid.

Complex dynamic responses of closed fish farms

The potential for closed, ocean-based aquaculture is significant, so are the challenges related to their wave-induced dynamic responses. For large-volume, impermeable structures diffraction forces will dominate the motions and loads. Diffraction is due to a fluid velocity field set up by the potential wave theory when the waves hits the structure wall. This changes the pressure field around the body (Faltinsen, 1990). The disturbances around the body changes the wave pattern, and waves will be reflected and radiated from the structure. Thus, the presence of a large-volume structure may make a complicated wave pattern in proximity to the structure, dependent on wave height and the relationship between wave length and diameter of the structure. The relative importance of forces acting on a wave-exposed structure is seen in figure 3.3, retrieved from Faltinsen, 1990.

Wave-excitation loads will further induce fluid motions inside the fish tank. These motions may develop into uncontrollable and complex fluid motions, called sloshing. These are connected to high fluid pressures causing slamming, i.e. large impulse loads. Sloshing may lead to damages and little research are yet published regarding wave-induced responses for closed fish farms.

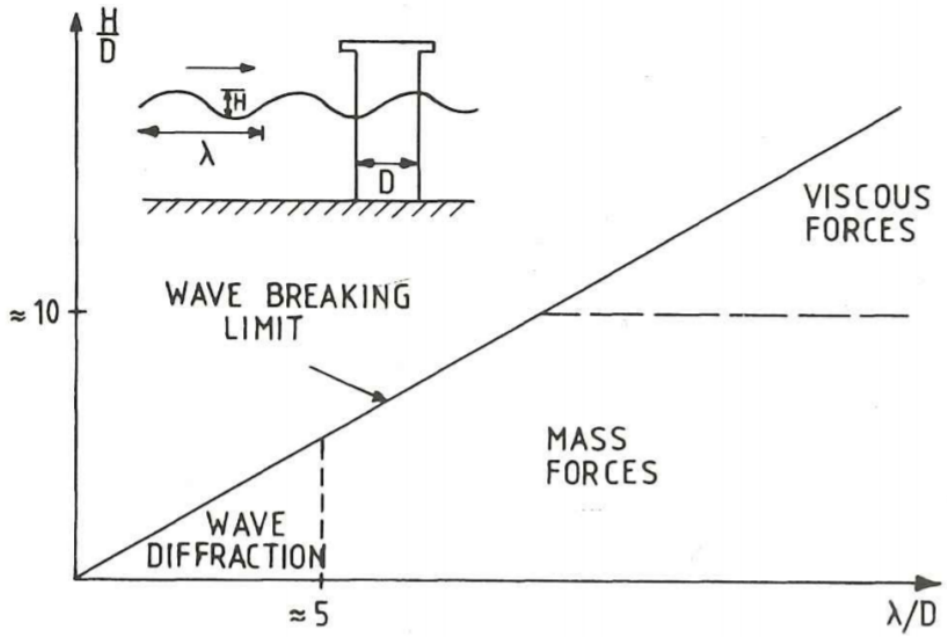

Figure 3.3: Relative importance of forces acting on a structure and the dependency of wave height, wave length and cross-sectional diameter of a structure (*Source: Faltinsen, 1990*).

Chapter 4

Wave theory - Description of the sea surface

There are different methods for describing sea waves, and in the following chapter some of the key points for describing and estimate the sea surface are presented. Wave phenomena and representation of sea states are addressed. Objectives of the chapter includes insights in met-ocean phenomena, their induced loads and further present techniques to represent met-ocean conditions for ocean engineering applications.

4.1 Linear and non-linear theory

A brief presentation of the mathematical background and assumptions for describing physical processes is necessary. We may distinguish between linear theory and non-linear theory applied to describe physical processes. The properties of these two theories will be given herein.

4.1.1 Linear theory

Motions of a system are often described by linear theory. The solutions of linear systems are, compared to its than its non-linear counterpart, widely accessible. There are two main characteristics of linear theory; homogeneity and superposition. An excitation of a homogeneous system will cause a response that is proportional to the excitation by a constant. The homogeneous process can be defined as:

$$Output(Response) = Input(Excitation) \cdot Constant \tag{4.1}$$

$$F(x\alpha) = \alpha F(x) \tag{4.2}$$

If the total response of a homogeneous system can be added by multiple excitations, the superposition principle is valid. The superposition principle can be defined as:

$$F(\alpha_1 x + \alpha_2 x) = F(\alpha_1 x) + F(\alpha_2 x) \tag{4.3}$$

The principles of homogeneity and superposition together form the basis for linear processes. Linear systems are of first order, i.e. their equations do not consists of polynomials (Store norske leksikon, 2014).

4.1.2 Non-linear theory

Non-linear processes and systems are treated differently than linear systems and there are no general and simple mathematical theorem covering non-linear processes as a whole. The non-linear processes and theory are described as everything else than linear processes (Hardesty, 2010). A common approach is to solve non-linear equations by numerical methods. Superposition is not valid and non-linear systems are not following the assumption of homogeneity.

Linearization

The majority of physical processes are inherent non-linear by nature. To simplify the description of these processes *linearization* is a useful method. When linearising a non-linear equation, the non-linearities are described by applying linear equations. The linear approximation is however only valid in a small region or a point of interest. Physical, non-linear processes in ocean engineering are commonly linearised due to the extensive simplification of problem solving. If not specified, linear theory is assumed valid in the following paragraphs.

4.2 Wave kinematics

Waves are physical phenomena of energy transport induced by spatial displacement of fluid particles, mainly caused by wind and other naturally occurring physical processes. Ocean waves can, in simplicity, be described as harmonic plane waves with a sinusoidal varying displacement often referred to as wave elevation:

$$\zeta(x,t) = \zeta_a cos(\omega t - kx) \tag{4.4}$$

Here, ζ_a is the wave amplitude, ω is the wave frequency. k is the wave number, which describes the relationship between the propagation of a wave and its wave length (Faltinsen, 1990; Patel, 1989, see also equation A.11 in appendix A.1.2). Equation 4.4 is also the basics of *regular wave theory*, described further in appendix A.1.

The term *kinematics* describes the motion of particles and their paths without considering their mass or the loads they are exposed to (Store norske

leksikon, 2016). Knowledge about the wave kinematics is an important tool for understanding the wave phenomena.

The fluid particles are assumed to move in orbits under a wave. The size are depending on the depth, as seen in figure 4.1. The assumption given in A.1.3 of no fluid disturbances deep down in the water column is visible. .

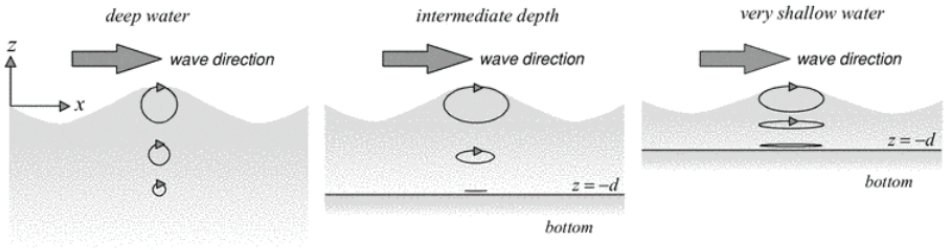

Figure 4.1: Fluid particle orbits various water depths (*Source: Holthuijsen, 2007, p. 122*)

At the surface orbits of fluid particles follow the wave shape, making the orbital period at the surface are equal to the wave period. Due to the kinematic boundary condition, the diameter of fluid particle orbits at the free surface must be equal to the wave height, $2\zeta_a$. Svendsen, 2006 approximates the phase velocity as a relationship between wave length and wave period:

$$C_p = \frac{\omega}{k} = \frac{\lambda}{T} \tag{4.5}$$

When depth decreases, the paths of fluid particles will be more elliptical shaped.

In summary, the wave motion is described by five parameters (Svendsen, 2006):

- ζ_a: wave amplitude
- λ: wave length
- h: water depth
- T: wave period
- C_p: phase velocity

Due to the fact that both the dispersion relation and the kinematic boundary condition (fluid orbital velocity at the surface must be equal to phase velocity), only three of these parameters can freely be selected.

Svendsen, 2006 present the most common combinations of wave parameters:

- h, ζ_a and λ
- h, ζ_a and T

For the second case, the wave length can be found by iterate the dispersion relation. Waves by definition do not transport mass, but is a phenomena transporting energy. The energy is transferred to the fluid by a various physical processes, such as wind and ocean currents. These phenomena displace fluid particles from their equilibrium position, inducing orbital fluid motions and waves to occur. The shape of a wave is influenced by a number of physical processes, among other the bathymetry and depth of the ocean bottom. Ocean wave phenomena and its dependency of among other depth will be presented in the following paragraphs.

4.2.1 Shoaling - Propagation of waves over uneven bottoms

Aquaculture sites are commonly located in areas with complex bathymetry, nearby islands and reefs or inside fjords. Wave motions are given by propagation direction and parameters such as amplitude, wave length and period, and will be affected by bathymetry. Shoaling is the change in wave phenomena due to change in water depth and the most common aspects of wave motions over uneven bottoms will be discussed in the following sections. The descriptions are based on linear theory and information can be found in Svendsen, 2006 and Holthuijsen, 2007.

Shoaling and refraction/ propagation of waves over uneven bottoms

The direction of propagation of a wave can be described by rays, which are aligned in the propagating direction of a long crested wave (Svendsen, 2006). When moving from deep to shallow water, the wave front change direction, caused by a reduction in phase speed. Rays hitting non-orthogonal to the depth contours will bend to compensate for the change in phase velocity, causing a change in wave direction, as seen in figure 4.2. The opposite occurs when a wave propagate from a shallow region to deeper areas and rays might end up crossing. Both phenomena are called *refraction*.

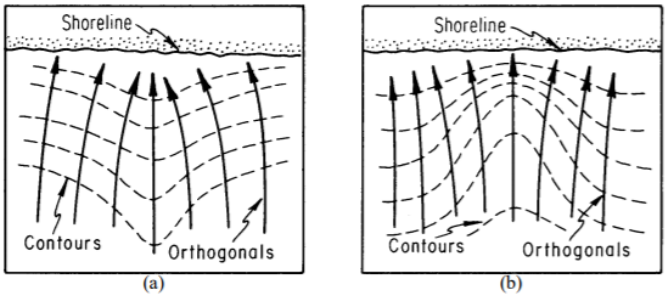

Figure 2-24. Refraction by a submarine ridge (a) and submarine canyon (b).

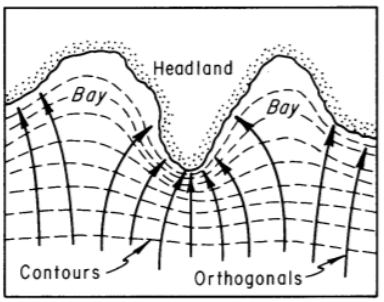

Figure 2-25. Refraction along an irregular shoreline.

Figure 4.2: Wave propagation and their rays over uneven bottoms (Source: Shore protection manual: Volume I and II, 1984, *p. 2-73*).

Consequences of shoaling are changes in wave height and wave length. Linear theory states that waves can not disappear or emerge, thus the wave periods are conserved and wave length and height must change. When shoaling occurs, the group velocity of the wave train will be decreased. This leads to an accumulation of wave energy, given by equation 4.10, increasing the wave amplitude and increasing the wave length (see e.g. Engebretsen, 2012; Holthuijsen, 2007 or Svendsen, 2006). The increase in wave amplitude can further lead to breaking, which is a non-linear phenomena discussed in the following section.

4.2.2 Energy dissipation - Application of non-linear theories to describe gravity wave phenomena

When the refraction pattern has been determined, the energy flux between two adjacent rays can be used to describe the wave heights. As stated above the wave energy must be conserved, making energy flux through two points at two adjacent rays equal. However, due to bottom friction and other non-linearities, such as breaking, wave energy will be dissipated. Wave breaking occurs due to an upper limit of stable wave height is exceeded (Patel, 1989).

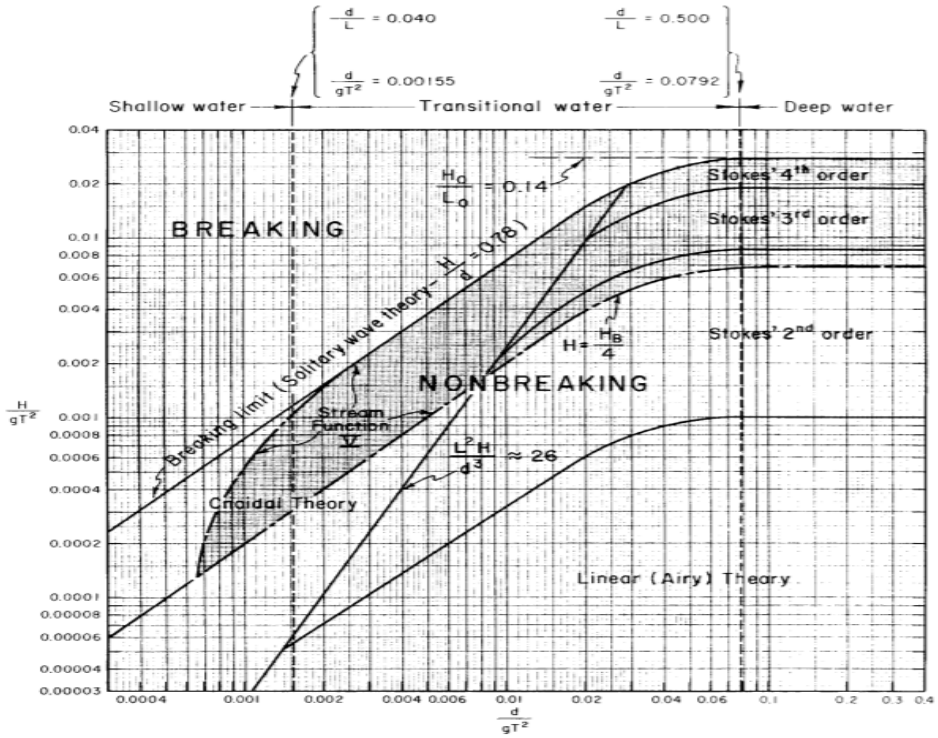

Figure 4.3: Applicability of linear and non-linear wave theories (*Source: Shore protection manual: Volume I and II, 1984*).

Breaking phenomena can cause wave slamming, a large impact wave load which must be considered and for some marine structures avoided.

Holthuijsen, 2007 limit linear theory for waves occuring in deep to finite depths. In figure 4.3, retrieved by Shore protection manual: Volume I and II, 1984, applicability of various wave theories are given. It is seen that the validity range of theories are dependent on depth, wave period and amplitude. A distinct border between the three main theories, Cnoidal, linear and Stoke's are seen. Cnoidal wave theory are applied for shallow waters, whereas Stoke's theories are suitable for steep waves in deep water.

It can be challenging to state a limit when non-linear theory should be applied. Waves can be locally non-linear and simultaneously be linear on a larger scale. This is the case when wave breaking at deep waters occurs (Holthuijsen, 2007). Non-linear waves are often treated as periodic in trains with constant shape, length and amplitudes. Some characteristic and visible wave phenomena can be described by non-linear theories and are explained below.

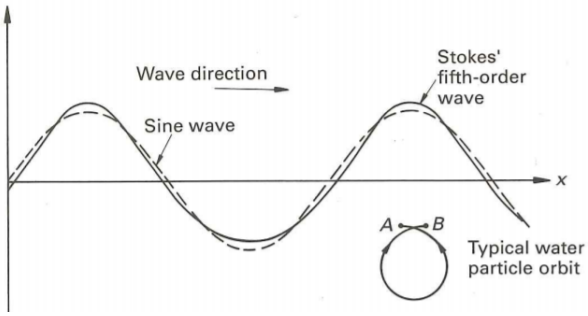

Figure 4.4: Wave kinematics of a linear wave and Stokes 5th order corrected wave with particle path caused by Stokes' drift theory (*Source: Patel, 1989, p. 132*)

Stoke's wave theory

In linear theory the wave profiles are assumed to be symmetric along the calm water surface. This is however not always an appropriate description of wave phenomena and a correction of the linear wave can be applied (Holthuijsen, 2007). By adding N harmonic waves to the primary linear sine-wave, the resulting wave become a N-th order (Stokes') wave with revised steepness. A N-th order Stokes wave correction is bound by having equal phase speed to its primary linear wave. The Stokes' wave is vertically asymmetric, with increased wave crests and reduced troughs, as seen in figure 4.4.

Haver, 2017 states that a Stoke's 5th order wave profile is a quite good description of a non-breaking extreme wave profile. *Stoke's wave profile is commonly used in a design wave method for analyzing dynamic loads on slender structures in finite waters.* To avoid slamming on marine structures, the steepness and increased wave crest elevations are important to consider (Patel, 1989).

Stoke's drift theory

Non-linear wave phenomena further affect paths of fluid particles. Linear theory assumes no mass transportation when looking at a fixed point in space. Nevertheless movement of fluid particles do occur when looking at fluid particles in a wave over time. Due to the asymmetrical shape of a Stokes' wave, the circular particle paths are changed to what seen in figure 4.4. This is the basics of *Stokes drift theory*, and the horizontal average fluid velocity, $\bar{u}$, over one period is equal to:

$$\bar{u} = \zeta_a^2 \omega k e^{2kz_0} \tag{4.6}$$

z_0 is the z-coordinate of the fluid particle in no waves (equilibrium position). Stokes drift velocity is influencing the motion of marine structures and should be considered when designing mooring systems as well its deflection mechanisms of the net pen.

4.2.3 Other gravity wave phenomena - diffraction and reflection

Standing waves and wave groups

When a 2D propagating linear wave hits a vertical wall, the wave will have zero horizontal velocity at the wall (Svendsen, 2006). The wave will be reflected and a wave opposite propagating with a period and amplitude equal to the incident wave will occur. In total the resulting wave will be:

$$\begin{aligned} \zeta_{incident} &= \zeta_a cos(\omega t - kx) \\ \zeta_{reflected} &= \zeta_a cos(\omega t + kx) \\ \zeta_{resulting}(t) = \zeta_1 + \zeta_2 &= 2\zeta_a cos(\omega t) cos(kx) \end{aligned} \tag{4.7}$$

A distinctive property of standing waves is seen from 4.7; the resulting wave have an amplitude twice of each of the components.

Diffraction and reflection caused by large volume structures or islands

When a wave train hits an object having large dimensions compared to the wave length, diffraction can occur. The interaction will modify the incident wave field and the diffraction will be a significant contributor to wave loads for a large, impermeable structures or islands. The wave field will further be influenced by these structures by reflection. Both phenomena are seen in figure 4.5, retrieved from Patel, 1989 .

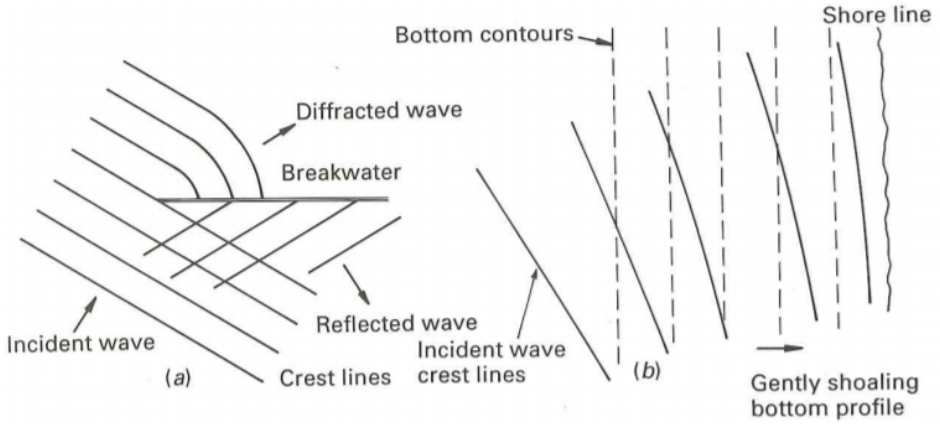

Figure 4.5: Wave phenomena - reflection and diffraction (a); refraction (b) (*Source: Patel, 1989*)

4.3 Representation of the ocean surface and wave phenomena

4.3.1 Wave generation - Wind-waves and swell

Wave phenomena can be divided into wind-generated waves and swells, where their physical properties are distinguished by their origin. Figure 4.6 is retrieved from LeBlond, 1978 and shows the characteristic periods of common wave phenomena in the ocean. Wind-waves are often steep, irregular and energetic. They are caused when energy are transferred from local wind to the sea (Ochi, 2005).

Swells are by Ochi, 2005 defined as wind-induced waves commonly generated by storm phenomena. They have generally large periods and travel long distances from the location where they were induced, such as across the Atlantic ocean. While travelling energy is lost, making swells become less steep and more regular of nature than wind-waves.

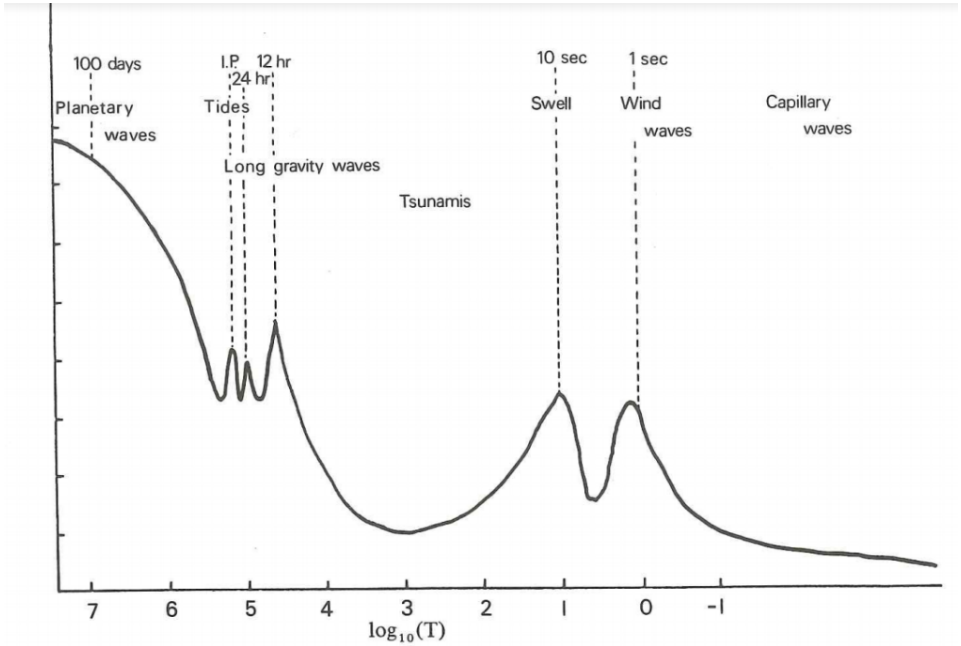

Figure 4.6: Schematic energy spectrum of oceanic wave phenomena. Swell and wind waves are characterized by periods of 10 seconds and 1 seconds, respectively (*Source: LeBlond, 1978*).

4.3.2 Long-crested waves

Linear theory assumes a mean elevation, z, to be zero. This will simplify the Fourier series expression of the wave elevation into a summation of multiple long-crested[1] wave components. Wave component i, has a random and designated phase angle, amplitude, circular frequency and wave number. When the total of I wave components are summed the expression of *long-crested wave elevation* is (Myrhaug, 2007):

$$\zeta(x,t) = \sum_{i=1}^{I} A_i cos(\omega_i t + \epsilon_i) \tag{4.8}$$

4.3.3 Short-crested waves

Wave components i, in reality, propagates in various spatial directions defined by the angles θ_j relative to the axis of propagation. Superposition is assumed valid. The sea surface elevation is now defined as a *short-crested wave elevation*, which is a summation of I long crested waves over J directions (Myrhaug, 2007):

$$\zeta(x,t) = \sum_{i=1}^{I}\sum_{j=1}^{J} \zeta_{Aij} cos(\omega_i t - x k_i cos\theta_j - y k_i cos\theta_j + \epsilon_{ij}) \tag{4.9}$$

4.3.4 Wave spectrum - representation of irregular waves

A long-crested wave elevation consists of a large number of wave components, each having a designated frequency. To simplify the representation of the wave elevation, a wave spectrum can be applied, describing the wave energy content. The spectrum is based on Fourier analysis, allowing transformation of a time dependent signal into frequency domain (see equation A.22 in appendix A.2). A wave elevation, ζ, made up by I linear, long-crested wave components with wave amplitudes ζ_{Ai} and frequencies ω_i has the energy density (Myrhaug, 2007):

$$\frac{E}{\rho g} = \sum_{i=1}^{I} \frac{1}{2}\zeta_{Ai}^2(\omega_i) = \sum_{i=1}^{I} S(\omega_i)\Delta\omega \tag{4.10}$$

[1] all wave components are going in the same direction

The area within a frequency interval $\Delta\omega$ with height $S(\omega)$ is equal to the the energy density of all wave components within this frequency interval. Then, if we let $\Delta\omega \to 0$, thus $I \to \infty$, the total energy of the long-crested wave elevation is defined as the area of the wave spectrum, where $S(\omega)$ is defined as the wave spectrum to the wave elevation $\zeta(t)$:

$$\frac{E}{\rho g} = \frac{1}{2}\zeta_A^2 = \int_0^\infty S(\omega)d\omega \tag{4.11}$$

The total energy of a short-crested wave elevation is defined by the total area of the omnidirectional wave spectra:

$$\frac{E}{\rho g} = \int_0^{2\pi}\int_0^\infty S(\omega,\theta)d\omega d\theta \tag{4.12}$$

For practical purposes it is often most interesting to analyze the wave propagation directions where maximum spectral density can be found. In other words, directions where the omnidirectional spectra have their highest peaks. The actual spectrum for the geographical area under consideration are commonly unknown and standardized spectra are then applied to analyze the wave conditions within the relevant area.

4.3.5 Wave parameters - representation of wave conditions

Significant wave height

The term significant wave height was first introduced in an article by Sverdrup and Munk, 1947. Based on the author's experiences, it was stated when observing irregular waves, it could be difficult to make a precise visual estimate of the characteristic wave height corresponding to the measured characteristic wave height. *Significant wave height is a statistical property describing wave phenomena and corresponds to the mean of the one third highest measured waves in a record.* The following mathematical definition is retrieved from Holthuijsen, 2007, where for instance j = 4 is the fourth highest wave of N waves:

$$H_s = H_{\frac{1}{3}} = \frac{1}{\frac{N}{3}}\sum_{j=1}^{\frac{N}{3}} H_j \tag{4.13}$$

Significant wave heights can alternatively be estimated by wave spectra, where their magnitudes depend on the area within the spectrum under consideration (Holthuijsen, 2007):

$$H_s = H_{m0} = 4\sqrt{m_0} \tag{4.14}$$

The spectral zero moment corresponds to the variance of a sample of wave elevations. The n-th moment of a spectrum is defined as (Myrhaug, 2005):

$$m_n = \int_0^\infty \omega^n S(\omega) d\omega; n = 0, 1, 2, ... \tag{4.15}$$

It is in Holthuijsen, 2007 stressed that the spectral moments and parameter estimates are sensitive to noise from measurements and integration. When obtaining the n-th moment from equation 4.15, an upper integration limit (for instance Nyquist, see appendix A.4.1) is in practice applied rather than ∞. Higher order moments are more sensitive to noise occurring at high frequencies than those of lower order. This is in particular affecting estimates for wave periods, as presented in the consecutive paragraph.

Wave periods

Following the description of wave height, it is possible to define wave period. Several wave period definitions are common, among other *zero-crossing wave period* and *peak period*. The mean zero-crossing period is the mean of the time interval between consecutive zero-crossings of wave elevations[2] (Holthuijsen, 2007). The zero-crossing period can be defined through spectral analysis (Myrhaug, 2007):

$$T_{m02} = 2\pi\sqrt{\frac{m_0}{m_2}} \tag{4.16}$$

Another common wave period is the *peak period, T_p, corresponding to the period of the highest peak in the wave power spectrum* (Myrhaug, 2007).

4.3.6 Standardized wave spectra

PM-spectrum

Spectra are used to simplify the description of a sea surface in terms of energy distribution of wave heights. They are applicable to describe irregular sea states for short term stationary sea states. One of the most used

[2]The wave elevation crosses the zero level between consecutive positive derivatives of the signal (Myrhaug, 2007).

standardized wave power spectrum is the Pierson-Moskowitz spectrum (PM-spectrum), based on dimensionless plotting of measurements done in the North Sea in 1964 (Pierson and Moskowitz, 1964). *One of the basic assumptions of a PM-spectrum is assuming a fully developed sea state*, in terms of equilibrium between the wind and the wind-induced waves. The PM-spectrum is a one-parameter spectrum, where only wind determine shape of the spectrum. For increasing wind speeds, the peak of the spectrum move to larger energies and its peak will tend to lower frequencies. The PM-spectrum is by Pierson and Moskowitz, 1964 defined as:

$$S(\omega) = \frac{A}{\omega^5} exp[-\frac{B}{\omega^4}] \tag{4.17}$$

where g is the gravitational acceleration and V is the wind speed in the following parameters:

$$A = 0.0081g^2 \; B = 0.74(\frac{g}{V})^4 \tag{4.18}$$

JONSWAP

Equilibrium between wind and waves is not possible everywhere. The interaction between wind and wind-waves are dependent on *fetch length, the free distance the wind blows from shore to the location of the waves.* The wind is assumed to have constant velocity within the fetch length. The PM-spectrum was revised in the Joint North Sea Wave Project, where measurements outside the coast of Sylt in Germany were obtained in a large measurement campaign (Hasselman; Barnett; Bouws, 1973). Sea states in North Sea are never fully developed, making it necessary to modify the PM-spectrum. In JONSWAP, peak frequency replaced the wind speed as parameter, due to the peaked shape of the spectrum obtained by the measurement campaign. Wind speed is still included by the following relationship:

$$\omega_p = 0.87\frac{g}{V} \tag{4.19}$$

Due to location dependency of a spectrum, it is possible to evaluate the validity of JONSWAP by parametrization[3]. This is based on an estimation of significant wave height from the spectrum H_{m0}.

[3]Process of presenting a state of a system by using independent variables, parameters

$$H_S \approx H_{m0} = 4\sqrt{m_0} = 4\sqrt{\int_0^\infty S(\omega)d\omega} \tag{4.20}$$

The valid area for appying the JONSWAP spectrum is given by peak period, i.e. $\omega_p = \frac{2\pi}{T_p}$, where T_p should lie within the area

$$3.6\sqrt{H_{m0}} \leq T_p \leq 5\sqrt{H_{m0}} \tag{4.21}$$

Torsethaugen spectrum

JONSWAP and PM-spectra are based on *wind-generated sea*. However, in some areas swells are predominant and JONSWAP can be replaced by a two-peaked spectrum developed by Torsetgaugen, 2004. This spectrum assumes deep water and open ocean areas. The peak at lowest frequency represents swells, whereas the peak located at larger frequency, represents wind generated seas. In the North Sea, local generated wind-sea and remotely generated swell sea simultaneously occur, making Torsethaugen applicable (Myrhaug, 2007).

4.4 Statistical representation of met-ocean conditions

Wave phenomena characteristics and wave parameters serves as a basis for describing met-ocean conditions, used in the design and operation of marine structures. The following sections discuss challenges of representing the actual met-ocean conditions. The objective is to give an introduction to wave estimation methods, which will be presented in section 5.1.1 and 5.1.2 in chapter 5.

4.4.1 Methodologies for wave data acquisition

Sampling of wave data is an important activity in the establishment of models for estimating environmental conditions in the oceans. Wave data are among main sources for information about the ocean. Both quantity and quality of the wave data available are important factors to consider, and the availability of wave data are moreover highly dependent on geographical area considered. In the North Sea, sampling and observation of waves have been done since the 1950s, whereas in other areas this is limited to a few years (Bitner-Gregersen, 2015; Haver, 2017). There are several methods available for wave data acquisition, including:

- Instrumental (physical) measurement
- Visual observations
- Hindcasting
- Remote-sensed data from satellites

Physical measurements are considered of having highest accuracy, but are expensive. Technical difficulties of doing routine measurements at sea and simultaneously cover a large area are some of the cost driving factors in conjunction with full scale measurements (Tucker, 1991).

Offshore wave data is important input in wave models applied in near-shore regions presented in 5.1.2. A common input is data acquired from hindcasting.

Hindcasting

Hindcasting are widely used methods providing information about the met-ocean conditions in a certain oceanic area, such as the North Sea. Hindcasting models use previously estimated and observed meteorological data, such as wind, current, temperature and waves as input data for mathematical models. The techniques of hindcasting are similar to forecasting applied in meteorology, but differs by establishing historical estimates of the met-ocean conditions. Haver, 2017 states that for the last decade, hindcast models have provided good quality for application in the Norwegian Continental Shelf.

Hindcasting is the preferred method for obtaining met-ocean data for design purposes in Norwegian offshore industry, and the hindcast database for North Sea covers the following information for every 3 hours average (*Retrieved from Haver, 2017*):

- *Mean wind speed at 10 m above sea level together with the corresponding mean direction the wind is blowing from.*
- *Total significant wave height, spectral peak period, spectral peak direction and mean direction from which waves are coming.*
- *Significant wave height for mean wind sea, spectral peak period for wind sea and spectral peak direction of propagation of wind sea.*
- *Significant wave height for swell sea, spectral peak period for swell sea and spectral peak direction of swell sea.*

NORA10 is a widely used hindcast database for the Norwegian Continental shelf. The met-ocean conditions presented above are in this model

calculated for every 10 km, where H_s and T_p values are given in a certain (and limited) resolution. The resolution is logarithmic, meaning the resolution is high for small values of T_p and decreases for increasing values of T_p. For H_s, the distribution function obtained from hindcast should be compared to measurements from the area under consideration to validate the hindcast data (Haver, 2017).

Hindcast databases do not account for complex bathymetry and islands (topography). According to Bore and Amdahl, 2017, hindcast data at nearshore locations in Norway are not existing, making it challenging to obtain long term information about the met-ocean conditions at typical aquaculture sites. Along with wind data and bathymetry information, hindcast data are important input data in wave models, such as SWAN (Simulating WAves Nearshore).

4.4.2 Challenges of representing the most probable met-ocean conditions

Subsequent to a measurement campaign, estimations of extreme values of met-ocean parameters and their corresponding loads can be done. Uncertainties and consequences of met-ocean estimation methodologies will in the following paragraphs be discussed.

Met-ocean description for a specific location consists of fitting the measurements of the conditions to a mixture of empirical, mathematical and statistical models. A detailed presentation of advances in ocean environment description can for instance be found in Bitner-Gregersen et al., 2014. The authors presents some of the challenges related to measurements and representation of met-ocean conditions, corresponding uncertainties and recent improvements in accuracy of the various methods applied for sampling and analyzing met-ocean conditions.

Precise estimations of environmental parameters at possible sites are critical for optimal design of fish farms. DNVGL-RP-C205 states in section *1.3.1.5 Environmental conditions* (p. 8) that recordings of *20 years should be available or that climatic uncertainty should be taken into account in the analysis.* In NS9415:2009, the required length of recording is only given for current measurements, where a measurement length of minimum 12 months should be obtained. Current measurements can alternatively consist of multiple consecutive samples with minimum duration of 4 weeks to represent and cover a 12 months period for further statistical analysis.

4.4.3 Uncertainties in met-ocean data acquisition

Uncertainty can be grouped in *aleatory uncertainty* and *epistemic uncertainty.* The natural randomness of a process over time is due to aleatory

uncertainty and can not be reduced. The epistemic uncertainties origin in for instance the method of data acquisition, model applied for fitting the data and/or climatic uncertainties, due to for instance climatic changes. This form of uncertainty can be minimized or at least reduced by collecting more information of the stochastic process considered, such as increasing the sampling time of the environmental parameters considered.

There are several challenges and uncertainties related to the validity of met-ocean conditions due to their spatial and transient variations. A common approach, which is discussed in Bitner-Gregersen et al., 2014, is to represent the conditions as stationary (short term) sea states, corresponding to a limited geographical area and period of time, represented by probabilistic models. Unlike waves, current and wind velocities, the parameters of a sea state vary much less over time. As an example; a sea state may be represented by estimated parameters such as a significant wave height (H_{m0}), a maximum wave height (H_{max}), a peak period (T_p) and zero-up crossing period (T_m02).

The final procedure of describing the met-ocean conditions within an area, consists of analyzing how sort-term sea states vary over time. A common approach is to establish a probabilistic sea state model describing the environmental conditions for the specific geographical area based on short term stationary sea states.

By the establishment of offshore oil production in the North Sea, a demand for accurate description of the met-ocean conditions was profound. This resulted in extensive studies of the environmental conditions in the North Sea, where long periods of samples have been acquired for describing the met-ocean conditions. Hindcasting is today widely used and much attention has been given to improve the precision of these data bases for numerous basins in several projects. Oceanographic studies of the North Sea have resulted in the establishment of several standardized scatter diagrams and wave spectra, such as the JONSWAP spectra (Joint North Sea Wave Observation Project) (Hasselman; Barnett; Bouws, 1973).

4.4.4 Description of near-shore met-ocean conditions

Contrary to offshore areas, descriptions of met-ocean conditions for near-shore areas are rather poor and are furthermore even more challenging to describe. Several articles published in conjunction to the OMAE 2017 (The International Conference on Ocean, Offshore and Arctic Engineering), addressed uncertainties in estimation of met-ocean conditions near-shore for aquaculture applications. Bore and Amdahl, 2017 stated that local bathymetry and topography induce large variations in the met-ocean parameters even within a small geographical area. Shallow water effects further may make

the spatial variations within a site considerable.

Bitner-Gregersen et al., 2014 stated that there is an increasing demand (and need) to replace subjective observation based wave data bases with instrumentally gathered information in combination with numerical models for use in marine applications. Uncertainties in met-ocean description will in the coming years provide large challenges in marine industries. *Location specific met-ocean description is needed both for establishing design and operational criteria are called for.*

Methods for probabilistic environmental description of aquaculture sites have among other been presented by Bore and Amdahl, 2017 and D. Kristiansen, Aksnes, Su, Lader, and V. Bjelland, 2017. The latter performed field measurements at two aquaculture sites and did statistical analyses of the collected data and compared results to the method of environmental characterization described in NS9415:2009. The authors stated that improvements in environmental description of aquaculture sites should be done to reduce the uncertainties in design.

Spatial estimation of wave conditions

Met-ocean estimations, in particular wave estimations for a specific area are most commonly done by measuring and evaluate wave elevations in one point, both for extreme value analysis, short and long term statistics. Nevertheless, it was by Forristall, 2011 validated that the maximum wave crest from a grid of wave measurements is larger than a single-point average maximum. It was shown that linear theory agrees well with measurements in a wave basin and simulations of the wave field when evaluating the ratio between area maximum and single-point maxima. The difference between multidimensional and single-point estimates are decaying as waves become long-crested, but area maxima is still 10% greater than point-extremes.

Barbariol, Benetazzo, Carniel, and Sclavo, 2015 stated that for short-crested sea states, estimations of wave extremes should rely on multidimensional wave field. The influence of wind, ambient currents and bathymetry conditions on wave extremes in a space-time domain was investigated. The ratio between wave extremes and significant wave height was in a space-time domain reduced by increasing wind speeds and by depth-induced shoaling. H_s increase as waves propagate to shallower waters, which counteracted extreme wave heights. Further it was shown that when enlarging the area analysed, the ratio between maximum wave height and H_s was increased.

Chapter 5

Site surveys and methodologies for wave load determination with respect to NS9415:2009

When establishing aquaculture activities in the ocean, an assessment of met-ocean exposure is necessary with respect to the following purposes: *Determine design loads/characteristic loads* (see i.e. Haver, 2017) or *obtain facility certificate/permission* (see NYTEK-forskriften, 2015). Met-ocean conditions must be documented in the NYTEK scheme, including wind-waves, swells (if occurring) and combined sea states. Main objectives of site surveys are to provide correct descriptions of the environmental loads at locations where fish farms are planned installed. By investigating the topography and degree of exposure to wind, waves and current, the site survey provides important information applicable for design and the operability of installation (NYTEK-forskriften, 2015). Several methodologies are available for estimating wave conditions, and in this section practical aspects of the site survey regarding wind and waves are presented.

5.1 Methodologies for wave load determination

Propagation and physics of ocean waves are random by nature and highly dependent on bathymetry and location. This makes it necessary to describe wave conditions thoroughly by stating the occurrence of various wave conditions at a site. According to NS9415:2009 and NYTEK scheme, wind-generated waves, swell and other wave conditions (caused by among other wave reflection, ships and wave-current interaction), must be assessed. Wind-waves and swells must be thoroughly described with return periods in NYTEK scheme, making it natural to emphasize only these herein.

The statistical parameter *return period* of a wave is described by the wave height or wave period that is exceeded only once during the respective period. According to the site analysis in NS9415:2009 both Hs_{10year} and $Hs_{50years}$ must be calculated based on measurements from a site. Wave

conditions can be represented in various ways, where information can be acquired by:

- Calculations
- Measurement campaigns
- Standardized spectra

In the following paragraphs methodologies for estimating wind-induced waves are presented, followed by methodologies for estimating swells.

5.1.1 Wind waves - Estimation of waves by use of fetch analysis

Methodologies presented herein for wind-wave estimation are selected based on the information stated in NYTEK scheme, retrieved by Directorate of Fisheries. NS9415:2009 only specify fetch length analysis as methodology for estimating wind-induced waves. Nevertheless, the standard does not limit the inspector to utilize other scientific well-respected methodologies if its use is adequately documented.

According to section 5.3.1.4 in NS9415:2009, wind-induced waves can be estimated based on wind data from measurements either of the two nearest weather stations or if available, from long-term statistics. The wind velocity shall be calculated by methods given in NS-EN 1991-1-4, in particular chapter 4. Wind velocity is in this standard defined as consisting of a mean velocity and a fluctuating component. The resulting wind magnitude is depending on topography, altitude and roughness of the surface where the wind blows.

Long-term wind velocities of 10 and 50 years return periods will serve as variables in calculations for the 10 and 50 years return periods of wind-induced waves. The following formulas are applied when estimating wind-induced waves. These can be found in section 5.3.1.4 of NS9415:2009.

Adjusted wind velocity U_A:

$$U_A = 0,71 U_{10/50 years}^{1,23} \quad [\mathrm{m/s}] \tag{5.1}$$

Significant wave height and peak period:

$$H_{s,\quad 10/50 years} = 5,112 * 10^{-4} U_A F_e^{1/2} \quad [\mathrm{m}] \tag{5.2}$$

$$T_{p,\quad 10/50 years} = 6,238 * 10^{-2} (U_A F_e)^{1/3} [\mathrm{s}] \tag{5.3}$$

Charts in Annex C of NS9415:2009 can substitute the formulas presented above, where the procedure also depend on fetch length, F_e, and wind velocity.

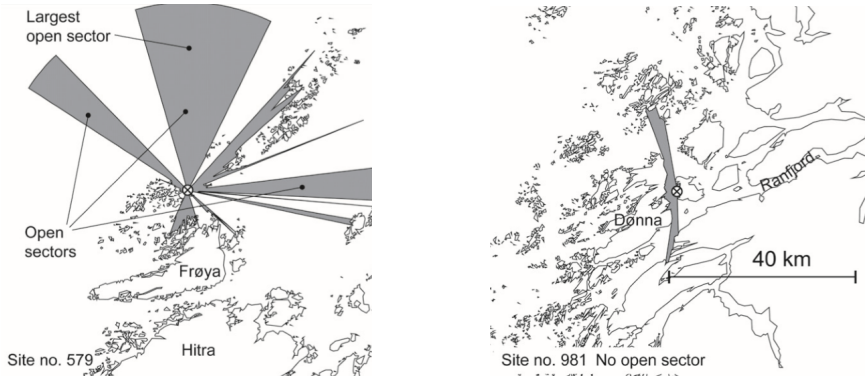

Figure 5.1: Fetch sector where wind-induced waves are assumed generated (*Source: Lader, Kristiansen, Alver, Bjelland, and Myrhaug, 2017*)

Finding most representative fetch length

Effective fetch length is defined as the distance wind blows freely over water without any disturbances from land, skerries or islands. An angle of maximum 12 degrees limits the area within a fetch length. Tables in NS9415:2009 Annex C specify 40 km as maximum fetch length. Figure 5.1 is retrieved from Lader, Kristiansen, Alver, Bjelland, and Myrhaug, 2017 and shows areas of fetch where wind-induced waves are assumed to be generated.

Wind direction varies over time, making it important to consider the directivity of wind and its consecutive wave loads (Jonathan, Ewans, and Forristall, 2008). NS9415:2009 requires documentation of waves, wind and current in at least 8 concurrent directions. This means that fetch length must be indicated in at least 8 directions when applying fetch length analysis to estimate wind-waves. Aquaculture sites features large variation in fetch length due to complex bathymetry and topography. This causes much larger directional dependency of sea state characteristics than what is typical at offshore sites. Bore and Amdahl, 2017 stated that a model including directional variation of waves significantly describes extremes better than one excluding directivity for met-ocean conditions at aquaculture sites.

5.1.2 Wave models

Wave models are used to numerically simulate wave fields by calculating wave parameters and spectra in predefined grid points when oceanographic measurements are limited. They are most commonly based on linear wave theory, utilizing equations and physical approximations of wave phenomena presented in section 4 and 4.2.1. Wave action models, as presented in Svendsen, 2006, are based on *assuming wave action,* $\frac{E}{\omega_r}$*, to be conserved* if moving

with the group velocity, $c_{gr\alpha}$ of a single monochromatic[1] wave propagating in direction α. Here E is the energy density of the wave with relative frequency $\omega_r = gktanh(kh)$, representing the frequency observed when moving with the current velocity, U_α, of the fluid particles.

Wave action models are applicable for irregular waves by defining a wave action spectrum, $N(f, \alpha)$, where a directional frequency spectrum and the relative frequency of the waves are defined. The wave action equation, retrieved by Svendsen, 2006, for each spectral components of a wave can be written:

$$\frac{\partial N(f,\alpha)}{\partial t} + \frac{\partial}{\partial x_\alpha}((U_\alpha + c_{gr\alpha})N(f,\alpha) = S_t \tag{5.4}$$

In wave models, this equation is solved with respect to $N(f, \alpha)$. The source term, S_t, describes the development in energy when a wave group is propagating (Hasselmann et al., 1988). The wave model source term includes the following physical contributions (notation as in Svendsen, 2006):

$$S_t = S_{br} + S_{bf} + S_w + S_{wc} + S_{nl} \tag{5.5}$$

- S_{br}: energy dissipation due to wave breaking
- S_{bf}: energy dissipation due to bottom friction
- S_{wc}: energy dissipation due to whitecap breaking of waves
- S_{nl}: nonlinear wave-wave interactions causing energy transfer and decay of wave motions
- S_w: input from wind, contributes to growth of wind-waves

The resolution of a wave model is user defined in spatial, frequency and/or time domains, depending on the model. Today, third-generation wave models developed from the deep-water wave model, WAM, are available (Hasselmann et al., 1988). In the following sections, wave models applied in registered NYTEK data will be presented briefly.

5.1.3 Estimation of wind waves by use of SWAN

SWAN (Simulating WAves Nearshore) is a numerical wave model simulating waves propagating from deep to shallow water, derived from WAM. It is an open-source model developed at Delft University of Technology first introduced by Booij; 1999. Information about SWAN is taken from Booij; 1999,

[1] conservation of wave crests (Svendsen, 2006)

Booij, Holthuijsen, and Battjes, 2001, Holthuijsen, 2007 and the SWAN User Manual (http://swanmodel.sourceforge.net/download/zip/swanuse.pdf).

As stated in section 4.2.1, physical properties of waves evolve while moving over uneven bottoms and into shallow regions. Unlike fetch length analysis and deep-water wave models, these effects are taken into account in SWAN and estimated in space and time domain by implicit numerical schemes.

Boundary conditions and constraints

Before running wave simulations in SWAN, boundary conditions and constrains must be determined. This includes:

- Computational domain and grid resolution: outputs are given in grid points in an earth fixed coordinate system
- Bathymetry information: To evaluate the development of waves over uneven bottoms, the model require information about change in depth and steepness. The accuracy of wave evolution rendering will depend on the resolution of bathymetry information.
- Boundary conditions: This includes defining what will happen to waves moving out of the computational grid or approaching land/beach. Furthermore wave reflection conditions must be determined.

Input data and resulting wave information

Hindcast data of met-ocean parameters (including wind data), standardized wave spectra (for deep water) and bathymetry are used as input data in SWAN. The resulting shallow-water wave spectra and estimates of wave parameters for a specific locations will be calculated. In case of irregular sea, i.e. when swell is occurring, NS9415:2009 states that a JONSWAP spectrum should be applied to describe both swell and wind-generated sea. In sheltered areas, where swell generally limited, a fully developed sea state should be assumed, making PM-spectre applicable.

Several improvements of the SWAN model have been incorporated since it was first presented by Booij et al., 2001. They stated that SWAN is capable of performing high-resolution calculations for near-shore regions, but should be avoided in oceanic, low-resolution calculations. Here, wave models WAM or WAVEWATCH III, developed by US National Oceanic and Atmospheric Administration, should be used. The model is directional dependent of the input data, which was discussed by Stefanakos and Eidnes, 2014. As presented previously, resulting directional variation in wave conditions at aquaculture sites were presented by Bore and Amdahl, 2017.

Figure 5.2a is retrieved by Stefanakos and Eidnes, 2014 and shows how SWAN can be applied to transfer offshore wave information and evaluate how this will evolve in near-shore regions. The study examples how SWAN can be applied in case of insufficient information about wave conditions in near-shore regions. The case displayed is from Norfold, England. SWAN was run three times and output data from one run was used as input data in the consecutive run, as seen in figure 5.2a. Figure 5.2b shows nested runs of SWAN, which are used due to complex topography and bathymetry. The computational domain of the second, nested run uses a finer grid. The red point is the input data point and the yellow points are target points, where output data (in this case spectra) of the run is given. Resulting wave conditions based on consecutive runs of SWAN will be dependent on the accuracy of the input wave information. In case of inaccurate input data or boundary conditions, this will propagate through the analysis and give bias in the resulting output.

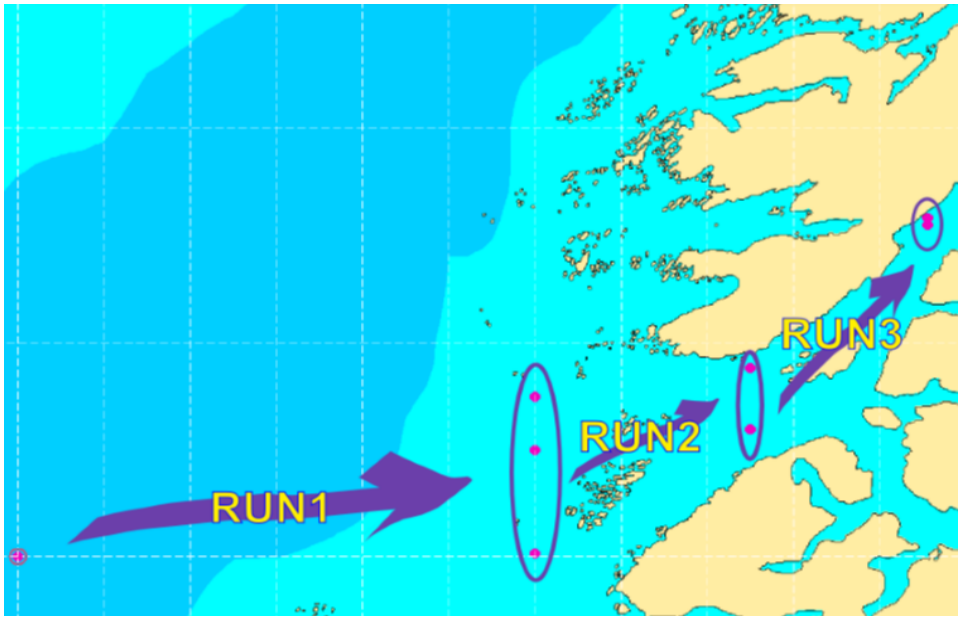

(a) Consecutive runs of SWAN. Starting point is an offshore location and is used as primary input in run 1 of SWAN giving wave conditions in three points. These outputs are used as input information in run 2.

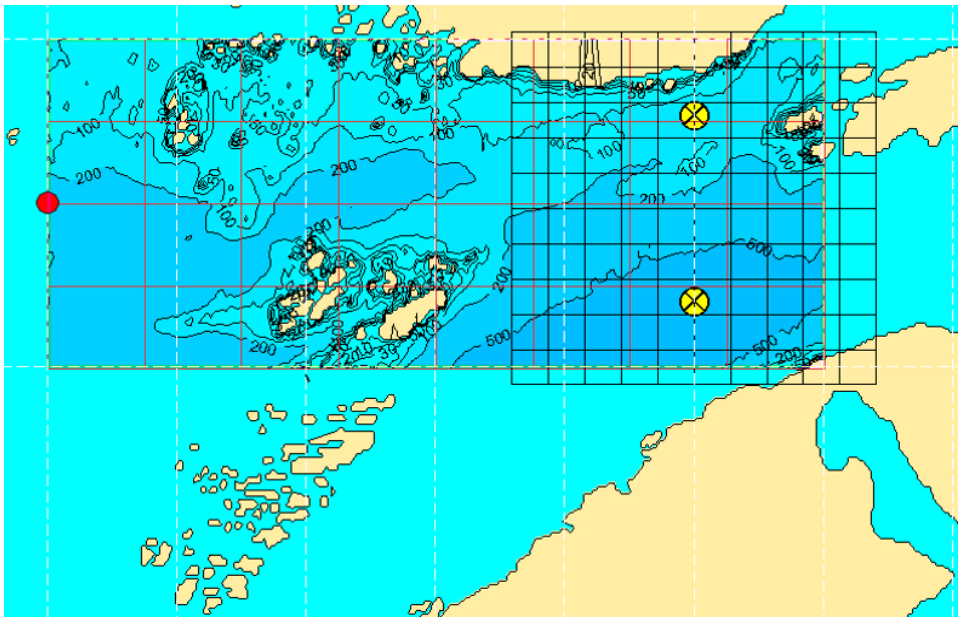

(b) Nested run of SWAN within a region. Red point is the input data point and the yellow points are target points, where output data in this case are given as spectra.

Figure 5.2: Set up of SWAN modeling for transferring offshore wave data to a near-shore location. (*Source: Stefanakos and Eidnes, 2014*)

5.1.4 Wave estimation by use of STWave and CMSWave

STWave (STeady state Wave model) is a half-plane wave model occurring a couple of times in the NYTEK scheme. This is developed by U.S. Army Corps of Engineers Waterways Experiment Station (Thomas C. Massey and Smith, 2011) and is based on equation 5.4. Main difference between this model and SWAN is that STwave assumes the following:

- Half plane: Waves propagating in half circles of 180 degrees
- Mild bottom slopes
- Neglects wave reflection

The half plane assumption allows only wave propagation from offshore to shore, but the simplification reduces requirements for computer memory.

CMSWave (Coastal Modeling System) is also developed by U.S. Army Corps of Engineers Waterways Experiment Station. It is similar to STWave, but *enhanced by including diffraction, reflection and transmission of waves by structures or islands.* Additional reading can be found in Lin, Demirbilek, Mase, Zheng, and Yamada, 2008.

Input data for both models include:

- Batymetry information
- Incident wave spectra
- Wind data
- Spatially varying bottom friction coefficients
- Current fields, surge and/or tidal water level adjustments

Outputs are among othe wave parameters and spectra for user defined grid points (Lin et al., 2008; Thomas C. Massey and Smith, 2011).

Suitability of a model will depend on user requirements, such as type of structure planned installed and met-ocean conditions around the site. If for instance closed and impenetrable structures are planned, the wave field will possibly be affected by the presence of the installation(s) and induce refraction and reflection phenomena. In coastal region, such as in outer archipelago, presence of swells may complicate the wave field additionally.

5.1.5 Swell estimation

Ocean wave models, such as WAM and WAVEWATCH III, are suitable for estimating swell generation in offshore regions. However, when approaching land and shallow depths, the accuracy of these models decrease. Browne et al., 2007 discuss approaches for effective and accurate swell estimations in near-shore regions. Currently, swell presence and estimation in near-shore regions can either be determined by visual observations or simulated by numerical wave action models, such as SWAN, STWave and CMSWave. Insufficient decision criteria for determine presence of swell can cause challenges in representing met-ocean conditions at aquaculture sites.

5.2 Possible challenges in met-ocean determination by NS9415

In NS9415:2009, fetch length analysis is specified for determining wind waves. This analysis is not applicable for evaluate swells, and other methods must be used to document their possible presence. The standard lists three possible approaches to determine wave height and period (Standard Norway, 2016):

- Diffraction and refraction analysis
- Measurements for determining swells with a return period of 10 and 50 years
- Other recognized methods which can document safety, validity and accuracy

Diffraction and refraction analysis can be interpreted as in numerical simulations of the wave field. If selecting measurements, the standard does not give any further details of duration, post-processing and statistical treatment of data.

According to D. Kristiansen et al., 2017, descriptions concerning acquiring of estimations of environmental loads are weakly described and inadequate in the standard. *Only fetch length analysis is described thoroughly, which is deficient in estimating wave conditions for sites in or nearby open ocean areas, due to the limiting fetch length condition.*

Representation of wind, waves and current return periods based on measurements are dependent on the chosen statistical models. No guidelines for statistical treatment are given in NS9415:2009 (Standard Norway, 2016), neither for any of the met-ocean phenomena. This leads to uncertainty in the calculated return periods based on the methods given in NS9415:2009,

where duration of measurement campaign and seasonal variability will influence the estimations (Bore and Amdahl, 2017).

5.3 Site surveys and level of exposure to met-ocean loads

NS9415:2009 states that measurements of current and assessment of wind and waves preferably shall be preformed in as an greenfield project activity, meaning the site should be without any kind of infrastructure or installations. Annex A of NS9415:2009 provides a table for site classification by exposure to waves and current. Table 5.1 was used in NS9415:2003, but is in NS9415:2009 attached as background information during site classification (D. Kristiansen et al., 2017; Standard Norway, 2016).

Table 5.1: Aquaculture site classes with respect to exposure

Exposure of aquaculture sites with respect to wave classes						
Wave class	H_s **[m]**	T_P **[s]**	**Degree of exposure**	**Current class**	V_C **[m/s]**	**Degree of exposure**
A	0,0 - 0,5	0,0-0,2	Small	a	0,0-0,3	Small
B	0,5 - 1,0	1,6-3,2	Moderate	b	0,3-0,5	Moderate
C	1,0 - 2	2,5-5,1	Medium	c	0,5-1,0	Medium
D	2,0 - 3,0	4,0-6,7	High	d	1,0-1,5	High
E	>3,0	5,3-18,0	Extreme	e	>1,5	Extreme

A classification of Norwegian salmon farms with respect to wind and waves was presented by Lader et al., 2017 at the *ASME 2017 36th OMAE conference*. The authors used long term wind data and fetch length to classify all Norwegian sites with respect to wind and waves. None of the 1070 Norwegian aquaculture sites were exposed to wave class *E - Extreme exposure*, whereas about 18 % of all the sites experienced wave conditions characterized as *C- Medium* or *D - High* at least once a year. The results from this study will be compared with data obtained from the Directorate of Fisheries in section 6.1.2.

There is a trend of moving sites to more exposed waters in Norway, however, *none aquaculture sites are yet located offshore*. Many stakeholders in the industry argue for moving fish farms to more exposed areas due to near-shore area conflicts, possible avoidance of sea lice in exposed areas and less challenges with emissions from the farms, stated by for instance Bjelland et al., 2015; Olafsen et al., 2012.

Preliminary concluding words

There are several methods available for assessing wave conditions at aquaculture sites and their characteristics and assumptions are quite dissimilar. For wind-wave estimations either fetch length or numerical wave models can be applied. Swell parameters, which are commonly occurring nearby open ocean areas, can be achieved by use of wave models or by measurement campaigns. Several studies have expressed that methods given in NS9415:2009 for evaluating wind-induced waves and swells are unclear.

5.4 Quantitative study of methodologies for wind-wave estimation

The following sections and chapter will be dedicated to a quantitative analysis of wave conditions at Norwegian aquaculture sites. The motivation for this is to reveal possible patterns and trends in the selection of wave estimation methods and further discuss possible causes and influencing factors for the selection. Resulting wave conditions are affected by among other accuracy of the wave estimation technique and the availability and quality of input data.

Gathering and preparing information have been a major work in this thesis and the process of establishing and classifying data sets will be presented in the following sections. Relevant files are described in conjunction to the process for the dedicated reader. Specific results from corporate and geographical analyses of causes affecting choices of wave estimation methodologies will be given in next chapter.

5.4.1 Resources and establishing data sets for analysis

The NYTEK data set was obtained by the Directorate of Fisheries in February 2018 and contains information about met-ocen conditions at 1027 sites in Norwegian waters. Based on objectives of the study, it was decided in cooperation with the Directorate to request only met-ocean conditions from non-public data. This was done by evaluating the guidance of NYTEK scheme (https://www.fiskeridir.no/Akvakultur/Registre-og-skjema/Skjema-akvakultur/NYTEK).

Supplementary publicly available information, such as site capacity, site operator, inspection body responsible for site survey, municipality and region for each site, was downloaded from online map service provided by the Directorate (https://kart.fiskeridir.no/).

Interviews of four inspection bodies were carried out in the final phase of the study. The purpose of this was to gain insights in what kind of decision

criteria inspection bodies values when they select methodology for wave estimation. The standardized questions given can be found in appendix B.2. Respondents identities and their respective inspection body are left anonymous.

5.4.2 Establishing data sets for analysis

When a site survey is updated, the outdated information about a site is not deleted from the NYTEK data bases, but adds up in the Directorate's data base. The data received from the Directorate contained much duplicated and outdated information which was necessary to remove. This was done by running the script *loadNYTEKF.m*. Based on the date of import, only newest versions of the site information was written from MATLAB into a xlsx file. This file has served as a primary cleaning file and is the foundation for all further analysis. After removing duplicates, a number of 1027 sites were available for analysis.

All aquaculture sites have a unique five digits identification number in governmental archives. The site number enables tracing of a site in various, unconnected data bases. Non-public NYTEK met-ocean data was linked to publicly available information by utilizing site numbers. Major parts of the public information is available as Excel files, which was used in a large extent to establish sheets for analysis.

For visualization and presentation of data, MATLAB and the business analytics software Power BI Desktop have been utilized depending on purposes of the visualizations.

Categorizing methodologies for wave estimation

Inspection bodies are required and responsible to enlighten methodology used for wave estimation. The scheme is formatted in a way making it possible to write comments or even long phrases of text stating what kind of method used in the site survey. Due to this inconvenience, a manual categorizing of the data was needed for further analyzing purposes. In most cases, methodology used in the locality analysis was stated clearly, but in some cases the information was inaccurate and insufficient for determine what kind of methodology originally used. For the latter case, these were categorized in a bin named "Not available". 501 sites were classified as "Not available" and have for most analysis purposes been excluded, yet this is specified for each presentation of data. Categories of classification for wave estimation methodologies given in NYTEK schemes can be found in appendix B.1.

Chapter 6

Results

Results from quantitative analyses of NYTEK data provided by the Directorate of Fisheries are presented here. The following approaches were taken:

1. Evaluating overall geographical differences in wave estimation methods
2. Comparing resulting wind-wave conditions at sites with an independent data set from a study by Lader et al., 2017 and evaluating the dependency of the methodology applied
3. Presenting geographical characteristics of sites where the occurrence of swells has been reported
4. Evaluating the relationship between company size, wave estimation methodologies and location of sites

Swells and wind-waves may be distinguished through analysis of met-ocean conditions at a site. In the scheme, one must specify wind-wave height, swell height and the combined wave height. This makes it natural to separate the presentations of statistics related to the different wave phenomena. Waves are most commonly generated by wind, and methods for wind-wave estimation have been emphasized throughout this thesis (see sections 4.3.1 and 5.1). The presence of swell and characteristics of associated sites will be presented and discussed in a separate section. Lastly, some findings regarding development licences will be discussed.

6.1 Geographical and overall quantitative distribution of wave estimation methods

Fetch length analysis is the only wind-wave estimation methodology specified in NS9415:2009 and accounts for 331 sites reported in the NYTEK scheme. The standard additionally permits inspection bodies to use other acknowledged methods. SWAN is the second most used methodology and has been applied for 187 sites. Interpretation of reported methodologies

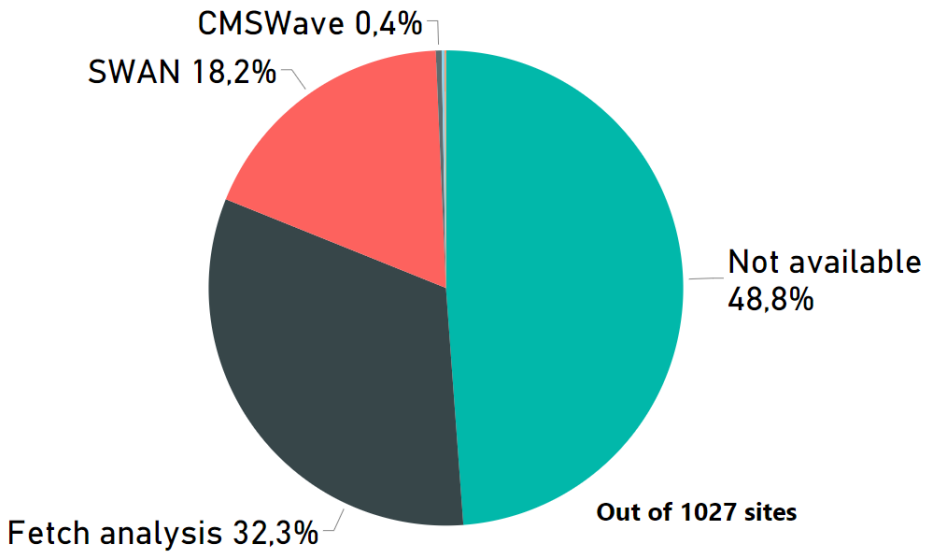

Figure 6.1: Distribution of methods for estimating wind-induced waves at 1027 sites reported in NYTEK scheme.

was performed as explained in section 5.4.2 and a distribution of wind-wave estimation methods was observed, as seen in figure 6.1.

CMSWave and STWave was reported at 4 and 2 sites respectively. For almost half of the sites the reported methodology was not possible to interpret. In the NYTEK scheme, inspection bodies have to report whether waves are estimated based on measurements or if they are calculated by wave models. Only at one location were waves measured, and for 125 sites, it was not stated whether waves were measured or calculated. The sites where calculation or measurements were unspecified were included in the "Not available" bin. There was no obvious reason as to why almost half of the sites did not report methodology for wind-wave estimation.

Due to the dominance of fetch analysis and SWAN, these methods have thus been given main focus. Figure 6.2 shows the distribution of estimation methods among counties. Fetch analysis is the dominant method for all regions excluding Trøndelag and Møre og Romsdal. Here, SWAN has a much larger share. This therefore motivated an investigation of the relative exposure level of sites among the regions. This was done in section 6.1.2.

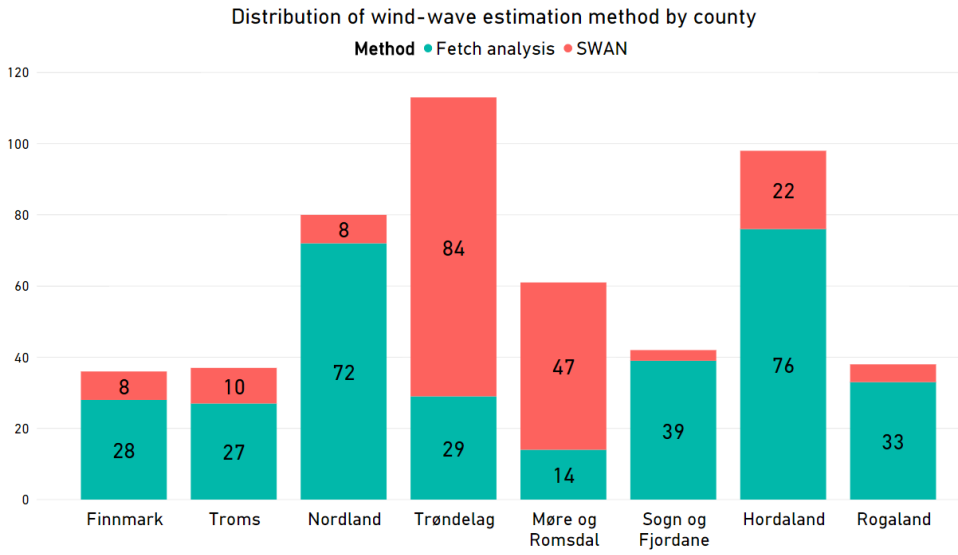

Figure 6.2: Distribution of wind-wave estimation method by region. Only fetch length analysis and SWAN are shown.

6.1.1 Methodologies for wind-wave estimation

In figures 6.3a and 6.3b, the distribution of wind-wave estimation methods are presented based on their reported wave heights.

The figures indicate fetch analysis as the preferred method for estimation of sites reported as having small to medium exposure to waves. In the next section this is further examined by comparing the NYTEK reported wave heights and corresponding methods with an independent data set. This may give further insights into deviations of the various methodologies for estimating wind-induced waves and will be discussed further in next section.

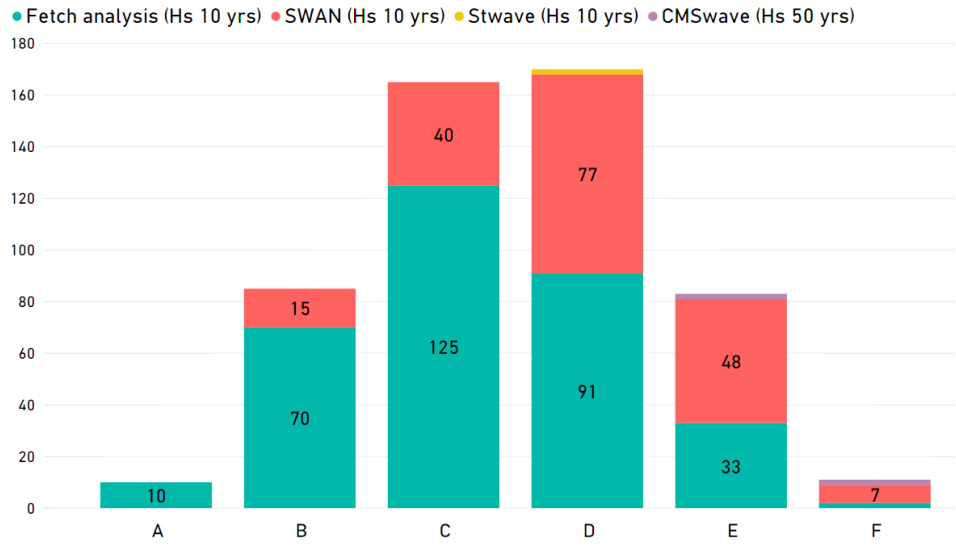

(a) Distribution of wind wave estimation methods for H_{s10yrs}.

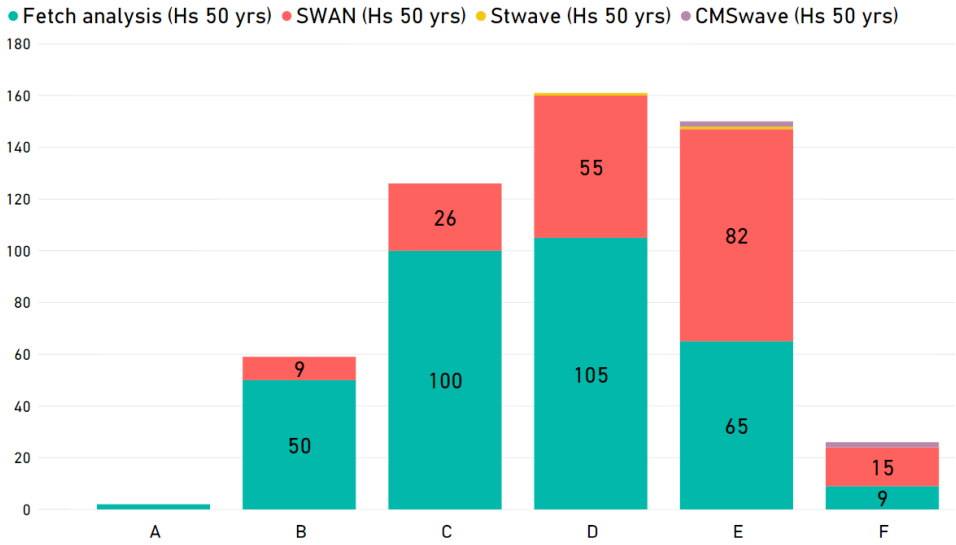

(b) Distribution of wind wave estimation methods for H_{s50yrs}.

Figure 6.3: Distribution of wind wave estimation methods based on exposure intervals given in table 5.1 for H_{s10yrs} and H_{s50yrs}. The x-axis displays classes of exposure, where A includes lowest wave heights and F the highest.

6.1.2 Comparative study of fetch length analysis and methodologies in NYTEK - significant wave heights

Data obtained from the NYTEK scheme (Directorate of Fisheries, 2018b) were compared to results from a study done by Lader et al., 2017. This analysis was done to provide a stringent basis for evaluation of the reported wave heights and their estimation methods.

Lader et al., 2017 evaluated wind-induced wave exposure at all Norwegian sites by utilizing fetch length analysis and formulae given in section 5.1.1. Their findings are discussed in section 5.3. The fetch length data set is from 2016 and contains simulated wave heights and significant wave heights for 1070 sites. Some of the sites present in the data set from Lader et al., 2017 have been discontinued while new sites have been established, resulting in 889 sites available for analysis.

The two data sets were combined by applying various built-in functions in Excel, where the site number was used as a link for comparison between the sets. Various parameters for each designated site was gathered in the file *ComparativeStudyNYTEKFetchMethodologies.xlsx, Sheet: NYTEK StrLen Ferdig.*

Significant heights of wind-induced waves with 10 and 50 year return periods given in NYTEK were compared to their equivalents from Lader et al., 2017. Figures 6.5 and 6.4 show met-ocean conditions for the 889 sites. Histograms and probability distributions of wave heights and their periods give an indication of common wave conditions at these sites.

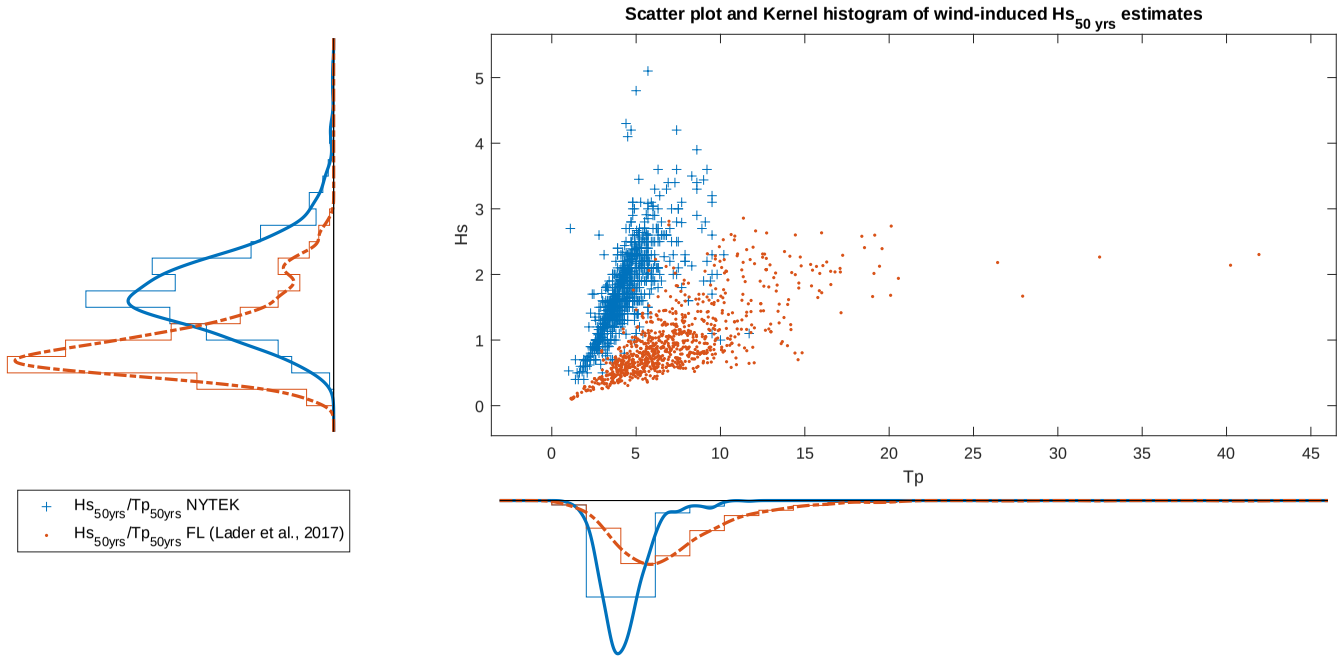

Figure 6.4: Wind-induced wave conditions with 50 year return periods at 889 Norwegian aquaculture sites based on two independent data sets (Blue: NYTEK data. Red: FL (Lader, Kristiansen, Alver, Bjelland, and Myrhaug, 2017)). Note the deviation between the data sets.

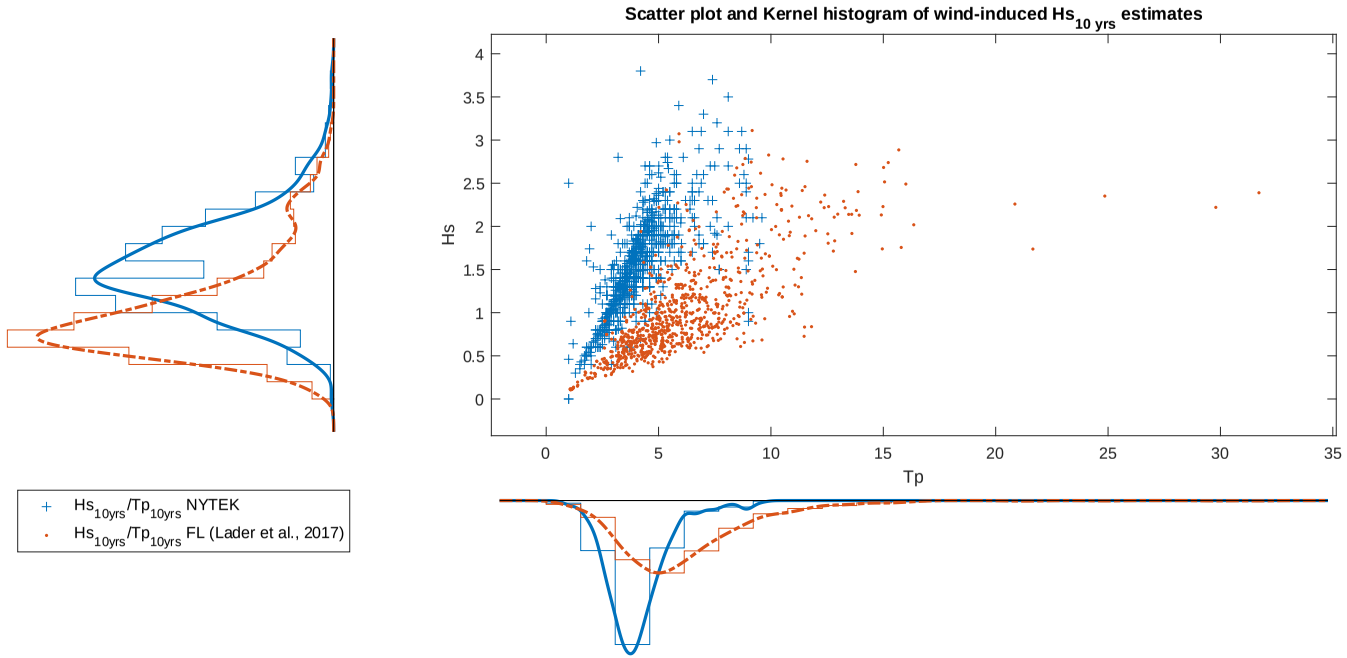

Figure 6.5: Wind-induced wave conditions with 10 year return periods at 889 Norwegian aquaculture sites based on two independent data sets (Blue: NYTEK data. Red: FL (Lader, Kristiansen, Alver, Bjelland, and Myrhaug, 2017)). Note the deviation between the data sets.

The visualizations show deviation between wave conditions reported in NYTEK and analyses done by Lader et al., 2017. The differences are summarized in table 6.1, and were derived from the script *FetchLengthNYTEKScatterF.m*. Here the individual bias between wave heights at each site are calculated, making it possible to evaluate an overall bias of the estimated wind-induced wave conditions. The wave height from fetch length analysis is divided by the wave height from NYTEK for each site and the overall bias is the mean of these results.

Table 6.1: Mean bias of wave conditions based on reported NYTEK data and results from fetch length analysis.

Ret. period	**Mean bias**	**Mean H_s -** *Fetch length*	**Mean H_s - NYTEK**
$H_{s,10yrs}$	0.78	1.04	1.54
$H_{s,50yrs}$	0.65	0.98	1.76

Mean bias is < 1 both for $H_{s,10yrs}$ and $H_{s,50yrs}$, and *indicates that results from fetch length analysis overall give smaller wave heights than what is reported in NYTEK*. This is also visible in figure 6.4. Wave heights based on fetch length analysis are in general smaller and results are more concentrated than their equivalents as reported in NYTEK. The possibility of estimation method dependence will be further investigated.

6.1.3 Wave height estimates V.S. estimation method

There are several factors influencing choice of wave estimation method. Wave heights from fetch length analysis are in general smaller than those reported in NYTEK, and one may consider fetch length analysis to estimate lower values than its alternatives. To evaluate this statement, the most frequent estimation methods are quantitatively examined.

In figure 6.6, the distribution of wind-induced wave estimation methods are given based on exposure to waves over a 50 year return period. For consistency, the level of exposure to waves was calculated based on results from Lader et al., 2017 for each site. Sites where estimation methods were not available were excluded.

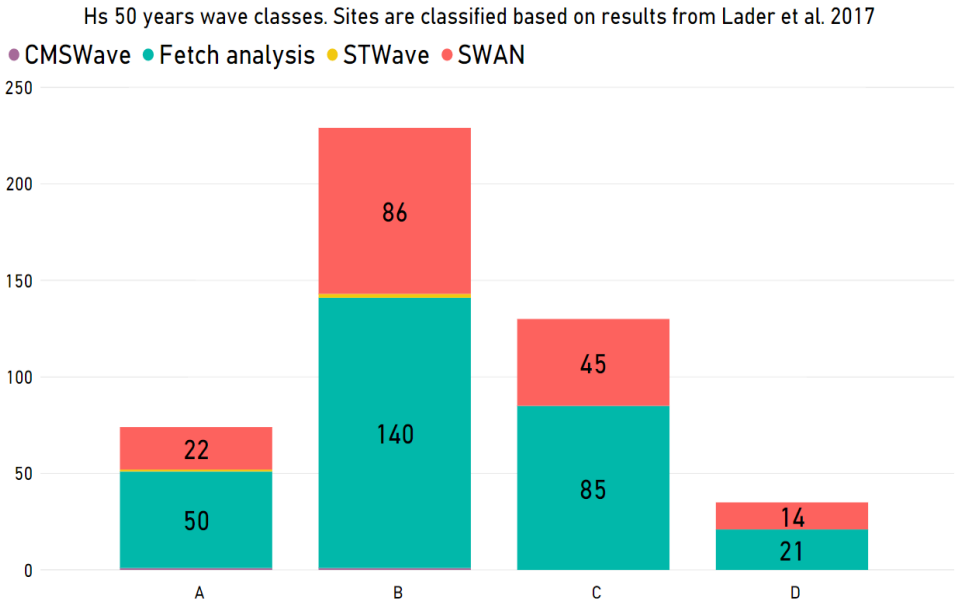

Figure 6.6: Share of $H_{s,50yrs}$ for wave classes based exposure. Sites are classified based on results from Lader, Kristiansen, Alver, Bjelland, and Myrhaug, 2017 and wind-induced wave estimation methods for sites within the class are summarized.

Table 6.2: Mean bias of wave conditions based on reported NYTEK data and results from fetch length analysis.

Ret. Period	*Mean bias – Fetch length/SWAN*	*Mean Hs_{SWAN} [m] NYTEK*	*Mean Hs_{SWAN} [m] Fetch length*
$Hs_{10\ yrs}$	0.62	1.83	1.02
$Hs_{50\ yrs}$	0.52	2.01	1.02

Table 6.3: Mean bias of wave conditions based on reported NYTEK data and results from fetch length analysis.

Ret. Period	*Mean bias – Fetch length/SWAN*	*Mean Hs_{SWAN} [m] NYTEK*	*Mean Hs_{SWAN} [m] Fetch length*
$Hs_{10\ yrs}$	0.81	1.43	1.00
$Hs_{50\ yrs}$	0.67	1.63	1.76

The majority of site surveys have been carried out by use of either fetch length analysis (as given in NS9415:2009) or SWAN and the share of estimation methods are constant for all levels of exposure. Based on the comparative data set made by combining NYTEK and fetch length analysis, no sites were exposed to waves higher than 3 meters over a 50 year return period. A similar distribution is seen in figure B.2 in appendix B.3.

Possible deviations between wave estimation methods can be evaluated by comparing a given method and its sites to results from Lader et al., 2017 for the same sites. In the appendix B.3 and figures B.3 - B.8 the distribution of wave heights at various sites are presented for different wind-wave estimation methods. Wave heights are categorized in bins depending on H_s magnitude, where number of sites in each bin are summarized.

In figures 6.7a and 6.7b, sites where SWAN has been used were compared to fetch length results and their respective significant wave heights. Deviation between the distributions by the two estimation methodologies indicate that application of SWAN tends to result in larger wave heights than fetch length analysis. One should further expect similar wave height results between sites where fetch length analysis was applied and reported in NYTEK, and from Lader et al., 2017. However, in figure 6.8a and 6.8b, this does not appear to be the case.

Deviation in figure 6.8a and 6.8b are smaller than for the case of SWAN, but the wave heights reported in NYTEK are in general larger than equivalent wave heights from Lader et al., 2017.

Bias parameters were calculated for data sets. For both 10 and 50 year return periods bias is in general smaller for sites where fetch length analysis has been reported. This may indicate that the data set from Lader

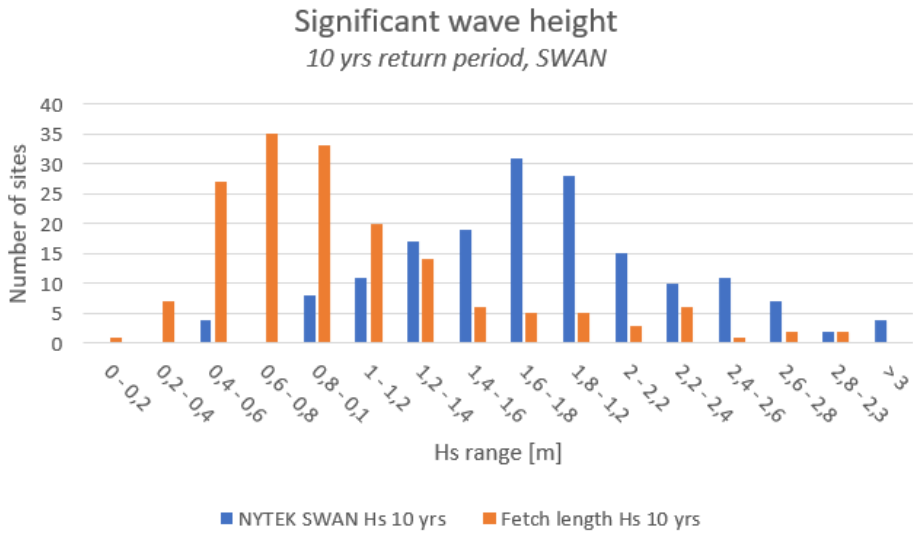

(a) Wind-induced $H_{s_{10yrs}}$ at sites - SWAN

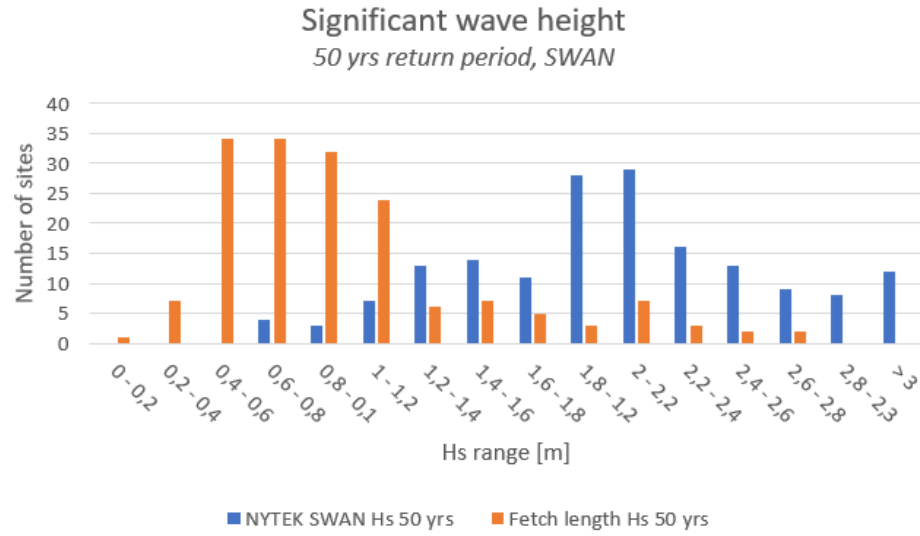

(b) Wind-induced $H_{s_{50yrs}}$ at sites - SWAN

Figure 6.7: Deviation between data sets when wind-wave methodology is evaluated.

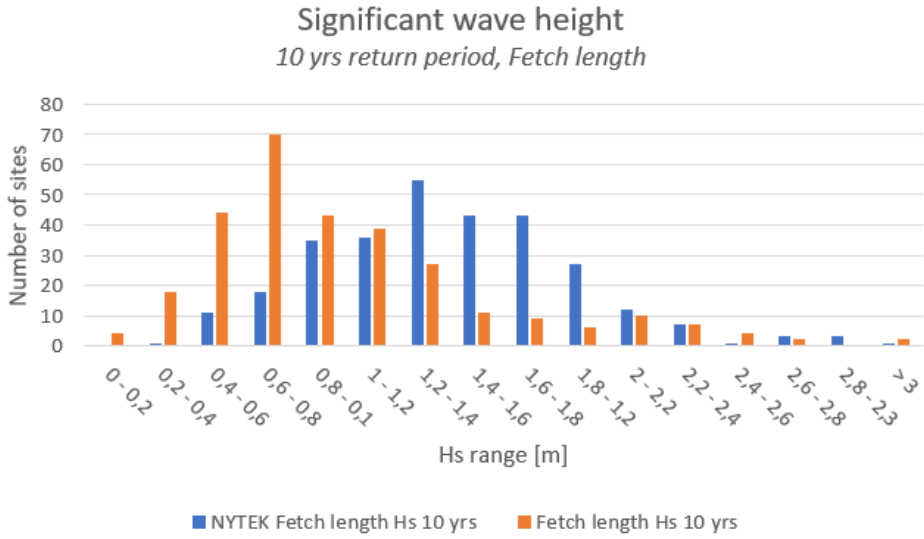

(a) Wind-induced $H_{s_{10yrs}}$ [m] at sites - fetch length analysis as given in NS9415:2009

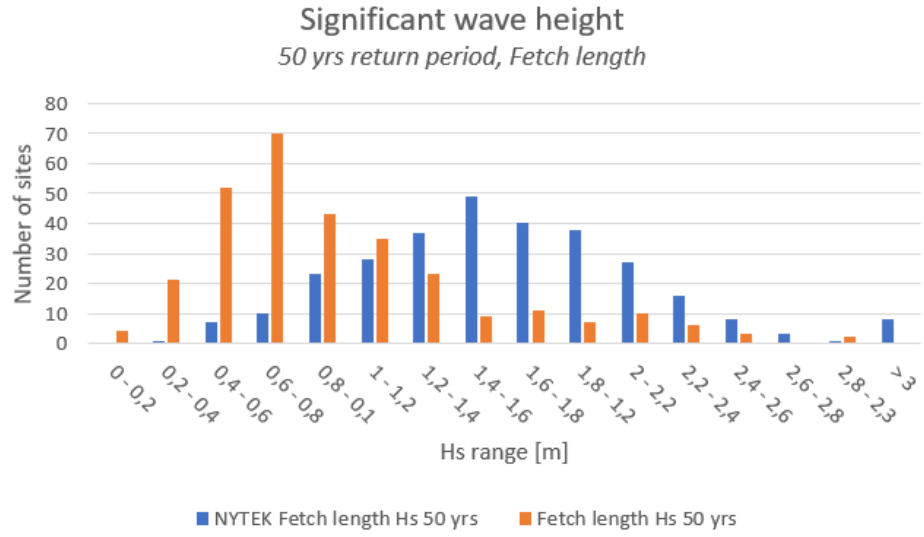

(b) Wind-induced $H_{s_{50yrs}}$ [m] at sites - fetch length analysis as given in NS9415:2009

Figure 6.8: Deviation between data sets when wind-wave methodology is evaluated.

et al., 2017 in general estimates lower wave heights than other comparative methods.

Mean wave height is larger for sites where SWAN was used compared to sites where fetch length analysis was used. Differences in mean wave heights may be caused by possible bias in estimation method or be simply due to the cause of exposure and site location. Figure 6.9 shows the distribution of wind-induced wave estimation methods based on region. Note the large differences in share of estimation methods among regions. Rogaland, Hordaland and Sogn og Fjordane are characterized by multiple long and narrow fjords. Exposure to open ocean areas are limited and fetch length analysis is widely used.

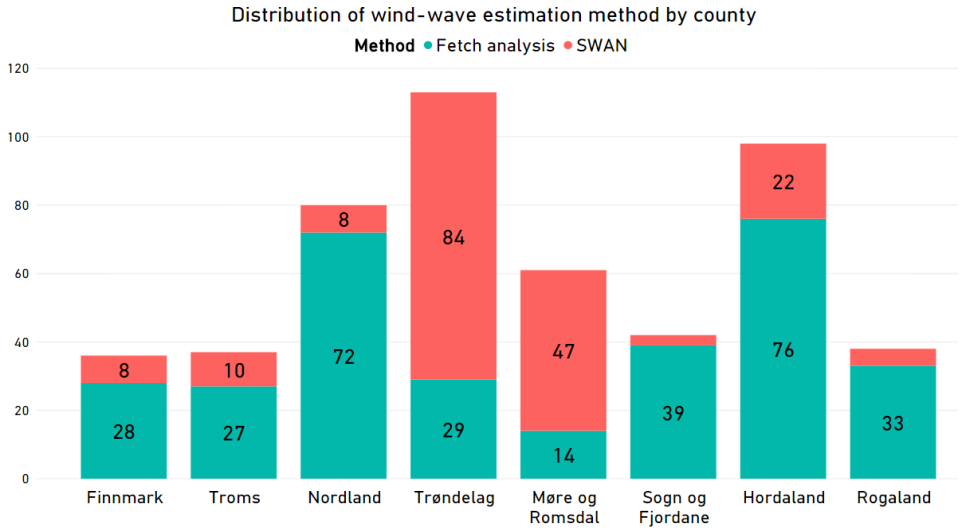

Figure 6.9: Distribution of wind-wave estimation method by county. Only sites where SWAN and fetch length analysis have been applied are included.

The converse is seen in Trøndelag and Møre og Romsdal. Only sites where fetch length and SWAN have been applied are shown because these are the preferred estimation methods. Figure 6.10 further shows the relative share of wind-induced wave exposure at these sites. It is seen that the relative share of sites classed as "High" to "Extreme" exposure are larger for Trøndelag and Møre og Romsdal than for Sogn og Fjordane and Hordaland. Here, sites are mainly located in archipelagos, near the Atlantic Ocean where swell is often present.

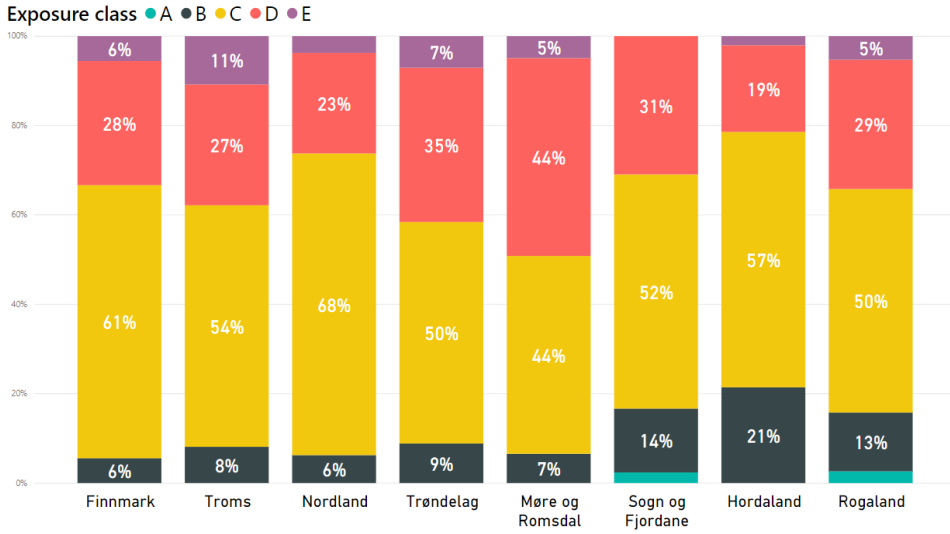

Figure 6.10: Share of exposure based on wind-induced wave heights reported in NYTEK. Only sites where SWAN and fetch length analysis have been used are included.

Figures 6.11 and 6.12, show locations where SWAN (green) and fetch length analysis (blue) have been used. Additional figures (B.9-B.10) of northern parts of Norway are found in appendix B.3. Within Nordland and Troms, which are counties without many protected fjord sites, fetch length analysis is widely used. Nevertheless, the share of sites within class C-E is still higher than for Sogn og Fjordane and Hordaland. Absence of swell could be the reason for why fetch length analysis is widely used in Nordland when exposure levels are relatively high. For the interested reader, a map showing all locations in Norway is found in appendix B, figure B.11.

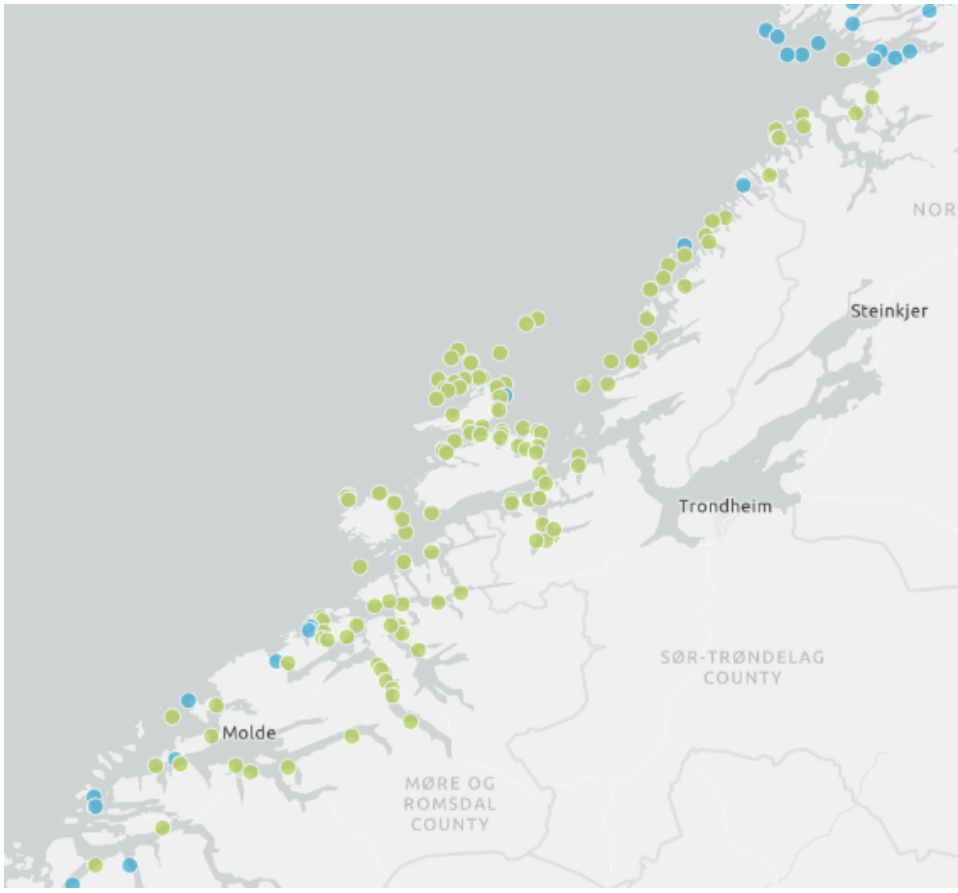

Figure 6.11: Locations in Trøndelag where SWAN (green) and fetch length (blue) have been used for wind-induced wave estimation.

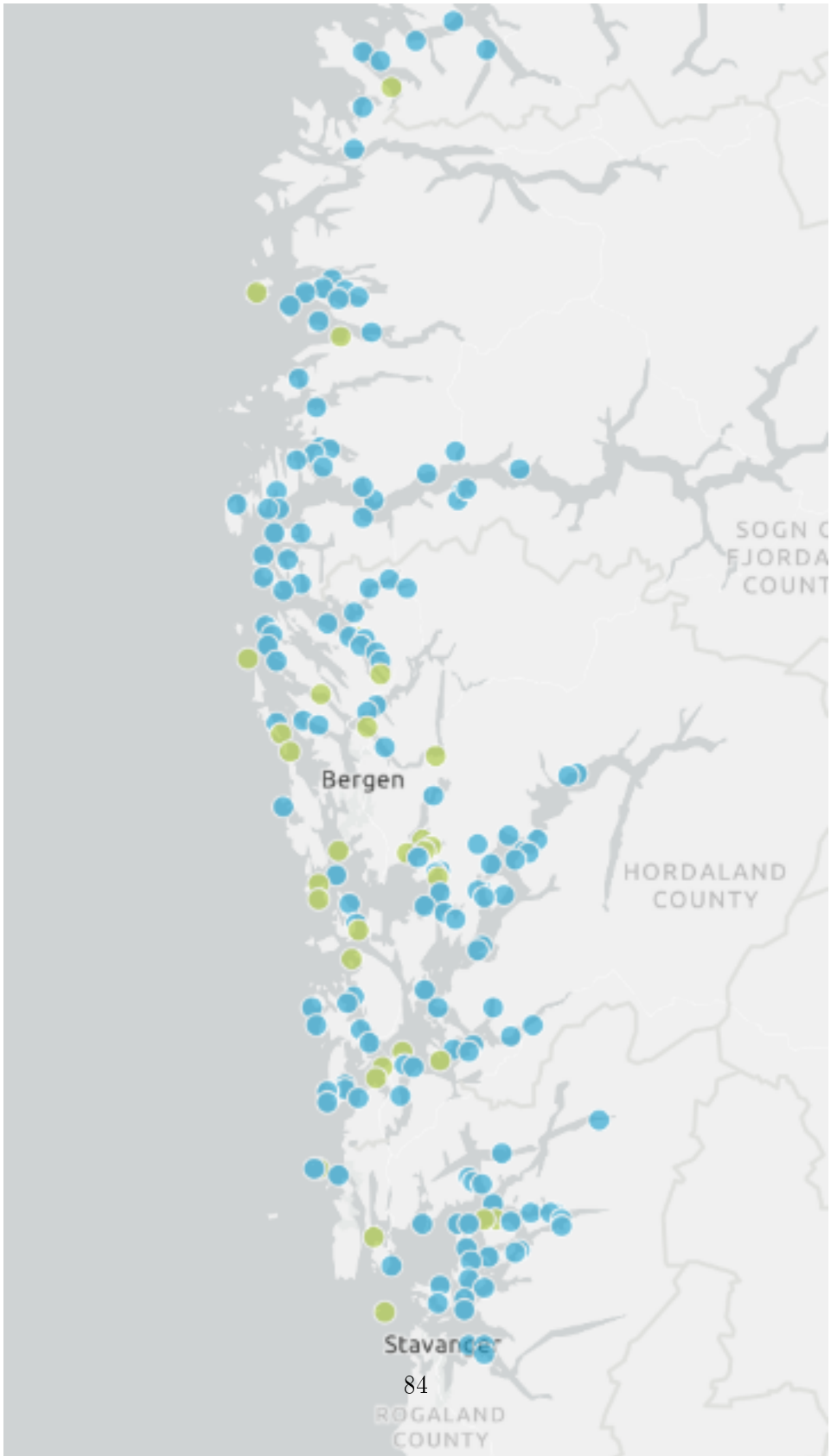

Figure 6.12: Locations in Vestlandet where SWAN (green) and fetch length

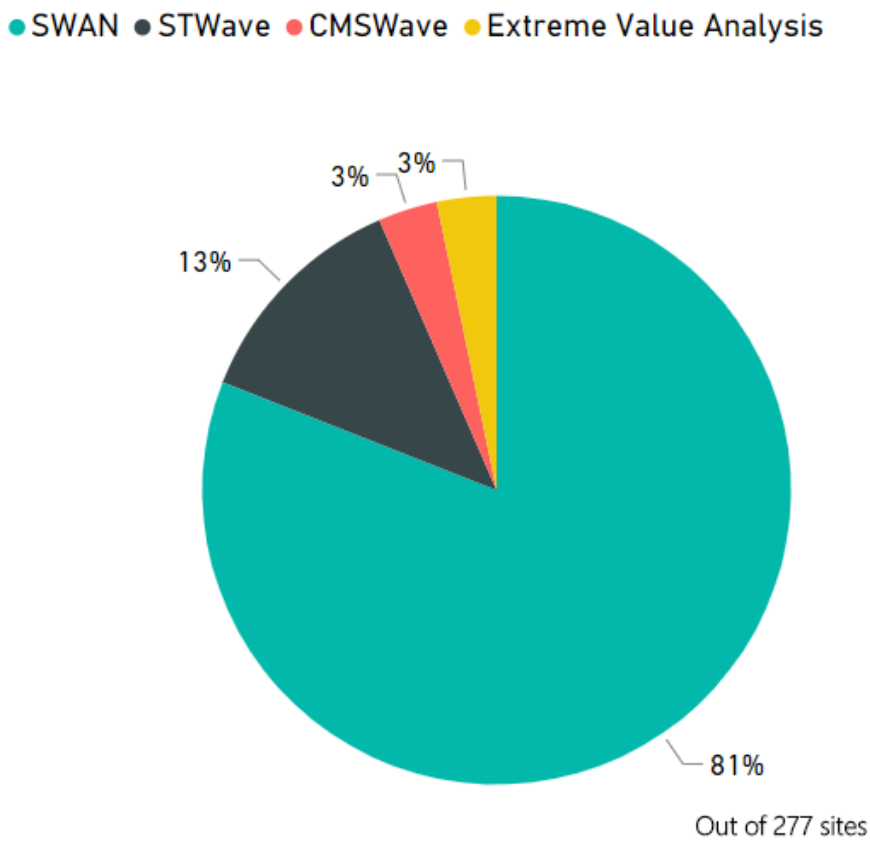

Figure 6.13: Share of estimation methods for swell.

6.1.4 Swell

During a conversation with one of the bodies providing site surveys (16th of May 2018), it was clear that the existence of swells influences selection of wave estimation methods. NS9415:2009 states that the existence of swell must be determined and documented. This is mainly done by assessing a site's exposure to open ocean and its surrounding topography. Swells are reported at 27 % of the sites in NYTEK data provided by the Directorate (nytek hoved1 - Tabulert med kategoriseringer.xlsx, Sheet: loadNYTEKres) and as for wind-induced waves, swell height and periods must be reported in the scheme.

Swell cannot be estimated by fetch length analysis, and software based on numerical approximations are widely used for this purpose, as seen in figure 6.13. If classifying the exposure distribution of swells by table 5.1, the majority of sites where swells are reported estimate swell heights to be less

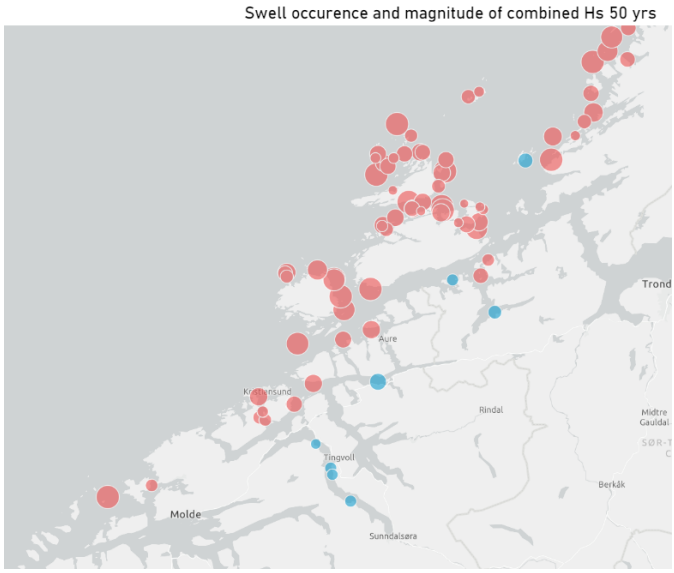

Figure 6.14: Localization of reported swell existence at sites in southern Trøndelag - red: occurring, blue: not occurring. Size of bubbles indicates magnitude of combined $Hs_{50yrs,combined}$

.

than 1 meter for 50 year return periods.

The combined wave height represents the expected wave conditions. In figure 6.15 the exposure of sites are classified by their combined wave heights. It is seen that as wave exposure increases, so too does the share of sites where swells are present.

Swells can be expected at sites exposed to open ocean areas, which are commonly characterized with higher waves. This is further exemplified in figure 6.14, where localization of swells at sites in southern Trøndelag is seen.

NS9415:2009 requires an inspection body to assess any occurrence of swells at a site. A possible approach to evaluate swell occurrence is to simulate waves using a numerical wave model. A member of an inspection body stated that their company in principal only performs numerical wave modelling, as this is the only method available for documenting swell to them (Inspection body, personal communication, May 22, 2018). Figure 6.17 gives an overview of presence and absence of swell at sites in Trøndelag. Only sites where SWAN, STWave and CMSWave have been applied are shown.

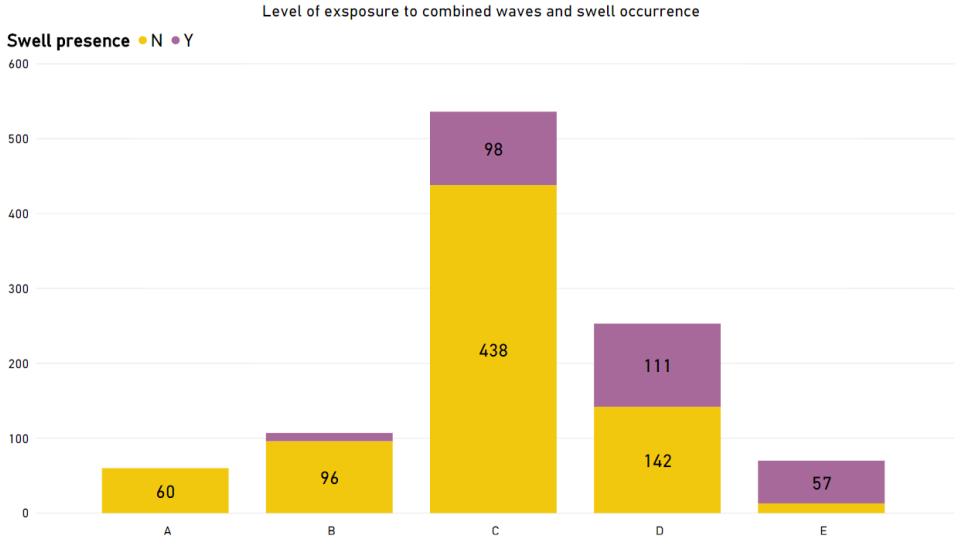

Figure 6.15: Distribution of swell existence by wave exposure $Hs_{50yrs,combined}$.

Figure 6.16: Methods for rejecting, confirming swell existence $Hs_{50,combined}$.

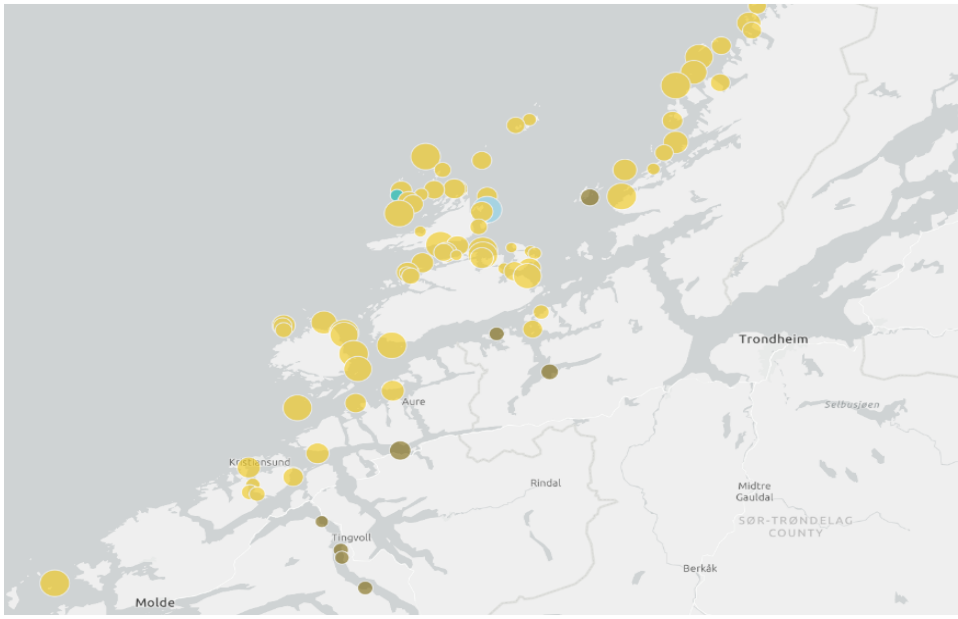

Figure 6.17: Presence and absence of swell at sites in Trøndelag. Size of bubbles indicate magnitude of $H_{s,50yrs,combined}$. Only sites where numerical wave models have been used are shown.

The number of sites in figure 6.16 and 6.15 are different. At some sites, it was not possible to distinguish the method used to evaluate the presence of swell. A member of an inspection body stated that the determination of swell existence was evaluated based on the inspector's experience, wind directions, assessment of the location by evaluating bathymetry and map information (Inspection body, personal communication, 15 May 2018). Thus, *the outcome of an assessment of swell existence highly relies on the decision-making process and thoroughness of available information.*

6.2 Corporate size and selection of wave estimation method

Numerical wave estimation methods are more extensive and require more time for analysis compared to fetch length analysis. *The inspection body can by law independently select the appropriate estimation method without interruption of its customer's requirements.* This is a main objective of the principle of independence, as stipulated in NYTEK §7 and presented in section 2.2.3. Prior to site survey, fish farmers source for price quotations from competitive inspection bodies and are free to select the inspection body offering site surveys at lowest price. Two inspection bodies stated in

conversations dated May 22, 2018 that fish farmers in practice may influence the extent and methodology of wave assessments based on price negotiation. This is hence the main motivation for investigating any possible relationship between company size and wave estimation methodology.

6.2.1 Classification of company size

We therefore decided to investigate any potential correlation between fish farm company size and selection of methodology for site survey. We first grouped companies into large, medium and small sizes. Definition of company size can be based on various other criteria, either single criterion or multiple criteria:

- Annual company revenue
- Number of employees
- Number of aquaculture licences
- Number of sites in operation

Aquaculture companies in Norway are required to report financial statements to the Register of Business Enterprises (The Brønnøysund Register Centre). The register provides legal and financial overview of sectors, by ensuring reliable information about business participants. Most information is public and can be retrieved either directly or through secondary sources.

www.proff.no is a search engine for corporate information in Norway, based on public information reported in the Register of Business Enterprises. Fiscal information from 2017 regarding aquaculture companies was found by using the search engine are given in table 6.4. Based on this information, aquaculture companies given in 6.5 were found to be largest.

Table 6.4: Parameters determining company size. All parameters can be expressed as total production capacity of a company.

Fiscal parameters	**Production parameters**
Operating Profit	Number of licences held by a company
EBITDA[1]	Number of sites operated by a company
	- Maximum allowed biomass (MAB) at sites
Assets	Number of licences affiliated sites
Employees	

Table 6.5: Five largest aquaculture companies based on operating profit and EBITDA (*Source: The Brønnøysund Register Centre via www.proff.no)*

Size	***Operating profit***	***EBITDA***
1	Marine Harvest AS *(13,2 bn NOK)*	Marine Harvest Norway AS *(4,6 bn NOK)*
2	Salmar Farming AS *(4,2 bn NOK)*	Salmar Farming AS *(1,6 bn NOK)*
3	Cermaq Norway AS *(3,3 bn NOK)*	Nordlaks Oppdrett AS *(1,12 bn NOK)*
4	Lerøy Midt AS *(2,9 bn NOK)*	Cermaq Norway AS *(0,9 bn NOK)*
5	Nordlaks Oppdrett AS *(2,7 bn NOK)*	Nova Sea AS *(0,9 bn NOK)*

Size	***Assets***	***Employees***
1	Marine Harvest Norway AS *(10,4 bn NOK)*	Marine Harvest Norway AS *(2287)*
2	Salmar Farming As *(5,3 bn NOK)*	Salmar Farming AS *(585)*
3	Nordlaks Oppdrett AS *(4,3 bn NOK)*	Cermaq Norway AS *(491)*
4	Cermaq Norway AS *(3,7 bn NOK)*	Lerøy Midt AS *(436)*
5	Lerøy Midt AS *(3,6 bn NOK)*	Lerøy Aurora AS *(403)*

Assets include many immediate factors determining production capacity. Information about production capacity was downloaded from the public Aquaculture register which is operated by the Directorate of Fisheries. Here, information about all Norwegian aquaculture licences can be found. One row in the registers' data set corresponds to one licence and multiple licenses are affiliated to a site. In figure 6.18, the parameters: number of employees, sites in operation and total production capacity based on the total number of licences held by a company, are shown for some of the largest fish farming companies. Marine Harvest Norway AS clearly stands out as the largest fish farming company in Norwegian waters, both in terms of financial and production parameters.

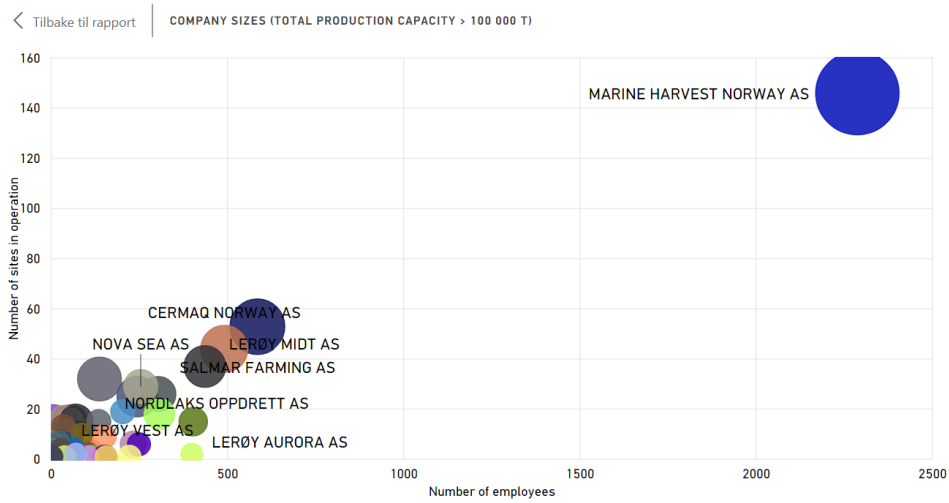

Figure 6.18: Distribution of companies based on number of employees and number of sites in operation. Sizes of bubbles are based on companies' total production capacity.

Business flow of wave estimation methods

Over the past 20 years development in Norwegian aquaculture business has been characterized by the consolidation of companies, as presented in section 2.1 and section 2.4 (see Aarset and Jakobsen, 2009; Bostock, 2011). *This is the main motivation to investigate any possible relationship between company size and site survey type.*

Companies are classified into groups based on their total production capacity and number of licences. Companies with total production capacity less than 10000 tonnes are not evaluated, excluding a total of 115 companies from analysis. The following classes are used to group companies:

- Large: Total production capacity $>$ 30000 tonnes
- Medium: 30000 metric tons $>$ Total production capacity $>$ 15000 metric tons
- Small: 15000 metric tons $>$ Total production capacity $>$ 10000 metric tons

Sankey charts are flow charts connecting two or more parameters and are used here to link information about fish farming company, inspection body performing site survey and the selected wave estimation method. Swells were not present at all sites, and we have chosen to focus only on wind-wave

estimation methods. Further, only fetch length analysis, SWAN, STWave and CMSWave were included.

Two observations can be made based on figure 6.21-6.19. First, there is no clear pattern between which inspection body a farmer select to use. *In all three cases, selection of inspection body seems quite random.* Both large, medium and small fish farming companies may use several inspection bodies for surveys.

The second observation is the differing share of methodology for wind-wave estimation between companies. 58% of estimations were done by SWAN for large companies, whereas this share is 29% and 23% for medium and small sized companies respectively. Site exposure could be a direct cause of this phenomena. Fiscal parameters could possibly influence a farmer's ability to operate more exposed and remote sites. Based on information provided in the questionnaire (see appendix B.2), survey-based numerical wave simulations take approximately 2-4 days, whereas the workload for fetch length analysis is approximately 1-2 days.

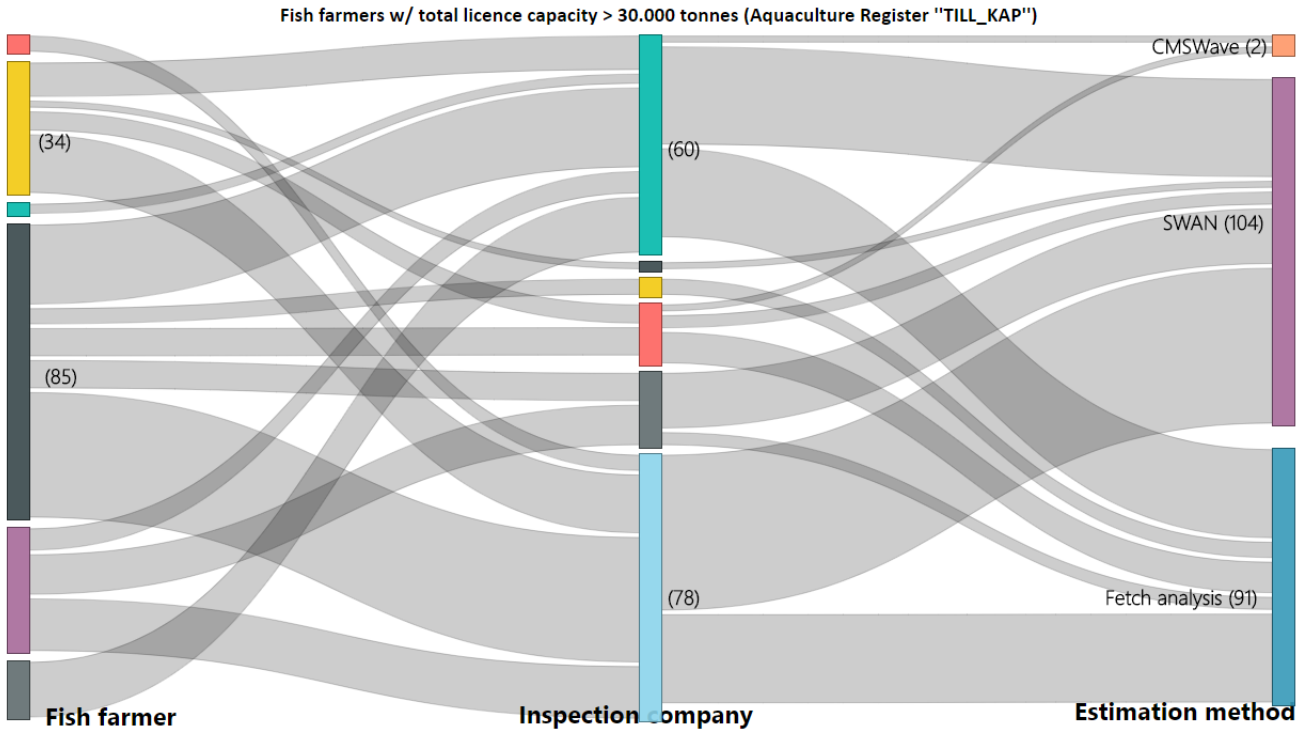

Figure 6.19: Business flow of wind-wave estimation methods for companies holding licences with total production capacities over 30000 tonnes.

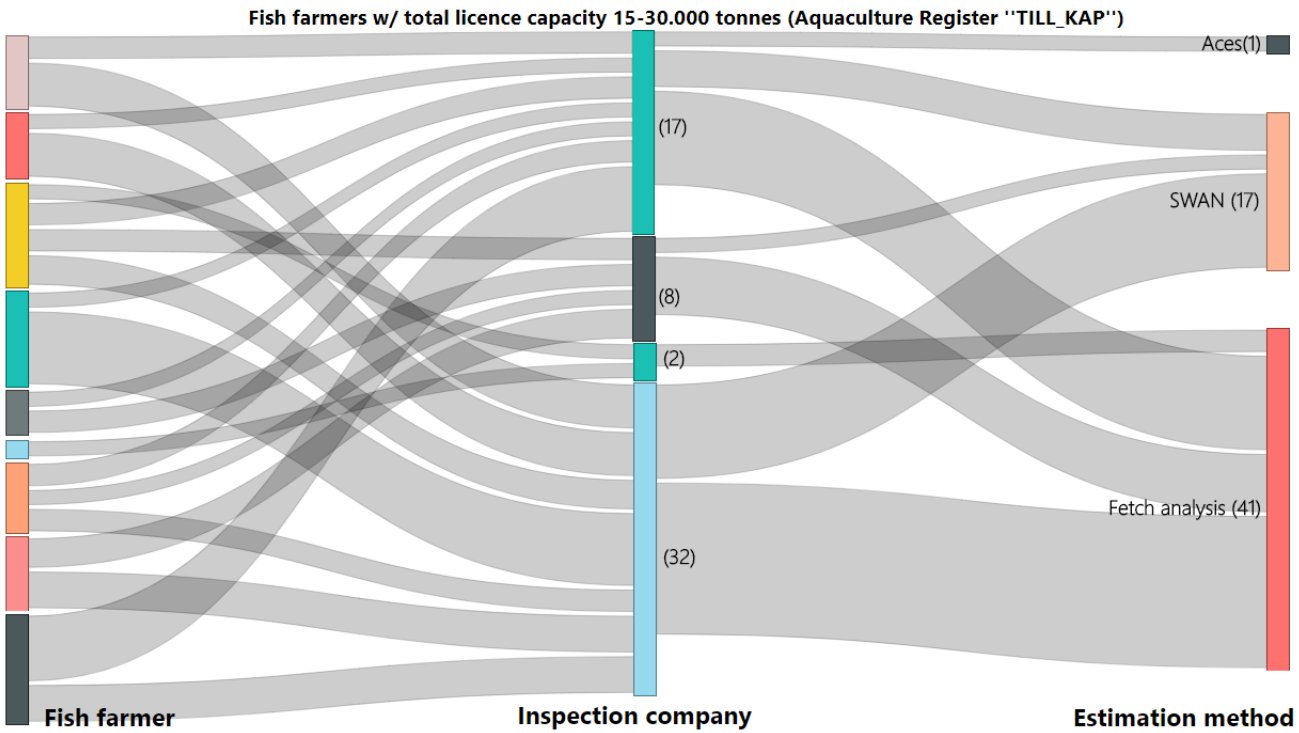

Figure 6.20: Business flow of wind-wave estimation methods for companies holding licences with total production capacities between 15000-30000 tonnes.

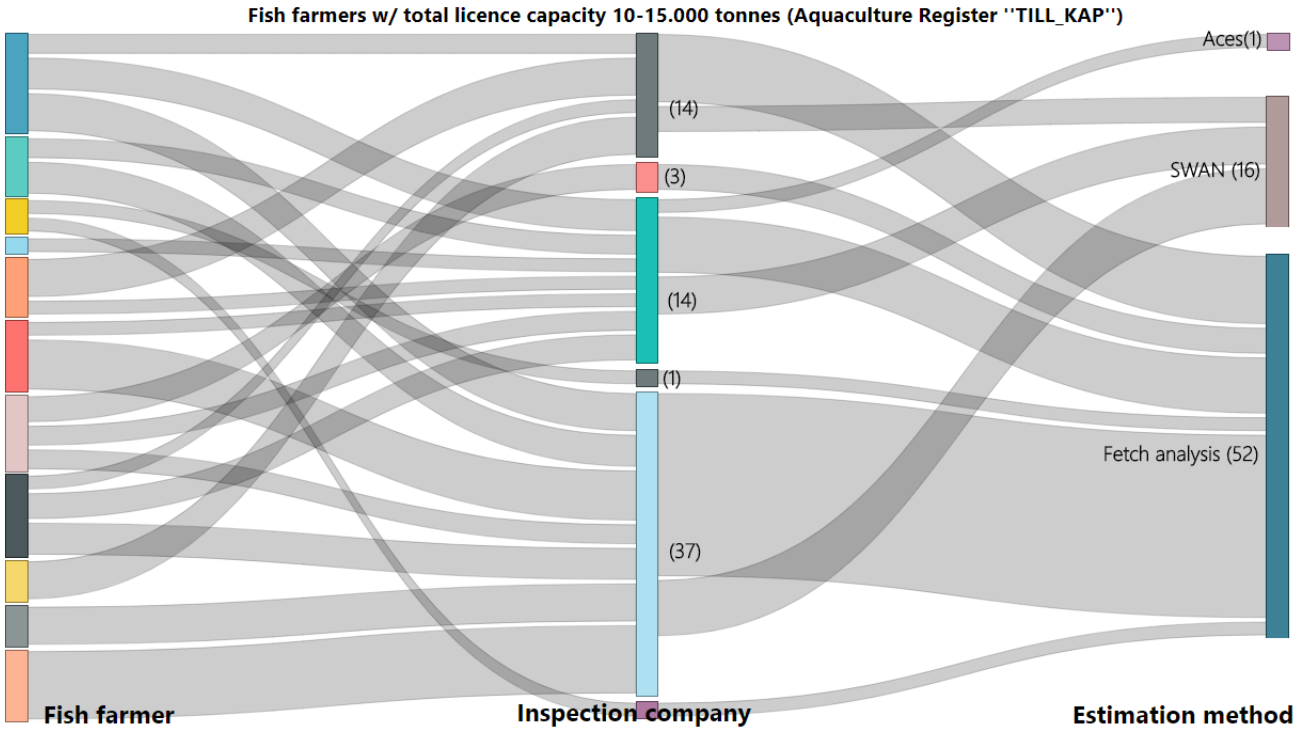

Figure 6.21: Business flow of wind-wave estimation methods for companies holding licences with total production capacities between 10000-15000 tonnes.

Wave conditions at exposed sites are frequently estimated by numerical methods, and this might suggest that fiscal parameters influence the selection of methodology for wave estimation and hence the thoroughness of site surveys. The distributions of fish farming company size and combined wave exposure level are shown in figures 6.22a and 6.22b. These figures also reflect the most representative exposure levels of sites operated by the companies. Additional figures (B.15b and B.15a) for Hs_{10yrs} can be found in the appendix B.3.

Exposure classes D and E (high and extreme) were present in 20% (43 sites), 19% (13 sites) and 15% (35 sites) for large, medium and small companies respectively. There were no significant differences between site exposure and fish farming company.

Figure 6.23 shows the degree of correlation between total production size and EBITDA. EBITDA (Earnings Before Interest, Taxes, Depreciation and Amortization) is a parameter describing the financial performance of a company. It takes into account debt and depreciation, associated with large investments and is thus commonly used to evaluate the financial standing of companies possessing significant manufacturing capital.

Figure 6.23 shows a positive correlation between the size total production capacity of a fish farming company and its financial performance. This suggests a possible relationship between the financial strength of fish farming companies and the specific wave estimation method selected for site surveys.

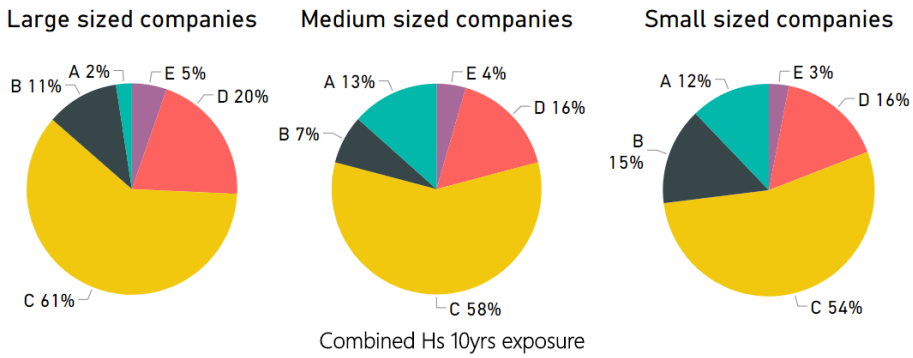

(a) Distribution of exposure level, $Hs_{10yrs \quad combined}$, and company size

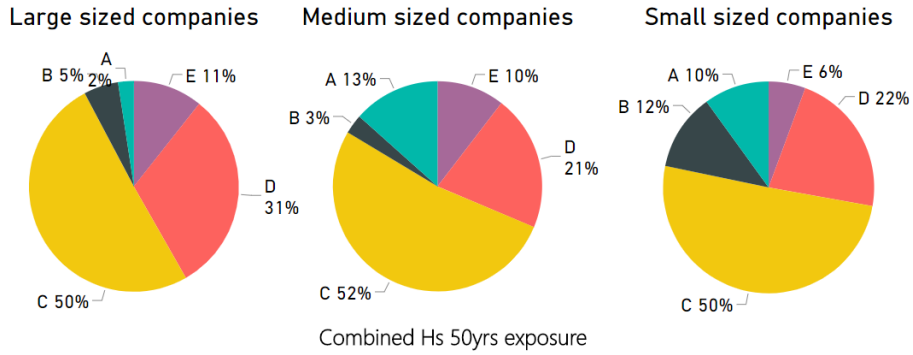

(b) Distribution of exposure level, $Hs_{50yrs \quad combined}$, and company size

Figure 6.22: Company sizes and site exposure with respect to combined waves (Hs_{50yrs} and Hs_{50yrs})

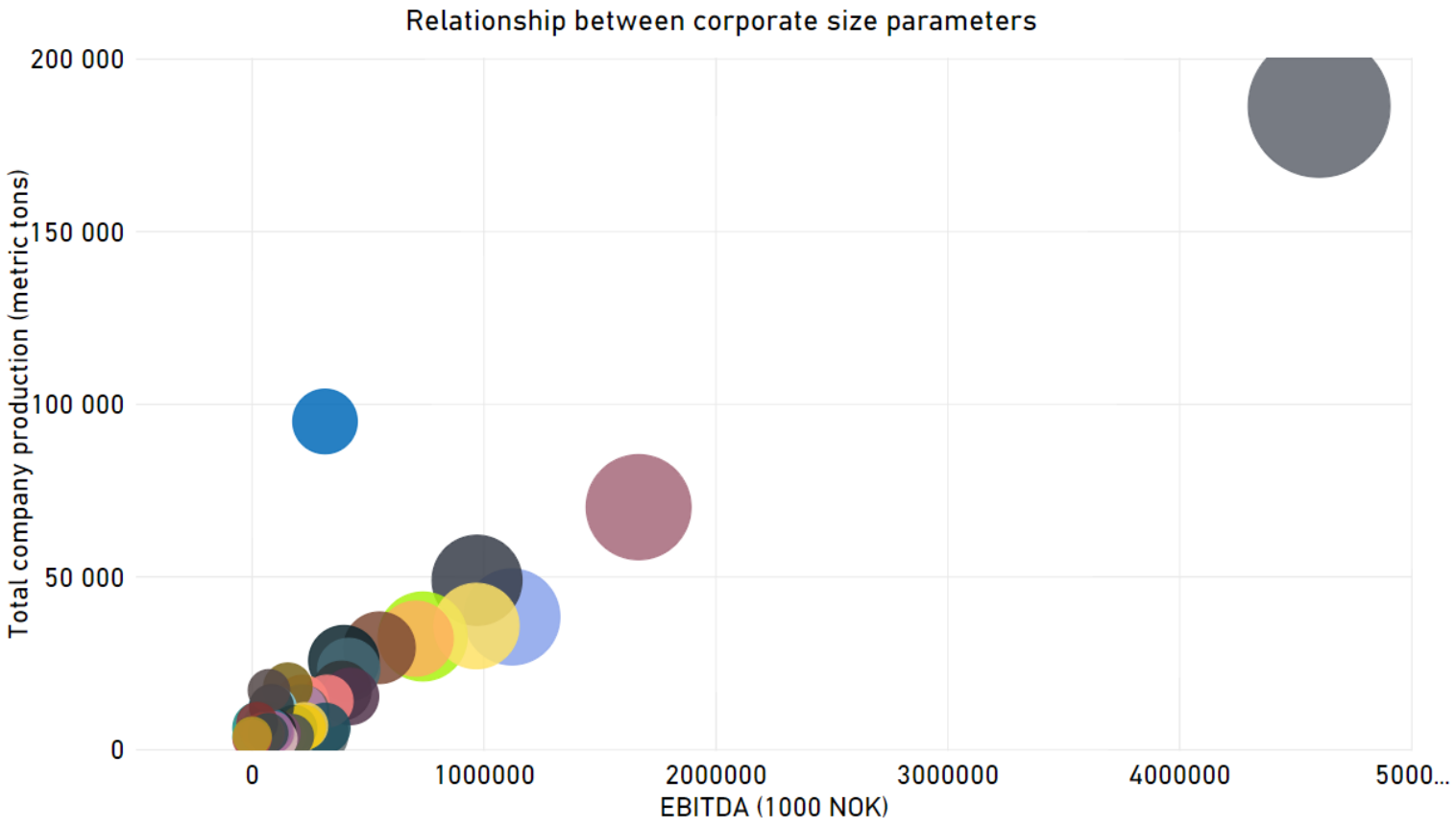

Figure 6.23: Relationship between production size and EBITDA of Norwegian fish farming companies. Only companies with annual total production over 10000 metric tons are included (*Source: Directorate of Fisheries, 2017 and The Brønnøysund Register Centre*)

Chapter 7

Discussion

7.1 Possible shortcomings and sources of error in data sets and analysis

Quantification of reported wave conditions at Norwegian aquaculture sites was done, and potential caveats with the analysis are discussed here.. The data concerning wave estimations in NYTEK scheme were obtained via poorly described methodologies, making potential errors related to subjective interpretation significant. Information about the wind-wave estimation method was not available for 53% of the sites in the original data set and have been excluded from many of the analyses. The results presented may only provide indications of the potential causes of variations in methodologies and weak patterns in decisions for wave estimation methods.

The grow-out phase of salmon is approximately 14-24 years. However, both business structure and the utilization of sites are temporally. Sources of data are (of course) not updated simultaneously, introducing challenges of comparing data sets from different sources.

Mapping out possible causes for variation in wave estimation methods is a complex task. There are numerous factors influencing an inspection body's decision for selection of methodology for wave estimations. These are related to location, availability of human sources and assets within the company, like knowledge, software and information about the site (Inspection bodies, 2018, personal communication, May).

Only companies with production capacity over 10000 metric tons are evaluated because these companies were thought to be of greatest importance. An expanded study could possibly include the historical development in number of companies and associated corporate size over the recent years to justify or reject the exclusion of very smallest fish farmers.

Wave condition assessments are dependent on inputs and the quality of input data will affect the quality of an analysis. In terms of standardized wave spectra, there are little information available about met-ocean conditions for near-shore regions. In the data received by the Directorate of Fisheries, no information about input data were available. This makes it

difficult to address effects of input data quality on variability in estimated wave conditions and any possible relations to localization.

The preliminary study presented in appendix A.5.4 was done as an attempt to evaluate spatial variation of wave conditions within an aquaculture site. There are many sources of error in full-scale measurements, and comprehensive work is needed to reveal and distinguish error from the wanted signal.

It is further bold to assume a one-to-one relationship between the dynamic response of the floating collar and the waves. Due to few, simple methodologies available for evaluating spatial variations of wave conditions, this assumption was nevertheless considered as a sufficient starting point for the objectives. Despite no clear findings at present time, the wave energy measurements does not reject that spatial variations in wave conditions within a site are insignificant. This can motivate for an evaluation of the importance of spatial distribution of waves at aquaculture sites and possibilities for including this in the site survey for new structures.

7.2 Consequences of the findings

New concepts and cages for fish farming will have different wave dynamic characteristics compared to the floating collar net pens widely used today. This makes it necessary to assess the reliability of presently available methodologies for site surveys . This could be done by further assessment of the spatial variations of wave conditions within aquaculture sites. As stated in section 2.4.2, there is a trend towards larger production units at aquaculture sites, which can result in larger environmental consequences of accidents. It is therefore important to lower the risk of accidents by implementing precautionary actions in the design and operation of fish farms.

Regulations and standards from offshore petroleum production could serve as a basis for the development of an legislative framework that safeguards both the environment and assets in future aquaculture activities. In conjunction with the main focus on technical development in aquaculture installations, revealing risks related to new and unproven solutions is important as well. This will entail comprehensive collection of met-ocean data and increasing the knowledge of met-ocean estimations in both near-shore and offshore regions.

NS9415:2009 does not stringently define the methodologies for estimations of met-ocean conditions. Its deficient descriptions of presenting met-ocean conditions have been addressed in several research papers (Arntsen et al., 2018; Bore and Amdahl, 2017; D. Kristiansen et al., 2017). None of the methodologies presented are ideal, making it necessary for the inspection body to select wave estimation method based on several factors. The

resulting wave conditions are dependent on the methodology applied and its input data, boundary conditions and assumptions.

There may be several causes of the differences between wave estimation methods of small and large companies. Selection of inspection body by the fish farmer may be influenced by available financial capital. This could be a possible cause for the pattern in share of wave estimation methods and may affect the principle of independence, as discussed in section 2.2.3. Another possible cause could be the degree of exposed and sheltered sites distributed between large and small fish farming companies. However, the distribution in site exposure level was not significantly uneven.

The findings presented here imply correlation between fish farming company size and methodology applied for wave estimation. A fish farmer is allowed open tender for inspection bodies and is therefore allowed to, in practice, choose the extent of the site survey. The relationship between fish farming company, its financial capability and methodology for wave estimation thus may be an infringement of the principle of independent inspection bodies as stipulated in NYTEK §7.

Chapter 8

Concluding remarks and further work

Advances in aquaculture have led to a need for evaluating and renewing legislation and technical standards comprising aquaculture installations. Wave conditions at Norwegian aquaculture sites have been studied by analyzing reported methodologies applied in site surveys. The new, emerging concepts for ocean based fish farming raise a need for evaluating present methodologies and requirements of site surveys.

Statutory site surveys in Norwegian waters include wave estimations at aquaculture sites based on NS9415:2009, where met-ocean conditions are reported to the authorities in the NYTEK scheme. Wave conditions provided in the NYTEK scheme are analyzed and possible influences among stakeholders based on wave estimation methods have been investigated. The main findings are as follows:

- Fetch analysis is the most applied wind-wave estimation method (32%), followed by the numerical wave model SWAN (18%)
- There are large geographical variations in the wind-wave estimation methods applied: Trøndelag and Møre og Romsdal deviate from other regions by having a large majority of sites where SWAN has been applied
- Comparative analysis of an independent data set indicates that SWAN gives larger resulting wave heights than fetch length analysis
- Numerical wave models are mainly used at sites operated by large sized fish farming companies
- Fetch length analysis is mainly used by small/ medium sized companies

The quality of site surveys vary, and methods may not cover spatial variations in wave conditions within a site sufficiently. Input-data for wave estimations are not documented in the NYTEK scheme. Effects of input-data quality in the resulting wave conditions and scope of wave assessments

should be further investigated. The preliminary findings of possible spatial deviations of wave energy content within the Hosenøyan site further reinforce these points.

The findings thus contribute to a platform for further evaluation of the legal framework governing aquaculture installations, reliability of site surveys in Norwegian aquaculture, documentation requirements, and spatial assessment of wave conditions at aquaculture sites.

Bibliography

Aarset, B., & Jakobsen, S.-E. (2009). Political regulation and radical institutional change: The case of aquaculture in norway. *Marine Policy*, *33*(2), 280–287.

AKVA Group AS. (2015). *AKVA Group Cage Models*. Retrieved November 9, 2017, from http://www.akvagroup.com/products/cage-farming-aquaculture/plastic-cages/cage-models

Akvakulturloven. (2006). *Lov om akvakultur (E: Aquaculture Act)*. Regulation. Nærings- og fiskeridepartementet. Retrieved from https://lovdata.no/dokument/NL/lov/2005-06-17-79

Altosole, M., Benvenuto, G., Figari, M., & Campora, U. (2009). Real-time simulation of a cogag naval ship propulsion system. *Journal of Engineering for The Maritime Environment*, *223*, 47–62. Figure.

Arntsen, M., Borge, J., Strømmesen, O.-H., & Hansen, E. (2018). *OMAE2018-77769: The effect of temporal length of current measurements on the derived design level*.

Asche, F., Roll, K. H., & Tveterås, R. (2012). FOU, innovasjon og produktivitetsvekst i havbruk ; historisk utvikling og strategier for fremtiden. *Magma*, *15*(1), 23–31. Retrieved March 30, 2018, from https://www.magma.no/fou-innovasjon-og-produktivitetsvekst-i-havbruk

Barbariol, F., Benetazzo, A., Carniel, S., & Sclavo, M. (2015). Space-time wave extremes: The role of metocean forcings. *Journal of Physical Oceanography*, *45*(7), 1897–1916. Retrieved May 30, 2018, from http://search.proquest.com/docview/1701482008/

Bi, C.-W., Zhao, Y.-P., Dong, G.-H., Zheng, Y.-N., & Gui, F.-K. (2014). A numerical analysis on the hydrodynamic characteristics of net cages using coupled fluid–structure interaction model. *Aquacultural Engineering*, *59*(Supplement C), 1–12. doi:https://doi.org/10.1016/j.aquaeng.2014.01.002

Bitner-Gregersen, E. M. (2015). Joint met-ocean description for design and operations of marine structures. *Applied Ocean Research*, *51*, 279–292. doi:10.1016/j.apor.2015.01.007

Bitner-Gregersen, E. M., Bhattacharya, S. K., Chatjigeorgiou, I. K., Eames, I., Ellermann, K., Ewans, K., ... Waseda, T. (2014). Recent developments of ocean environmental description with focus on uncertainties. *Ocean Engineering*, *86*. doi:10.1016/j.oceaneng.2014.03.002

Bjelland, H. V., Føre, M., Lader, P., Kristiansen, D., Holmen, I. M., Fredheim, A., ... Schjølberg, I. (2015). Exposed aquaculture in norway: Technologies for robust operations in rough conditions. In *Oceans 2015 - mts/ieee washington* (pp. 1–10). doi:10.23919/OCEANS.2015.7404486

Booij; R. H. (1999). A third-generation wave model for coastal regions: 2. verification. *Journal of Geophysical Research: Oceans*, *104*(C4), 7667–7681.

Booij, N., Holthuijsen, L., & Battjes, J. (2001). Ocean to near-shore wave modelling with swan. In *Coastal dynamics 2001* (pp. 335–344). American Society of Civil Engineers (ASCE).

Bore, P. T., & Amdahl, J. (2017). OMAE2017-61413: Determination of environmental conditions relevant for the ultimate limit state at an exposed aquaculture location. In *36th international conference on ocean, offshore and arctic engineering (OMAE2017)*, June 20, 2017. The American Society of Mechanical Engineers. doi:10.1115/omae2017-61413

Bostock, J. (2011). The application of science and technology development in shaping current and future aquaculture production systems. *The Journal of Agricultural Science*, *149*(S1), 133–141.

Braithwaite, J. (2008). Regulatory capitalism; how it works, ideas for making it work better. *Reference and Research Book News*, *23*(3). Retrieved from http://search.proquest.com/docview/199628063/?pq-origsite=primo

Browne, M., Castelle, B., Strauss, D., Tomlinson, R., Blumenstein, M., & Lane, C. (2007). Near-shore swell estimation from a global wind-wave model: Spectral process, linear, and artificial neural network models. *Coastal Engineering*, *54*(5), 445–460. doi:https://doi.org/10.1016/j.coastaleng.2006.11.007

Chakrabarti, S. K. (2002). *The theory and practice of hydrodynamics and vibration* (W. Scientific, Ed.). Advanced series on ocean engineering. River Edge, N.J: World Scientific.

Cimbala, Y. A. C. J. M. (2014). *Fluid mechanics - fundamentals and applications* (3rd ed.). Mc Graw-Hill Education.

Directorate of Fisheries. (2011, February). *Delegasjon av myndighet etter akvakulturloven*. Retrieved February 20, 2018, from https://www.fiskeridir.no/Akvakultur/Akvakulturloven-og-forskrifter

Directorate of Fisheries. (2015). *Kategorisering av 109 innmeldte rømningshendelser i 2015*. Retrieved November 14, 2017, from https://www.fiskeridir.no/Akvakultur/Statistikk-akvakultur/Roemmingsstatistikk

Directorate of Fisheries. (2017). *Key figures from aquaculture industry 2016*. Retrieved November 30, 2017, from https://www.fiskeridir.no/Akvakultur/Statistikk-akvakultur/Statistiske-publikasjoner/Noekkeltall-for-norsk-havbruksnaering

Directorate of Fisheries. (2018a). *Oversikt over søknader om utviklingstillatelser*. Retrieved May 15, 2018, from https://www.fiskeridir.no/Akvakultur/Tildeling-og-tillatelser/Saertillatelser/Utviklingstillatelser/Soekere-antall-og-biomasse

Directorate of Fisheries. (2018b). *Statistics for aquaculture - Atlantic salmon and rainbow trout*: Number of licenses per 31.12 1994-2017. number of sites in sea water 2006-2017. number of companies and licenses with grow out production 1994-2016. Retrieved February 20, 2018, from https://www.fiskeridir.no/English/Aquaculture/Statistics/Atlantic-salmon-and-rainbow-trout

DNV-GL. (2017a). *DNVGL-RP-C205: Environmental condritions and environmental loads, recommended practice*. DNV-GL. DNV-GL. Retrieved October 17, 2017, from https://rules.dnvgl.com/docs/pdf/DNVGL/RP/2017-08/DNVGL-RP-C205.pdf?utm_campaign=&utm_medium=email&utm_source=Eloqua

DNV-GL. (2017b). *DNVGL-RU-OU-0503: Offshore fish farming units and installations*. https://rules.dnvgl.com/docs/pdf/dnvgl/ru-ou/2017-07/DNVGL-RU-OU-0503.pdf. [https://rules.dnvgl.com/docs/pdf/dnvgl/ru-ou/2017-07/DNVGL-RU-OU-0503.pdf] (25th Dec 2017). DNV-GL. Retrieved May 22, 2018, from https://rules.dnvgl.com/docs/pdf/dnvgl/ru-ou/2017-07/DNVGL-RU-OU-0503.pdf

Engebretsen, E. A. (2012). Wave conditions for offshore wind turbine foundations in intermediate water depths. Master thesis. Institutt for marin teknikk, Norwegian University of Science and Technology. Retrieved from http://hdl.handle.net/11250/238204

EY. (2016, May 17). *The Norwegian Aquaculture Analysis 2016*. EY. Retrieved March 1, 2018, from http://www.ey.com/Publication/vwLUAssets/EY_The_Norwegian_Aquaculture_Analysis/

Faltinsen, O. (1990). *Sea loads on ships and offshore structures*. Cambridge Ocean Technology. Cambridge University Press.

Forristall, G. (2011). OMAE2011-49837: Maximum crest heights under a model tlp deck. In *Proceedings of the international conference on offshore mechanics and arctic engineering - OMAE2011* (Vol. 2, pp. 571–577). The American Society of Mechanical Engineers.

Fossen, T. I. (2011). *Handbook of marine craft hydrodynamics and motion control* (Wiley, Ed.). Wiley.

Fredheim, A., & Langan, R. (2009). Advances in technology for off-shore and open ocean finfish aquaculture. In *New technologies in aquaculture: Improving production efficiency, quality and environmental management* (pp. 914–944).

Hardesty, L. (2010). *Explained: Linear and nonlinear systems*. Retrieved March 2, 2018, from http://news.mit.edu/2010/explained-linear-0226

Harris, F. J. (1978). On the use of windows for harmonic analysis with the discrete fourier transform. *Proceedings of the IEEE*, *66*(1), 51–83. doi:10.1109/PROC.1978.10837

Hasselman; Barnett; Bouws, H., Carlson. (1973). *Measurements of wind-wave growth and swell decay during the joint North Sea wave project (JONSWAP)* (D. H. Institut, Ed.). Ergänzungsheft zur deutschen hydrographischen Zeitschrift. Reihe A. Hamburg: Deutsches Hydrographisches Institut.

Hasselmann, S., Hasselmann, K., Bauer, E., Janssen, P., Komen, G., Bertotti, L., ... A. Ewing, J. (1988). The wam model - a third generation ocean wave prediction model. *Journal of Physical Oceanography*, *18*, 1775–1810.

Haver, S. (2017). *Metocean modelling and prediction of extremes*. Lecture notes in *TMR4195 - Design of Offshore Structures*. Department of Marine Technology, Norwegian University of Science and Technology.

Holthuijsen, L. H. (2007). *Waves in oceanic and coastal waters*. Cambridge: Cambridge University Press.

Hovem, J. M. (2012). *Marine acoustics : The physics of sound in underwater environments*. Los Altos Hills, Calif: Peninsula Publishing.

International Organization for Standardization. (2009). *ISO 19901-6:2009 Petroleum and natural gas industries - Specific requirements for offshore structures - Part 6: Marine operations*. International Organization for Standardization. Retrieved November 15, 2017, from http://www.standard.no/no/Nettbutikk/produktkatalogen/Produktpresentasjon/?ProductID=520410

International Organization for Standardization. (2015). *NS-EN ISO 19901-1:2015 Petroleum and natural gas industries - Specific requirements for offshore structures - Part 1: Metocean design and operating considerations*. Standard Norway. International Organization for Standardization, Geneva, CH. Retrieved March 15, 2018, from https://www.standard.no/no/Nettbutikk/produktkatalogen/Produktpresentasjon/?ProductID=800599

International Organization for Standardization. (2016). *NS-EN ISO 17776:2016 - Petroleum and natural gas industries - Offshore production installations - Major accident hazard management during the design of new installations*. Standard Norway. International Organization for Standardization, Geneva, CH. Retrieved March 22, 2018, from http://www.standard.no/no/Nettbutikk/produktkatalogen/Produktpresentasjon/?ProductID=881512

Jia, H., Moan, T., & Jensen, Ø. (2012). Coupled hydrodynamic analysis between gravity cage and well boat in operation. *Proceedings of the International Offshore and Polar Engineering Conference*, 1055–1062.

Jonathan, P., Ewans, K., & Forristall, G. (2008). Statistical estimation of extreme ocean environments: The requirement for modelling directionality and other covariate effects. *Ocean Engineering*, *35*(11), 1211–1225.

Klebert, P., Lader, P., Gansel, L., & Oppedal, F. (2013). Hydrodynamic interactions on net panel and aquaculture fish cages: A review. *Ocean Engineering*, *58*.

Kristiansen, D., Aksnes, V., Su, B., Lader, P., & V. Bjelland, H. (2017). OMAE2017-61531: Environmental Description in the Design of Fish Farms at Exposed Locations. In *36th international conference on ocean, offshore and arctic engineering (OMAE2017)*, June 19, 2017. The American Society of Mechanical Engineers. doi:10.1115/omae2017-61531

Kristiansen, & Faltinsen. (2015). Experimental and numerical study of an aquaculture net cage with floater in waves and current. *Journal of Fluids and Structures*, *54*(100), 1–26.

Lader, P., Dempster, T., Fredheim, A., & Jensen, Ø. (2008). Current induced net deformations in full-scale sea-cages for atlantic salmon (salmo salar). *Aquacultural Engineering*, *38*(1), 52–65.

Lader, Kristiansen, Alver, Bjelland, & Myrhaug. (2017). OMAE2017-61659: Classification of Aquaculture Locations in Norway with Respect to Wind Wave Exposure. In *36th international conference on ocean, offshore and arctic engineering (OMAE2017)*. The American Society of Mechanical Engineers. doi:10.1115/omae2017-61659

Lai, E. (2004). *Practical digital signal processing*. Elsevier Science.

Laksetildelingsforskriften. (2015). *Forskrift om tillatelse til akvakultur for laks, ørret og regnbueørret (laksetildelingsforskriften)*. Regulation. Ministry of Trade, Industry and Fisheries. Retrieved from https://lovdata.no/forskrift/2004-12-22-1798/%C2%A78

LeBlond, P. H. (1978). *Waves in the ocean*. Elsevier oceanography series. Amsterdam: Elsevier.

Levi-Faur, D. (2005). The global diffusion of regulatory capitalism. *Annals Of The American Academy Of Political And Social Science*, *598*, 12–32.

Li, P. (2017). *A theoretical and experimental study of wave-induced hydroelastic response of a circular floating collar* (Doctoral dissertation, Norwegian University of Science and Technology).

Lin, L., Demirbilek, Z., Mase, H., Zheng, J., & Yamada, F. (2008). *Cms-wave: A nearshore spectral wave processes model for coastal inlets and navigation projects*. U.S. Army Corps of Engineers Waterways Experiment Station (USACE-WES).

Ministry of Petroleum and Energy,Ministry of Trade, Industry and Fisheries. (2017). *Regjeringens havstrategi - ny vekst, stolt historie (eng: The maritime strategy of the government of norway- new growth, proud*

history). Retrieved January 24, 2018, from https://www.regjeringen.no/no/dokumenter/ny-vekst-stolt-historie/id2552578/

Ministry of Trade, Industry and Fisheries. (2005). *Technical requirements for fish farming installations*. Norwegian Ministry of Fisheries and Coastal Affairs. Retrieved January 31, 2018, from https://www.regjeringen.no/globalassets/upload/kilde/fkd/bro/2005/0013/ddd/pdfv/255320-technical_requirements.pdf

Ministry of Trade, Industry and Fisheries. (2017, March). *Strategi mot rømming fra akvakultur*. Retrieved October 18, 2017, from https://www.regjeringen.no/contentassets/9dca61fe798145ea89e83b8981bc46cc/w-0017_strategi-mot-romming-fra-akvakultur.pdf

Moe, H., Olsen, A., Hopperstad, O. S., Jensen, Ø., & Fredheim, A. (2007). Tensile properties for netting materials used in aquaculture net cages. *Aquacultural Engineering*, *37*(3), 252–265. doi:https://doi.org/10.1016/j.aquaeng.2007.08.001

Myrhaug, D. (2005). *Tmr4235 stochastic Theory of Sea Loads - Statistics of Narrow Band Processes and Equivalent Linearization*. Institutt for marin teknikk, Fakultet for Ingeniørvitenskap og Teknologi, NTNU. Trondheim, Norway.

Myrhaug, D. (2007). *Tmr4180 Marin Dynamikk - Uregelmessig sjø*. Institutt for marin teknikk, Fakultet for Ingeniørvitenskap og Teknologi, NTNU. Trondheim, Norway.

Næss, & Moan. (2005). Chapter 5 - Probabilistic Design of Offshore Structures. In S. K. Chakrabarti (Ed.), *Handbook of offshore engineering* (pp. 197–277). London: Elsevier. Retrieved from https://www.sciencedirect.com/science/article/pii/B9780080443812500084

Newland, D. E. (2005). *An introduction to random vibrations, spectral & wavelet analysis* (3rd ed.). Mineola, N.Y: Dover.

Newman, J. N. (1977). The motions of a floating slender torus. *Journal of Fluid Mechanics*, *83*(4), 721–735. doi:10.1017/S0022112077001426

Nistov, Nylund, Opedal, Boe, Halle, Onsum, ... Rebo. (2016). *Prosjekt NORSOK-analyse: NORSOK-eiernes anbefalinger vedrørende ressursinnsats og prioriteringer for videre arbeid med NORSOK-standardene*. Retrieved November 22, 2017, from https://www.norskoljeoggass.no/Global/2016%20dokumenter/Rapport%20NORSOK%20analyse.pdf

Norwegian Food Safety Authority. (2017). *Fiskevelferd (E: Fish welfare)*. Retrieved October 4, 2017, from https://www.mattilsynet.no/fisk_og_akvakultur/fiskevelferd/

NYTEK-forskriften. (2015). *Forskrift om krav til teknisk standard for flytende akvakulturanlegg (NYTEK-forskriften) (E: Regulation on technical standards for floating aquaculture plants (NYTEK Regulation))*. Ministry of Trade, Industry and Fisheries. Kingdom of Norway. Re-

trieved May 9, 2018, from https://lovdata.no/dokument/SF/forskrift/2011-08-16-849

Ochi. (2005). *Ocean waves: The stochastic approach*. Cambridge ocean technology series. Cambridge, U.K: Cambridge University Press.

Olafsen, T., Winther, U., Olsen, Y., & Skjermo, J. (2012). *Verdiskaping basert paa produktive hav i 2050*. Retrieved October 1, 2017, from http://www.sintef.no/globalassets/upload/fiskeri_og_havbruk/publikasjoner/verdiskaping-basert-pa-produktive-hav-i-2050.pdf

Patel, M. H. (1989). *Dynamics of offshore structures*. London: Butterworths.

Pierson, W. J., & Moskowitz, L. (1964). A proposed spectral form for fully developed wind seas based on the similarity theory of s. a. kitaigorodskii. *Journal of Geophysical Research*, *69*(24), 5181–5190. doi:10.1029/JZ069i024p05181

Salmar ASA. (2017). *OFFSHORE FISH FARMING - A new era in fish farming is on its way*. Salmar ASA. Retrieved February 15, 2018, from https://www.salmar.no/en/offshore-fish-farming-a-new-era/

Samsing, F., Solstorm, D., Oppedal, F., Solstorm, F., & Dempster, T. (2015). Gone with the flow: Current velocities mediate parasitic infestation of an aquatic host. *International Journal for Parasitology*, *45*(8), 559–565. doi:https://doi.org/10.1016/j.ijpara.2015.03.006

Shen, Greco, & Faltinsen. (2016). Simulations of well boats at fish farms in waves and current. In *The 12th international conference on hydrodynamics*, September 19, 2016. The 12th International Conference on Hydrodynamics, 18 – 23 september 2016, Egmond aan Zee, The Netherlands, Egmond aan Zee, The Netherlands.

Shore protection manual: Volume I and II. (1984, January 1). *Shore protection manual: Volume i and ii*.

Standard Norway. (2016). *NS 9415.E:2009 - Marine fish farms - Requirements for site survey, risk analyses, design, dimensioning, production, installation and operation*. Standard Norway. [http://www.standard.no/no/Nettbutik Standard Norway. Standard Norway.

Statistics Norway. (2017). *Another record high for salmon*. Retrieved October 25, 2017, from https://www.ssb.no/en/jord-skog-jakt-og-fiskeri/artikler-og-publikasjoner/another-record-high-for-salmon

Stefanakos, C., & Eidnes, G. (2014). Transferring wave conditions from offshore to nearshore: The case of nordfold. *International Conference on Offshore Mechanics and Arctic Engineering*, *4*.

Store norske leksikon. (2014). *Lineær Algebra (E: Linear Algebra)*. Retrieved March 2, 2018, from https://snl.no/line%C3%A6r_algebra

Store norske leksikon. (2016). *Kinematikk (E: Kinematics)*. Retrieved from https://snl.no/kinematikk

Svendsen, I. A. (2006). *Introduction to nearshore hydrodynamics*. Advanced series on ocean engineering. Hackensack, N.J: World Scientific.

Sverdrup, 1.-1., H. U., & Munk, W. H. 1. (1947). *Wind, sea and swell: Theory of relations for forecasting*. Contribution / Scripps Institution of Oceanography. New series ; no. 303. Hydrographic Office and the Supt. of Docs. Retrieved from https://www.biodiversitylibrary.org/item/86149

Thenozhi, S., Yu, W., & Garrido, R. (2013). A novel numerical integrator for velocity and position estimation. *Transactions of the Institute of Measurement and Control*, *35*(6), 824–833. doi:10.1177/0142331213476987. eprint: https://doi.org/10.1177/0142331213476987

Thomas C. Massey, M. E. A., & Smith, J. M. (2011). *Stwave: Steady-state spectral wave model - user's manual for stwave, version 6.0*. Retrieved from http://www.dtic.mil/dtic/tr/fulltext/u2/a550608.pdf

Torsetgaugen, S., Knut; Haver. (2004). Simplified double peak spectral model for ocean waves. In *International society of offshore and polar engineers*. SINTEF Fisheries and Aquaculture.

Tucker, M. (1991). *Waves in ocean engineering: Measurement, analysis, interpretation*. Ellis Horwood series in marine science. New York: Ellis Horwood.

Ursell, F. (1953). Short surface waves due to an oscillating immersed body. *Proceedings of the Royal Society of London. Series A, Mathematical and Physical Sciences (1934-1990)*, *220*(1140), 90–103.

Utne, I., Schjølberg, I., Holmen, I., & Marie Skjøndal Bar, E. (2017). OMAE2017-61845: risk management in aquaculture: Integrating sustainability perspectives. In *36th international conference on ocean, offshore and arctic engineering (OMAE2017)* (V07BT06A054). The American Society of Mechanical Engineers.

Xu, T.-J., Zhao, Y.-P., Dong, G.-H., Li, Y.-C., & Gui, F.-K. (2013). Analysis of hydrodynamic behaviors of multiple net cages in combined wave–current flow. *Journal of Fluids and Structures*, *39*, 222–236. doi:https://doi.org/10.1016/j.jfluidstructs.2013.02.011

Appendix A

Full scale measurements at Hosenøyan

This chapter address a preliminary study of spatial variation of wave conditions within an aquaculture site. Improved knowledge about spatial variations of met-ocean conditions at sites are relevant for optimization of design and operation. Despite the rising need, estimation techniques concerning spatial variation within aquaculture sites are limited. As stated in the introduction, *deficient research concerning prediction of met-ocean conditions at aquaculture sites are available.*

The objective of this study is to investigate the second sub-questions given in the introduction:

1. What is the variance in spatial wave conditions within a site?
2. How may spatial wave energy content affect the reliability of site surveys?

A full-scale measurement campaign has been carried out in relation to the problem statement. Due to limited time and some postponements, the work is not finished. Nevertheless, the preliminary study identify the potential for further investigation of spatial variations of wave conditions within an aquaculture site.

This chapter is organized by presenting:

1. Relevant theory complying:
   (a) Wave theory
   (b) Dynamics of floating collars
   (c) Full-scale ocean measurements by accelerometers
2. Post-processing techniques:
   (a) Experiences made through post-processing and what to avoid when processing full-scale recordings

3. Presentation of the site and preliminary results of the measurement campaign

The objective of the chapter is to outline what to notice and consider when conducting full-scale studies. Discussions relevant for both the full-scale measurements and the quantitative analysis are given in chapter 7 in main part of the thesis. Proposals for further work relevant for continuing the measurement campaign are given in section A.5.4 whereas recommendations comprising the overall topic of the thesis are given in 8.

A.1 Regular wave theory

Waves are physical phenomena of energy transport induced by spatial displacement of fluid particles, i.e. vibrations. The fluid particles want to restore their equilibrium state, giving the formation of forces acting to obtain this resting position. The motion of fluid particles can be described as harmonic plane waves with a sinusoidal varying displacement:

$$\zeta(x,t) = \zeta_a sin(\omega t - kx) \tag{A.1}$$

The fluid, herein sea water, is assumed to be incompressible and inviscid, with a constant density of $\rho = 1025 \quad kg/m^3$. Incompressibility implies a conservation of mass, known as the equation of continuity:

$$\frac{\partial u}{\partial x} + \frac{\partial v}{\partial y} + \frac{\partial w}{\partial z} = 0 \tag{A.2}$$

A velocity potential, ϕ, is used to describe the irrotational fluid motion $\vec{U} =$ [u, v, w] in time [t] and space [x, y, z]:

$$u = \frac{\partial \phi}{\partial x}, v = \frac{\partial \phi}{\partial y}, w = \frac{\partial \phi}{\partial z} \tag{A.3}$$

When inserting A.2 into A.3, the Laplace equation, $\nabla^2 \phi = 0$ appears. This is applied to solve for the velocity potential with relevant boundary conditions for the fluid. To summarise, the assumptions made for describing the fluid are:

- Invicid
- Incompressible
- Irrotational

Bernoulli equation

With the assumptions made above, the Bernoulli equation can be introduced. The Bernoulli equation originates from the Euler equations (*conservation laws*); conservation of mass, conservation of momentum (Newton's 2nd law) and conservation of energy. It is an approximate description of a fluid, because the assumptions of incompressible, steady and inviscid fluid must be valid. Çengel and Cimbala (2014) states that the Bernoulli equation describes the relationship between pressure (flow energy), fluid elevation (potential energy) and fluid velocity (kinetic energy), where *C(t)* is a time-varying arbitrary function (Cimbala, 2014):

$$p + \rho z g + \rho \frac{\partial \phi}{\partial t} + \frac{\rho}{2} \vec{U} \cdot \vec{U} = C(t) \tag{A.4}$$

A.1.1 Boundary conditions

Application of the following the boundary conditions are done to solve the potential flow problem in accordance with the Bernoulli equation:

- *Kinematic boundary condition*: It is assumed that no fluid enter or leave a body surface, thus the tangential velocity component in a potential flow on a fixed body is zero, $\frac{\partial \phi}{\partial n} = 0$. The wave elevation of the free-surface is defined as $z = \zeta(x, y, z, t)$, where ζ is the wave elevation. Next it is assumed that a fluid particle on the free-surface stays on the free-surface, which is also the main assumption when defining the kinematic boundary condition:

$$\text{Kinematic condition:} \quad \frac{\partial \zeta}{\partial t} + \frac{\partial \phi}{\partial x}\frac{\partial \zeta}{\partial x} + \frac{\partial \phi}{\partial y}\frac{\partial \zeta}{\partial y} - \frac{\partial \phi}{\partial z} = 0 \quad \text{at} \quad z = \zeta(x, y, t) \tag{A.5}$$

- *Dynamic boundary condition*: This condition assumes that the water pressure at the surface is equal to the atmospheric pressure on the free-surface. At the fluid side of the surface we can utilize the Bernoulli equation: $p_0 + \rho g z + \rho \frac{\partial \phi}{\partial t} + \frac{\rho}{2} \nabla^2 \phi = p_{atm}$, where $p_0 = p_{atm}$.

$$\text{Dynamic condition:} \quad g\zeta + \frac{\partial \phi}{\partial t} + \frac{1}{2}\left(\left(\frac{\partial \phi}{\partial x}\right)^2 + \left(\frac{\partial \phi}{\partial y}\right)^2 + \left(\frac{\partial \phi}{\partial z}\right)^2\right) = 0 \tag{A.6}$$

It is further assumed that the wavelength, λ, and the wave elevation, ζ , are much smaller than the water depth, H:

$$\lambda << H \quad \text{and} \quad \zeta << H \tag{A.7}$$

The velocity potential can be derived by applying the Laplace equation, boundary conditions and satisfying the Bernoulli equation. To do so, the dynamic free surface condition must be linearized by Taylor expansion at the mean surface $z = \zeta(x, y, t) = 0$. The kinematic and dynamic conditions from A.5 and A.6 can now be written as Faltinsen, 1990, p. 15:

$$\text{Kinematic condition (on} \quad z = \zeta(x, y, z, t) = 0): \quad \frac{\partial \zeta}{\partial t} = \frac{\partial \phi}{\partial z} \tag{A.8}$$

$$\text{Dynamic condition (on} \quad z = \zeta(x, y, z, t) = 0) \quad \frac{\partial \phi}{\partial t} + g\zeta = 0 \tag{A.9}$$

The solution for the Laplace equation are different for shallow water and deep water, but the procedure and assumptions made for solving are almost identical. By applying techniques for second order ordinary differential equations, the expressions for ϕ are found.

A.1.2 Arbitrary (shallow) water assumption

When derived by use of separation of variables, the aforementioned assumptions will result in the velocity potential for arbitrary water depth, h:

$$\phi = \frac{g\zeta_a}{\omega} \frac{cosh(k(z+h))}{cosh(kh)} cos(\omega t - kx) \tag{A.10}$$

ω is the frequency, $k = \frac{2\pi}{\lambda}$ is the wave propagation number, g is the gravity and ζ_a is the wave amplitude. This expression is valid for arbitrary water depths, thus both shallow and deep waters, but because the expression can be simplified for deep water, it is common to use A.10 for shallow water only.

Dispersion relation for general water depths

The wave propagation number (or simply wave number) gives the relationship between the propagation of a wave and its wavelength (e. g. Faltinsen, 1990; Patel, 1989). If linked to the free-surface condition, the *dispersion relation* can be found on a general form for all water depths:

$$\tanh(kh)k = \frac{\omega^2}{g} \tag{A.11}$$

Shallow water assumption

When the water depth becomes very small compared to the wave length, i.e. $h \ll \lambda$, the expression for $tanh(kh)$ simplifies to kh. The expressions for respectively wave length and dispersion can then be written:

$$\lambda = T\sqrt{gh} \tag{A.12}$$

$$k^2 h = \frac{\omega}{g} \tag{A.13}$$

The *phase speed, defined by the wave number and the dispersion relation, dependent of frequency.* When shallow water is assumed, there is no longer a relation between frequency and phase speed. The waves are *non-dispersive* and the wave length is $\lambda = T\sqrt{gh}$. Svendsen, 2006 states that *shallow water assumption is valid when* $\frac{h}{\lambda} < \frac{1}{20}$.

A.1.3 Deep water assumption

Deep water is assumed when $h > \frac{\lambda}{2}$. Wave interactions at the sea surface induce displacements of fluid particles. Down in the water column these motions are required to die out. When $z \to -\infty$ no displacements are occurring at all. The solution of the Laplace equation then gives the following velocity potential:

$$\phi = \frac{g\zeta_a}{\omega} e^{kz} cos(\omega t - kx) \tag{A.14}$$

Dispersion relation for deep water

The dispersion relation is similar as for shallow water, however when h gets large and $tanh(kh) \to 1$, the deep water dispersion relation can be simplified to:

$$\omega^2/g = k \quad \text{when} \quad h \to -\infty \tag{A.15}$$

A.1.4 Wave velocities

The dispersion relation is closely connected to phase velocity, C_p, and group velocity, C_g, of a wave. These describe the velocity of a single wave form and the propagation of a wave train (energy propagation velocity) respectively:

$$\text{Group velocity:} \quad C_g = \frac{\mathrm{d}\omega}{\mathrm{d}k} \tag{A.16}$$

$$\text{Phase velocity:} \quad C_p = \frac{\omega}{k} \tag{A.17}$$

By applying the dispersion relation for deep water into A.16, the group velocity can now be written as:

$$C_g = \frac{d\omega}{dk} = \frac{1}{2}\frac{g}{\omega} = \frac{1}{2}C_p \tag{A.18}$$

Summation of linear wave components can also be used to describe wave groups. When two linear waves propagates in same direction with equal amplitude but slightly different frequency, they form a wave motion called *wave group*:

$$\zeta(x,t) = Z(x,t)_a cos(\frac{\omega_1 + \omega_2}{2}t - \frac{k_1 + k_2}{2}x) \tag{A.19}$$

where $\zeta(x,t)$ is composed by the linear components $\zeta_1\zeta_2$ and $Z(x,t)_a$ is the wave amplitude

$$Z(x,t)_a = 2\zeta_a cos(\frac{\omega_1 - \omega_2}{2}t - \frac{k_1 - k_2}{2}x) \tag{A.20}$$

The group velocity is derived from the phenomena when $\omega_1 \to \omega_2$, i.e. $\lambda'_g = \frac{2\pi}{k_1 - k_2} \to \infty$, which is an infinitely long wave group. The group speed of the wave train, $C'_g = \frac{\omega_1 - \omega_2}{k_1 - k_2}$, corresponds to the definition of group speed given in A.18.

A.2 Irregular wave theory

The previous sections presented *regular wave theory*, which forms basis for describing a regular sea surface. The sea surface consists of multiple wave components labelled i. A representation of the sea surface elevation at time t in a fixed spatial location observed within a period of duration T can be given as a Fourier series:

$$\zeta(t) = \sum_{i=1}^{\infty}[a_i cos(\frac{2n\pi}{T}t) + b_i sin(\frac{2n\pi}{T}t)], t \in [-\frac{T}{2}, \frac{T}{2}] \tag{A.21}$$

Establishment of spectrum from measurements

If measurements are available, it is possible to evaluate sea states by establishing spectra. In practice the Fast Fourier transform calculates an average estimate of the power spectral density based on a discrete and limited number of records. The following definitions of the spectral density and Fast Fourier Transform are retrieved from Chakrabarti, 2002. Wave data, sampled in a duration of T_s in time-domain, are converted into the frequency domain by the FFT of the sample:

$$X(\omega, T_s) \int_0^{T_s} x_k(t) exp(-\omega t) dt \tag{A.22}$$

This will provide the spectral density $S(\omega)$ as a function of the expected value of the *k-th* signal in frequency-domain of n_s signals:

$$S(\omega) = \lim_{T_s \to \inf} \frac{2}{T_s} E[|X_k(\omega, T_s)|^2] \tag{A.23}$$

A.3 Dynamics of floating collar fish farms

In this section, the interactions between waves and a floating collar will be studied. The main motivation for this is to map out necessary assumptions to transform known measurements of the responses of a floating collar to wave motions. The dynamics of a torus is investigated, with the aim of finding an appropriate transfer function for a floating collar of a fish farm.

A.3.1 The hydrodynamic response of a floating collar in waves

A floating structure in the ocean is exposed to wave forces exiting oscillating motions. Based on theory given in for instance Faltinsen, 1990, the hydrodynamic response problem of the floating structure consists of two phenomena:

- *Wave excitation loads*: Froude Kirloff forces, diffraction forces and diffraction moments
- *Hydrodynamic added mass, damping and restoring loads*

The first phenomena can be described as when the structure is restrained from oscillating in the water column. It is further exposed to incident waves, creating an unsteady pressure field due to undisturbed waves. This causes *Froude-Kirloff forces*. The presence of the structure will change the incident wave fluid field and causes *diffraction forces*.

The *hydrodynamic loads* are characterized by forced body oscillations with the wave excitation frequency in calm water. These will accelerate the surrounding fluid particles and inducing fluid pressure forces at the body surface.

Linearity is assumed and allows superposition of the two hydrodynamic load phenomena. Hydrodynamic coefficients present in both the wave excitation loads and the hydrodynamic loads due to added mass, damping and restoring are applied to solve the equation of motion of the structure and identify responses due to wave exposure:

$$\sum_{n=1}^{6} [(M_{kj} + A_{kj}\ddot{\eta}_k + B_{kj}\dot{\eta}_k + C_{kj}\eta_k] = F_j e^{-i\omega_e t} \tag{A.24}$$

Motion in direction k is due to an exciting force F_j induced in direction j. M_{kj} is describing the mass matrix (see Faltinsen, 1990, p. 67) and further η_k describes the position and motions of the structure.

A.3.2 Added mass and damping forces

When a structure is exposed to a forced harmonic motion in calm water, the fluid disturbance will generate waves. Fluid particles surrounding the object will simultaneously start oscillating, resulting in an oscillating pressure field in the fluid domain. These phenomena are origin to the coefficients *added mass,* A_{kj} and *damping,* B_{kj}. The hydrodynamic pressure induced added mass and damping force in direction k due to motion in direction j can be written (Faltinsen, 1990, p. 69):

$$F_k = -A_{kj}\frac{d^2\eta_j}{dt} - B_{kj}\frac{d^2\eta_j}{dt} \tag{A.25}$$

The dimensions of added mass and damping coefficients depend on motion mode and direction of the force. Some are in terms of mass, some in terms of moment of inertia, others in terms of mass and length. Their sizes are often empirically determined and depend upon several factors, such as geometry of the object, frequency of oscillation, forward speed of the object and depth of the surrounding fluid (Faltinsen, 1990, p. 42).

A.3.3 Wave induced motions of a torus

A floating collar commonly used in aquaculture can be assumed to consist of two toruses lying closely together. Each torus has a cross sectional tube radius of a and a torus radius of c, illustrated in figure A.1.

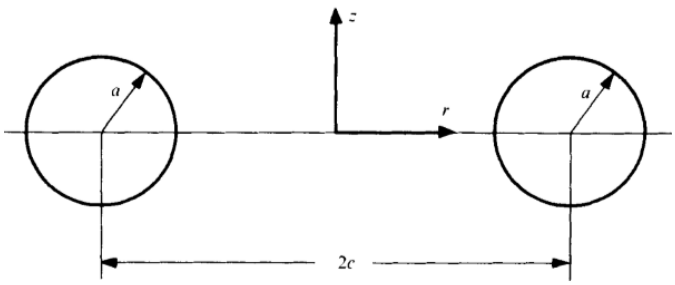

Figure A.1: Cross section of a torus (*Source: Newman, 1977*)

The added mass can be found by assuming that the radius of the tube is much smaller than the radius of the torus (Newman, 1977; Ursell, 1953). A consequence of slender body theory is a flow profile which is constant

in the longitudinal direction of the tube and have large variations in the cross sectional direction. Slender body theory is further a requirement for applying strip theory. The formalization of these assumptions are defined in the slenderness parameter, ϵ, given by Newman, 1977 and later Li, 2017:

- Slender structure: $\frac{a}{c} = \epsilon \ll 1$
- Short wavelength compared to torus radius: $\frac{\lambda}{c} \ll 1$
- Large wavelength compared to tube radius: $\frac{a}{\lambda} \ll 1$
- Freely floating torus in presence of incoming deep water waves.

Expressions for added mass and damping coefficients in 3D can be challenging to determine. Newman, 1977 investigated the motions of a slender torus and derived expressions these coefficients based on 2D added mass and damping coefficients derived by Ursell, 1953. The assumptions for 2D added mass and damping coefficients were based on:

- An immersed circular slender cylinder exposed to vertical motions
- Potential theory, neglecting surface tension at the cylinder surface and viscosity at cylinder surface

Based on strip theory, Newman, 1977 assumed that the 3D added mass for a torus could be calculated as the product of the circumference of the torus and the 2D added mass for a slender cylinder.

The resulting 3D and the basic 2D added mass coefficients for a torus results for a slenderness ratio $\frac{a}{c} = 0,2$ are shown in figure A.2. A fluctuating behaviour of the added mass is observed. Newman, 1977 stated that this occurs due to effects of tuned resonant modes in the inner basin of the torus, depending on the slenderness of the torus.

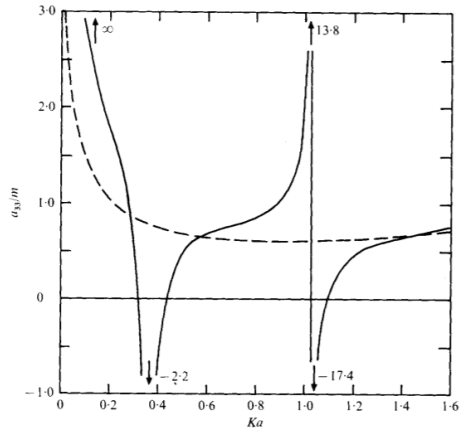

FIGURE 3. Heave added-mass coefficient for a torus with $a/c = 0{\cdot}2$. The dashed line denotes the corresponding two-dimensional coefficient for the circular cylinder, and the arrows denote peak values as shown.

Figure A.2: 3D added mass coefficient in heave (*Source: Newman, 1977*).

A.3.4 Natural frequency of a floating collar

If wave conditions at the site is known, one can use this to design a solution with the purpose of avoiding unfavourable dynamic responses, such as resonance motions. These are induced when incident waves are in order of the natural frequency of the structure. Hence, it is desirable to know the natural frequency of the structure.

The natural period of a freely floating structure in heave is defined in Faltinsen, 1990 as:

$$T_{3n} = 2\pi\left(\frac{M + A_{33}}{\rho g A_W}\right)^{\frac{1}{2}} \quad [\text{s}] \tag{A.26}$$

$T_n = \frac{2\pi}{\omega}$, A_{33} is the *added mass* and A_W is the *water-plane area*. The added mass originates in accelerated fluid particles surrounding the oscillating object and depends on the shape of the object and direction of motion.

Li, 2017 addressed wave-induced response of a floating collar. Through experiments and theoretical (numerical) analysis, he investigated among other the RAO, added mass and other hydrodynamic properties of a floating collar in waves with absence of current. Net, bottom ring, weights and mooring system were neglected in the study. A minor focus was given the natural frequencies of the floating collar. Using A.26, the natural frequency of a semi-submerged torus was decribed by:

$$T_{3n} = 2\pi\left(\frac{M + A_{33}}{\rho g A_W}\right)^{\frac{1}{2}} = 2\pi\left(\frac{\frac{1}{2}a^2\pi\rho + A_{33}}{\rho g 4\pi c a}\right)^{\frac{1}{2}} \quad [\text{s}] \tag{A.27}$$

Here a is equal to the cross-sectional radius of the tube. The numerically predicted undamped natural frequencies were calculated to be 22.63 rad/sec

(n=0) to 29.11 rad/sec (n=10), where mode n has mode shape $cos(n\beta)$. These values are larger than those that were found experimental range of the linear incident waves.

A.3.5 Transfer function for a torus

When an object is exposed to waves with an amplitude ζ_a, an oscillating motion of the object with amplitude, η_{3a}, will occur. As it will be explained in section 4.1, a linear system is assumed. This testifies the use of transfer functions, which represents the connection between the linear response of an object and an exciting motion. The term "transfer function" is general for all kinds of linear processes, and the more specific *Response Amplitude Operator (RAO)* will herein be used to describe the relationship between wave excitation and the response of the torus. The RAO in heave is defined as in Faltinsen, 1990 as:

$$RAO_3(\omega) = |\frac{\eta_3}{\zeta_a}| \tag{A.28}$$

Li, 2017 studied RAOs obtained by application of three theories at multiple positions along the torus. The results can be seen in figure A.3, where it can be seen that the RAO is both dependent on the angle to the incoming waves, their frequencies and wave number. The wave number is here given as a non-dimensional wave number, $\nu = k = \frac{2\pi}{\lambda} = \frac{\omega^2}{g}$, for deep water.

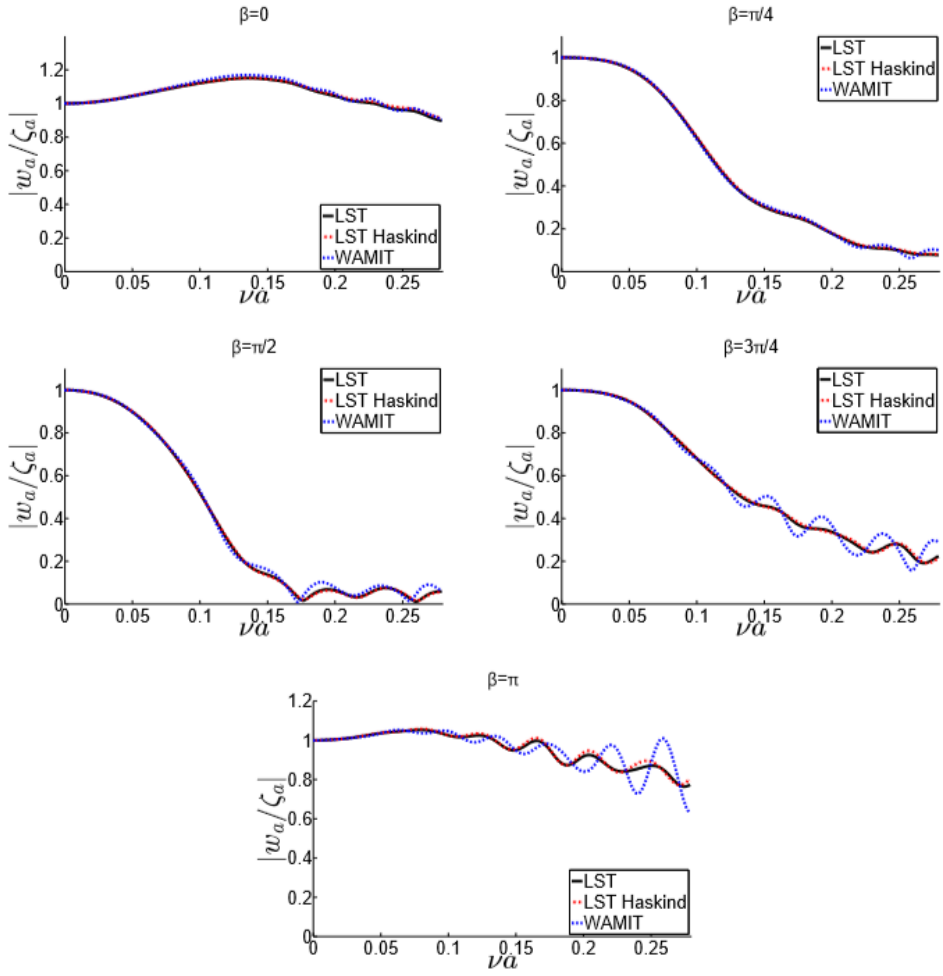

Figure A.3: Response amplitude operators (RAO) for five locations at a torus with $\frac{a}{c} = 0.0253$ in deep water. (*Source: Li, 2017*)

The study by Li, 2017, compares application of low-frequency slender body theory (LST), Haskind and the potential theory-based computer program WAMIT.

Net, bottom weights and moorings will affect the wave-induced motions and the RAO of a floating collar fish farm. Nevertheless, a preliminary one-to-one relationship between the linear response and the exciting motions due to waves is assumed. This simpifies the processing of measurements and is suitable for the purpose of the preliminary study.

A.4 Practical aspects of data acquisition

An accelerometer is a device measuring the acceleration relative to a reference frame in space. At rest all objects are exposed to gravity, and an accelerometer will measure this acceleration as 1 g, correspodning to $9,81 m/s^2$. Accelerometers are commonly based on the principle of a mass-spring system and its corresponding equation of motion (Thenozhi, Yu, and Garrido, 2013):

$$\vec{F} = m\vec{a} = k\vec{x} \tag{A.29}$$

Here m is the mass is displaced from its resting position, and the elongation, x, of a spring with stiffens k will be measured by a sensor in the accelerometer.

Axis orientation

Spatial orientation can be described by a various reference frames, and a detailed description on seakeeping and motion control of marine crafts can be found in Fossen, 2011. Reference frames can be divided into two main categories; *Earth-Centred Reference Frames* and *Geographic reference frames*. The first one consists of a *Earth-fixed inertial reference frame* and the latter of a *Non-inertial (body fixed) reference frame*. These reference frames can be used jointly to describe motions of a floating collar relative to a fixed location in space.

Body-fixed, non-inertial reference frame

A non-inertial reference frame is commonly applied to describe the wave-induced motions for a floating structure. The reference frame is following the spatial orientation of the object, herein the accelerometer. The non-inertial reference frame is equivalent to a body-fixed reference frame. It is convenient to describe the motions of a floating structure, which will pitch and roll in the water plane at the centre of flotation (CF) and centre of gravity (CG).

Earth-centred inertia frame

When the object is exposed to a non-zero net force, the object and the non-inertial reference frame will be accelerated. The accelerometer will measure this acceleration relative to an inertia reference frame. This reference frame represents the object at rest or moving with constant velocity, when the net force acting on the object is zero. The relative location of the spatial coordinates x_n, y_n, z_n to the earth centred earth fixed (i.e. a reference frame

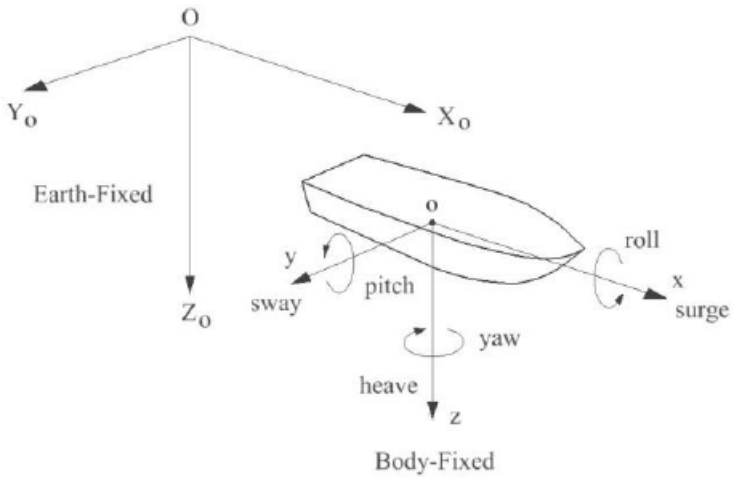

Figure A.4: Definition of reference frames and motion of marine vessels. (*Source: Altosole, Benvenuto, Figari, and Campora, 2009*)

rotating with the angular rotation velocity of the earth), is in this reference frame described by the angles *latitude* and *longitude*. z_n is pointing into the centre of earth, y_n is directed to the east and x_n to the north. Figure A.4, from Altosole, Benvenuto, Figari, and Campora, 2009, displays the two coordinate systems.

Quaternion - reference frame transformation

For the case of the accelerometer applied in this thesis, the body-fixed reference frame is aligned to the inertia, as seen in figure A.5: the bottom of the device is located at the surface of earth, the short side is pointing north and the right side is directed east.

If the body fixed reference frame of an object is not aligned with the inertia frame, quaternion transformation must be done. This enables description of body motions in a earth-fixed inertia reference frame.

Motions of an object

The motions of a non-fixed structure can be described by $\vec{\eta}$, where the translatoric motions are defined by η_1, η_2, η_3. These describes the relative translatoric displacement of the body-fixed reference frame (x_b, y_b, z_b) to the inertial reference frame $(x_n, y_n, z_n$. The relative angular displacement of the body-fixed reference frame to the inertial reference frame can further be described by Euler angles, displayed in figure A.4. These are also included in the latter components of the vector η_4, η_5, η_6. These describe the rotational

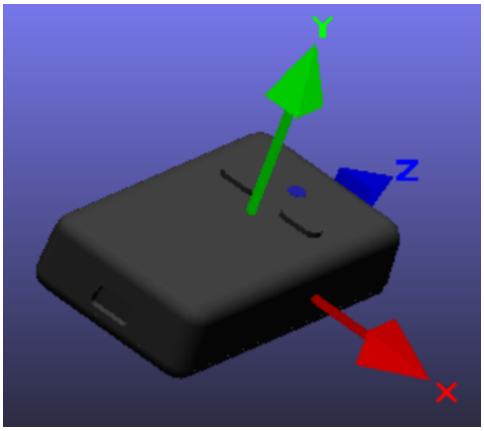

Figure A.5: Reference frame of the accelerometer used for full-scale measurements (*Source: 3-Space Sensor Suite Manual* from *Yost Engineering, Inc.*)

motions *roll,* ϕ, *pitch,* θ and *jaw,* ψ respectively.

The motions of an object are defined as the following, retrieved from Faltinsen, 1990:

$$\vec{s} = \eta_1\vec{i} + \eta_2\vec{j} + \eta_3\vec{k} + \vec{\omega} \times \vec{r} \tag{A.30}$$

where $\vec{\omega} = \eta_4\vec{i} + \eta_5\vec{j} + \eta_6\vec{k}$ and $\vec{r} = x\vec{i} + y\vec{j} + z\vec{k}$.

The time derivative of the displacement vector corresponds to the velocity of the structure, whereas the double derivative corresponds to the acceleration of the structure.

$$\vec{v} = \frac{\partial \vec{s}}{\partial t} \tag{A.31}$$

$$\vec{a} = \frac{\partial \vec{v}}{\partial t} = \frac{\partial \vec{v}^2}{\partial^2 t} \tag{A.32}$$

Application of equations A.31 and A.32 in post-processing allow evaluation of the elevation of the elevation and velocity of a structure based on acceleration measurements.

A.4.1 Wave measurements

When conducting wave measurements, several factors might influence the results of the measurements and give biased data, among other duration and time of the recording, device used in the measurements and sampling frequency. Influences of these factors will in this section be presented.

Biased data

Tucker, 1991 discusses issues and possible sources of biased measurements. During storm events, sea states may be too severe for sensors in the measurement device to register, which could lead to seasonal bias and gaps in the data sets. When gaps are occurring, a correction must be done when post-processing the data by applying some kind of averaging technique. One possible method is to weight the sampled by a weighting factor proportional to the total number of H_s. Another method is to apply a *folding in-technique*. Gaps are divided into two parts and the first half-gap is filled by duplicated data from the preceding data sequence and the consecutive half-gap with duplicated data from the subsequent recordings (Tucker, 1991).

Another typical error could be malfunctions in the measurement devices leading to systematic biased data.

Sampling frequency and the Nyquist theorem

An important factor to consider when performing wave measurements is the sampling frequency. It is in practice not possible to record wave elevation in a continuous time domain, and a time step of the measurements must be selected. This sampling frequency will influence what kind of wave periods that will be registered and define the resolution of the sample.

The relationship between sampling frequency and sampled wave periods is given by the *Nyquist theorem*. This theorem states that the sampling frequency must be minimum twice the target frequency of the sample. The Nyquist frequency can be stated as:

$$f_{Nyq} = \frac{1}{2\Delta t} = 2f_0 \leqslant f_s \tag{A.33}$$

The target frequency could for instance be the natural frequency of an object, f_0. The Nyquist frequency gives the upper limit of possible sampled frequencies, i.e. the *cut-off frequency* of the sample. When doing measurements one should ensure that the sampling frequency, f_s, is well above f_{Nyq}. A consequence of undersampling and not fulfilling the Nyquist requirement could be aliasing; a misidentified wave elevation with much lower frequency than the actual wave, as seen in figure A.6.

The sampling frequency and resolution of the sample furthermore influence the estimation of the spectra for the waves (Haver, 2017).

A.4.2 Post-processing and presentation of sampled data

Samples from accelerometers need to be post-processed to evaluate the wave elevation and establish a statistical description of the wave exposure. There are a certain important steps, given below:

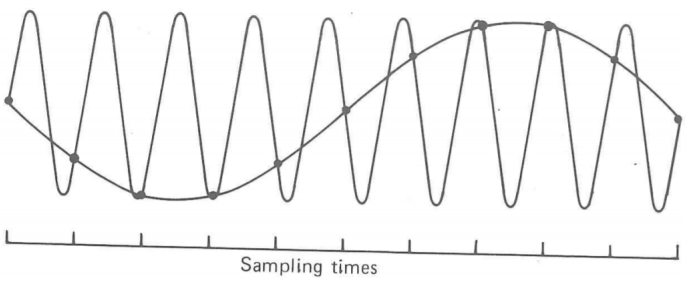

Figure A.6: Aliassing of an input wave with much higher frequency than the output (sampled) wave. (*Source: Tucker, 1991*)

- Determine sampling frequency and duration of the measurements
- Calculate the wave elevation from acceleration
- Filter the data: Find and determine the valid of the Response Amplitude Operator and linear theory
- Establish spectra and probability papers for statistical assessment

A.4.3 Post processing of accelerometer data

When a measurement campaign is finished, treatment of the recorded data is needed. This is done through the process of post-processing, where the purpose is to filter out the wanted signals and discard disturbing components from the wanted signal. Techniques applicable for post-processing and consequences for the resulting signal will be addressed here.

Filtering

Measurement devices record all signals within a predefined frequency range limited by the device's features. This means that the frequency band of a recording could include noise, which from acoustics is defined as undesirable signals (Hovem, 2012). Signals are commonly recorded in time-domain. To detect frequencies where noise are occurring, a Fast Fourier Transform can be applied to transform the signal into frequency domain and plot a power spectrum of the signal. An unfiltered and filtered (smoothed) signal from Yost Lab 3D Sensor is shown in figure A.7, which is attached only for visualization.

Filtered makes it easier to detect patterns in the data. Various filters are available, depending on the purpose of the analysis. This could be in terms of number of samples and development in peaks or minima. Filtering

can either be done by while measurements are sampled or as post-processing activity. Only a brief introduction to filtering application will here be given.

Low-pass filtering

A low pass filter is applied when noise is located at frequencies higher than a defined cut-off frequency. The *cut-off frequency* is by Hovem, 2012 defined as the frequency where wave number k and group speed approaches zero and phase speed goes to infinity. This filter *allows frequencies lower than the cut-off frequency to pass through and leaves out low-frequency signals.*

High-pass filtering and band pass filtering

The counterpart of low-pass filter is the high-pass filter. This *leaves out noisy signals located below a defined cut-off frequency.* If both high and low-pass filtering are applied this is called *band-pass filtering.*

Ocean waves are characterized by periods of 0.5 s to 25 s, corresponding to a frequency band from 0.04 Hz to 2 Hz frequency band (Haver, 2017). An appropriate band-pass filter could thus be designed to attenuate signals outside this range. By plotting the signals in a spectre, an appropriate bandwidth for the filter can be determined.

Smoothing signals

In highly fluctuating signals, overall patterns can be difficult to recognize. Averaging the signal makes trends easier to discover, reduces data size and processing time for further analysis. An example of a smoothed signal is shown in figure A.7, where zero-phase digital filter is applied. This filter can be found in the Signal Processing Toolbox distributed by The MathWorks, Inc.

A.4.4 Acceleration to elevation - challenges with bias and drift

To transform a signal of acceleration to elevation several approaches can be applied. Their success depends on several factors originating in the recording and measurement device. Bias can easily build up if not care is taken when transforming the signal into velocity and position. A common approach is to assume constant acceleration within a time step and utilize equations A.24, A.31 and A.32 specified as:

$$\dot{\zeta}(t) = \dot{\zeta}_0 + \int_0^t \ddot{\zeta}(t)dt = v_0 + a(t)t \tag{A.34}$$

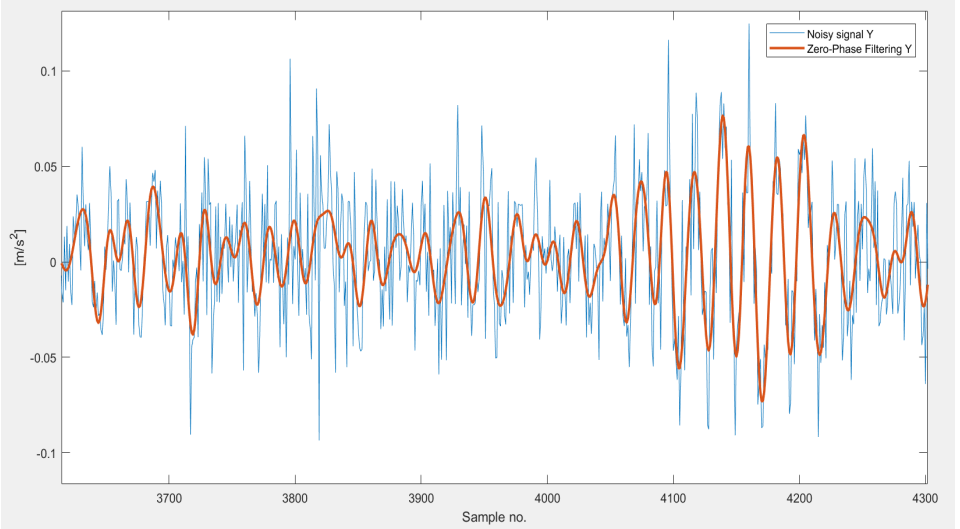

Figure A.7: Unfiltered and smoothed signal of linear acceleration recorded by Yost Labs 3-Space Sensor processed by Zero Phase Digital filter in MATLAB.

$$\zeta(t) = \zeta_0 + \int_0^t \int_0^t \ddot{\zeta}(t)dt = v_0 t + \frac{1}{2}a(t)t^2 \tag{A.35}$$

By applying numerical integration techniques between sample points, approximations of the integration in A.34 and A.35 can be found. The trapezoidal rule is one of several a possible choices for numerical solving of the integration:

$$\int_a^b f(x) \approx [\frac{f(a) + f(b)}{2}](b - a) \tag{A.36}$$

Bias and drift from accelerometer data

Calculating velocity and position from accelerometer data might be easier said than done. Signals from IMUs (Inertia Measurement Unit) consist of the following components (Thenozhi et al., 2013):

$$a(t) = k_a \ddot{\zeta(t)} + w(t) + d \tag{A.37}$$

where k_a is accelerometer gain (sensitivity), w(t) is noise and disturbances on the measurement and d is the offset, originated in absence of gravity or motion (0g).

When applying numerical integration to a signal, bias from noise and offset will accumulate over time and will make bias predominant. The accumulation of errors from measurements after integration is called *drift*.

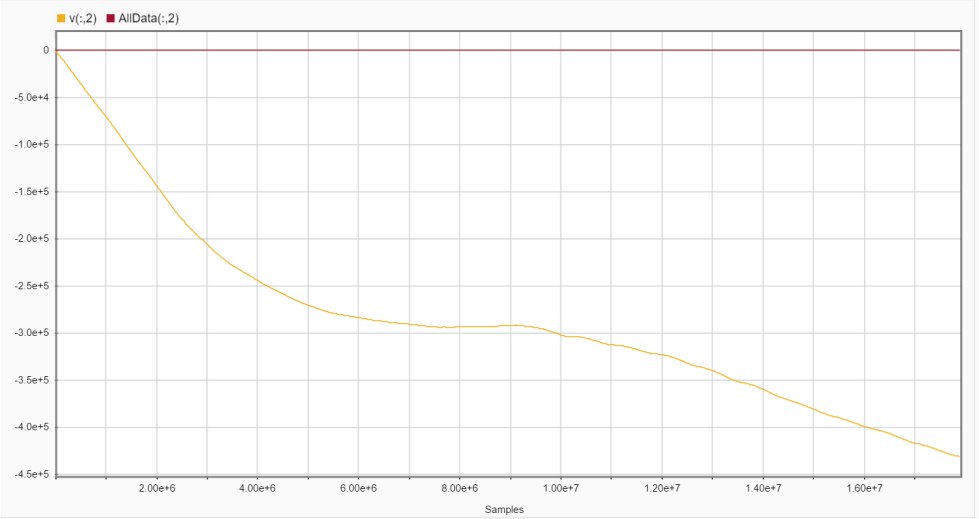

Figure A.8: Bias when using trapezoid numerical integration to find velocity (v(:,2)) from accelerometer data measured by Yost Labs 3-Space Sensor.

Offsets might origin from inaccurate initial calibration of the accelerometer. Another offset can be caused by change in the relationship between displacement of the mass and acceleration measured. Temperature changes might also cause offsets. One way to remove offsets are periodic re-calibration of the velocity and position.

Results of numerical integration are shown in fig A.8, where accelerometer data are integrated once and twice with respect to time step without any removal of noise and bias.

In figure A.8, 17 millions samples are evaluated simultaneously. One way to avoid the occurrence of drift could be to evaluate much less samples at a time. This allows easier detection and removal of drift by carrying out a calibration and "reset" the velocity (and position) when they move out of a predefined range. When doing this, the input should have a zero mean, i.e. a *normalized* signal.

Analysis in frequency domain

Another approach to avoid accumulation of bias is to evaluate the signal in the frequency-domain after a Fast Fourier transformation (Thenozhi et al., 2013). Then the following relationships can be utilized, retrieved by Newland, 2005:

$$S_{\dot{\zeta}}(\omega) = \frac{S_{\ddot{\zeta}}(\omega)}{\omega^2} \tag{A.38}$$

$$S_\zeta(\omega) = \frac{S_{\dot{\zeta}}(\omega)}{\omega^2} = \frac{S_{\ddot{\zeta}}(\omega)}{\omega^4} \tag{A.39}$$

Here, $S_{\ddot{\zeta}}(\omega)$ corresponds to the frequency spectrum of measured acceleration, $S_{\dot{\zeta}}(\omega)$ is the spectrum for velocity and $S_\zeta(\omega)$ for the position. ω is frequency range of the samples. Next an inverse FFT is necessary to evaluate the results from equations A.38 and A.39:

$$\zeta(t) = \int_{-\infty}^{\infty} S(\omega) e^{i\omega t} d\omega \tag{A.40}$$

Window function and spectral leakage

There are certain requirements for signals undergoing a Fourier transform. Waves are random and their signal of infinite length. Fourier transformation assumes a periodic time domain signals, where the data are repeated after a certain time or are of indefinite length. The reason for this can be seen in equation A.22, where the signal is integrated over an indefinite period of time, making it necessary to assume that the signal is periodic. The signal can furthermore be presented as a sum of a finite number of sine waves (Harris, 1978).

If the signal is non-periodic, *spectral leakage* can occur when performing a Fast Fourier Transform (Harris, 1978). This is due to sharp transitions between repeated signals, and will produce a resulting broad banded spectrum. This is equivalent to running the signal through a pass-band filter, where attenuation of the signal will occur if the frequency of the signal does not coincides with the bandwidth of the filter.

Spectral leakage can be avoided by truncating the signal. This is done by multiplying the signal with a window function. The simplest is the rectangular window function, *w(n)*, retrieved by Lai, 2004:

$$w(n) = x = \begin{cases} 1, & \text{if } |n| \leq M, \\ 0, & \text{otherwise.} \end{cases} \tag{A.41}$$

where M is the interval of interest, i.e. $2M = N$, and N is the total number of samples. In the transition region, i.e. in the area where $n \to M$, this window will introduce non-uniform convergence of the Fourier series. Another simple, yet much used window function, is the Bingham window function, retrieved by Newland, 2005 as:

$$w(n) = 0.5 + 0.5cos(\frac{2n}{N}\pi), \quad n = -\frac{N}{2}, ..., -1, 0, 1, ..., \frac{N}{2} - 1. \tag{A.42}$$

Effects of band-pass filtering and Bingham window functions on measurements from Hosenøyan are seen in figure A.15. Windowing is applied on the full length of a sample, corresponding to a sea state of 1 hour.

Analysis of acceleration in frequency domain

There are several approaches available to compare signals. When evaluating the total energy in a measurement and comparing this to equivalent signals, it is possible to detect possible variations in wave load exposure. A convenient theorem is the Parseval's theorem (Newland, 2005):

$$\frac{1}{T}\int_0^T x^2(t)dt = \sum_{i=-\infty}^{\infty} X_i * X_i \tag{A.43}$$

where T is the period of the signal, $x(t) = x(t+T)$ and X is frequency-transformed signal. If a measurement is composed by N discrete signals, equation A.43 can be re-written to:

$$\sum_{n=0}^{N-1} |x[n]|^2 = \frac{1}{N}\sum_{k=0}^{N-1} |X[k]|^2 \tag{A.44}$$

These relationships can be utilized when investigating total energy within a frequency band.

A.4.5 Probabilistic theory of sea loads and statistical description of sea states

Waves are inherent random of nature. When summed up, a large number of random stochastic realizations are approaching a *Gaussian distribution*, as defined by the *central limit theorem*. If infinite water depth, the sea surface is thus assumed to be a random, Gaussian distributed process. Gaussian description can be further extended to include shallow water, but *assumes no severe wave conditions such as storms*. The horizontal asymmetry of troughs and crests in finite water depths is a contributing factor for this exclusion (Ochi, 2005, see p.2, 142-143 and 280).

The term *ergodicity* is applied when one single realization of a process is representative and provide all statistical properties for the stationary, stochastic process as a whole (Newland, 2005). Time averaging will replace and is equal to ensemble averaging, causing the assumption of constant statistical properties for one sea state. The recordings of linear acceleration is one hour, making it practical to calculate and assume constant statistical properties for one hour long sea states.

It is further common to assume the following when analyzing the environmental conditions influencing the installation or operations:

- Sea states are ergodic and stationary within a duration of 20 minutes to 3 hours.
- Wave elevation is a stochastic Gaussian process with variance σ^2 and mean equal zero.

By making the above mentioned assumptions it is possible to describe met-ocean phenomena with probabilistic models. It is common to base the long term statistics of environmental conditions within an area on identically distributions of the samples obtained by short term statistics. Stationary sea states must be independent of each other, assuming that a sea state is not influenced by its predecessors. This assumption is however questionable in case extreme weather conditions are emerging, for instance in build-up of a storm event.

A.5 Practical aspects of full-scale measurements at Hosenøyan

Spatial variation of met-ocean conditions is an important topic when assessing the quality of site surveys. The spesific location applied in analyses may affect the outcome of a survey. As pointed out in section 4.4.4, site surveys are based on point extremes, and are deviating from area extremes (Barbariol et al., 2015; Forristall, 2011). The analyses done herein are preliminary and a very first review of the spatial variation of wave elevation within an aquaculture site. Due to practical issues and related to full-scale measurements, only effects of filtering and spatial variation of energy content in linear acceleration are analyzed. The following sections describes how theory presented in appendix A.3 and A.4 are applied for the data from the full-scale measurements at Hosenøyan.

A.5.1 Description of the Hosenøyan site

The aquaculture site used in this study is located in Flesafjorden at 64°53'52" N, 9°53'189" E, which is north east of Frohavet outside Stokkøya in Trøndelag (figure A.9. The farm is protected to the open ocean by some small islands and skerries, but unprotected to waves and wind coming in from south west from the relatively open ocean area in Frohavet, figure A.10.

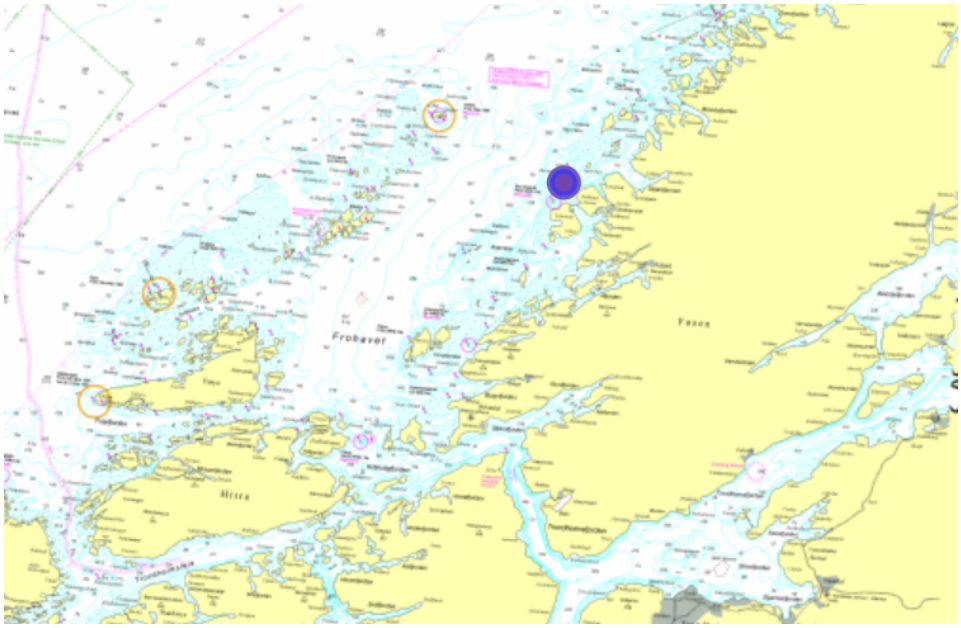

Figure A.9: Overall location of Hosenøyan site in Trøndelag (*Source: Kartverket*)

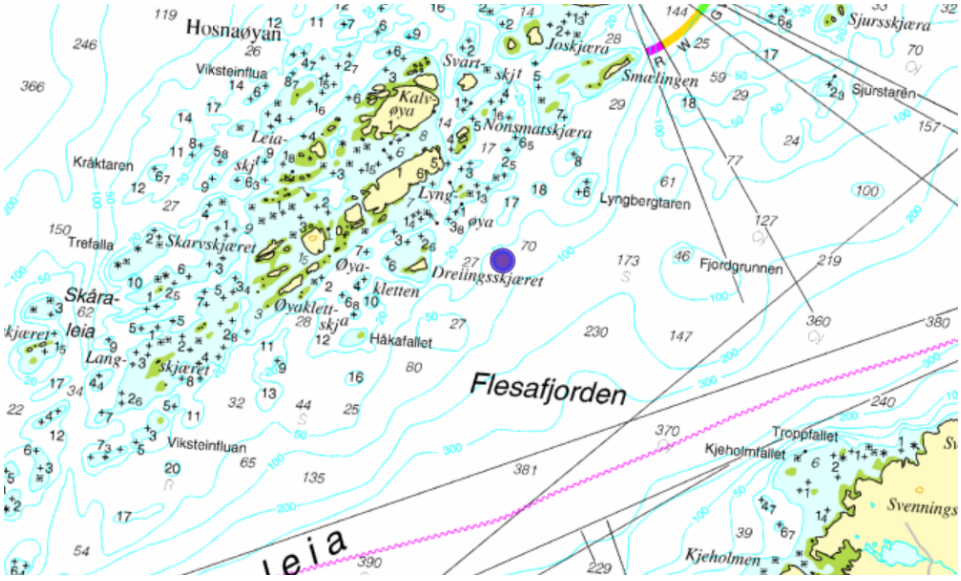

Figure A.10: Detailed location of Hosenøyan site in Trøndelag (*Source: Kartverket*)

Alignment of moorings and floating collars

The plant is aligned across of the strait, with a mooring system able to keep 12 net pens, as seen in figure A.11. The feed barge is located north east, closest to the islets and reefs, protected from waves coming in from south east.

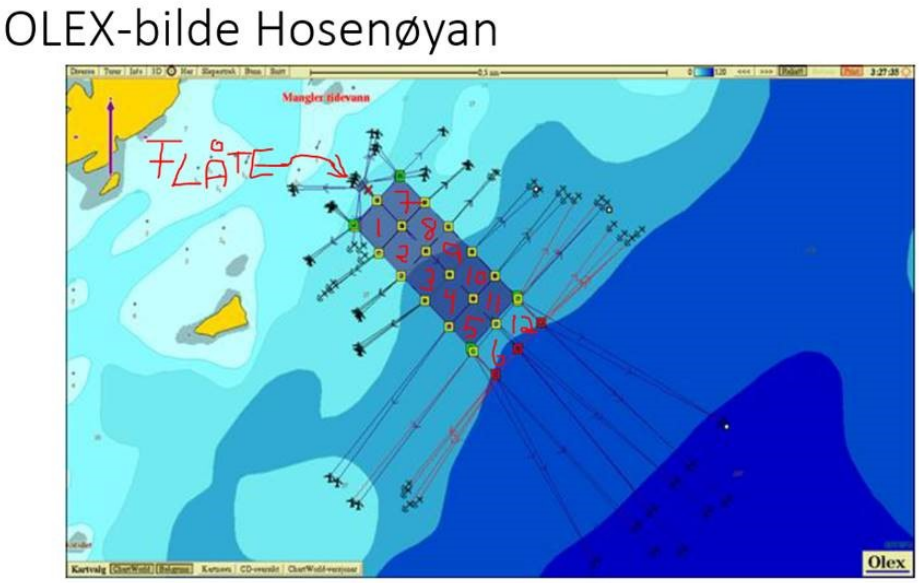

Figure A.11: Alignment of mooring system at Hosenøyan fish farm. (Flåte = Feed barge)

8 cages manufactured by Aqualine with the following technical description were in use at the site:

- Each floating collar consists of two tubes with circumference 157 [m] and pipe diameter 0,5 [m] (i.e. torus radius $c = 25$ [m] and pipe radius $a = 0,5$ [m] respectively)
- Sinker tube of 80 [kg/m] at depth 17,5 [m] outside the net pen on each cage
- Sinker of 1000 [kg] at bottom of each net pen

Based on data from NYTEK schemes obtained from the Norwegian Directorate of Fisheries, met-ocean conditions characterizing the Hosenøyan plant are given in table A.1. If the exposure levels presented in table 5.1 are used, *Hosenøyan can be categorized as having a high to extreme degree of exposure to waves.*

Table A.1: NYTEK data from Hosenøyan fish farm (*Source: Norwegian Directorate of Fisheries*)

$Hs_{wind,10yrs}$[m]	$Tp_{wind,10yrs}$[s]	$Hs_{wind,50yrs}$[m]	$Tp_{wind,50yrs}$[s]	$Hs_{comb.,10yrs}$[m]
2,9	7,7	3,3	8,6	1
$Hs_{swell,10yrs}$ [m]	$Tp_{swell,10yrs}$[s]	$Hs_{swell,50yrs}$ [m]	$Tp_{swell,50yrs}$ [s]	$Hs_{comb.,50yrs}$[m]
3,2	16,3	3,6	16,3	1

Description of accelerometers

Six *Yost Labs 3-Space Datalogger* accelerometers (https://yostlabs.com/product/3-space-data-logger/) have been installed at the site. These are funded within the research program Exposed Aquaculture (see www.exposedaquaculture.no/), where a purpose is to provide data for upcoming master students and their research work. Set up and calibration of accelerometers were done in cooperation with Eirik Svendsen and Gunnar Senneset, reasearchers in SINTEF Ocean.

Alignment of accelerometers

The initial plan by alignment of accelerometers was to compare spatial deviation of linear acceleration and if possible, wave elevation at various locations within the fish farm. Without having any prior knowledge about the detailed wave propagation pattern at the site, it was assumed that exposure was greatest along the strait, for waves coming from south-west and north-east. The innermost cages (no. 1 and 7), were assumed to be most protected to waves, and the outermost cages (no. 6 and 12) most exposed to waves propagating in the strait. It was further important to validate measurements by align accelerometers in pairs.

The alignment of loggers are marked as green dots in figure A.14. It can be seen that the alignment deviates from the initial objectives. Cage 1, 7, 6 and 12 were not installed due to fallowing, and as a compromise it was chosen to align one logger inside the power cabinets at cages 2, 7, 3, 9, 5 and 11.

The power cabinets are placed at the walk-ways at the floating collars at each cage at height 1,25 m above sea level and are seen in figure A.12.

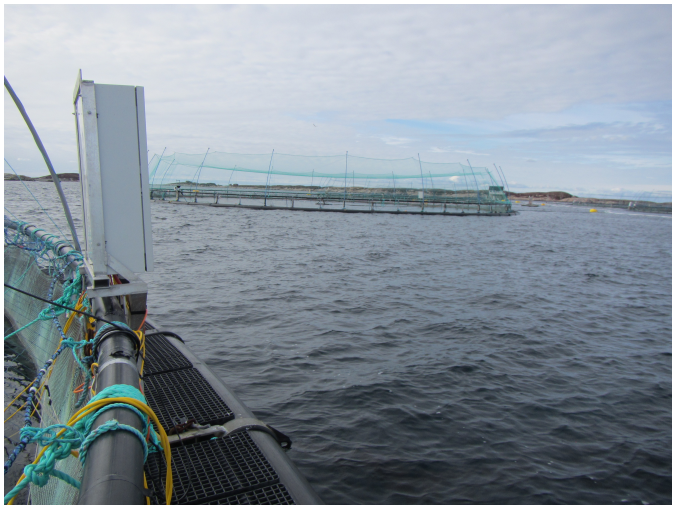

Figure A.12: Set-up of accelerometers and alignment of power cabinets. There is one cabinet at each collar, at 1,25 m above sea level. *Photo: Gunnar Senneset*

Figure A.13: Alignment of accelerometer inside power cabinet. All loggers are directed equally inside cabinets. *Photo: Gunnar Senneset*

Figure A.13 shows the alignment of an accelerometer inside a power cabinet. Sea water entering the cabinets might occur. This caused failure of accelerometers at cage 2 and 11, which are red collars in figure A.14. Only data from cage 3, 5, 8 and 9 were obtained.

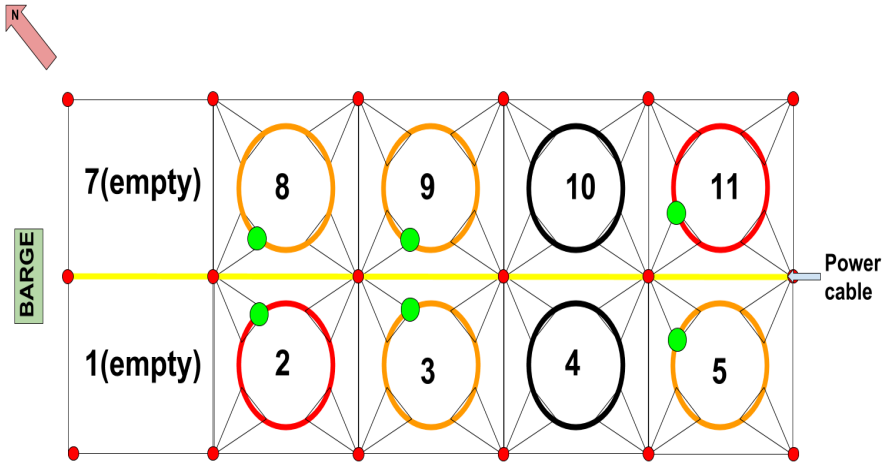

Figure A.14: Alignment of loggers at Hosenøyan site. Green dots display where loggers were placed. Orange collars are cages where linear acceleration was obtained, red are collars where measurements were interrupted due to salt water entering accelerometers.

Data sampling

The measurement campaign was conducted between April 11th and May 8th 2018. A total of 645 hours with 10 Hz samples were recorded by each accelerometer. The accelerometers do not save samples in a permanent file until a recording finished, and made it necessary to split recordings into one hours intervals to reduce risk of losing data.

Sampling frequency was determined based on the floating collar's natural frequency. This was calculated by use of equation A.30 and assuming the dynamics of a semi-submerged tube, as presented in section A.3.4. A small script (*naturalFreqTorusKOPI.m*) written for these calculations can be found in appendix C.

The calculated natural period was found to be 1.7288 s.

A.5.2 Post-processing of sampled data from Hosenøyan

Loading data to software

Due to a very large amount of data (approximately 2600 text files), an automated loading algorithm was written. For each accelerometer the main

script *importfileForMHosF.m* was runned, which resulted in a *NxM* cell array (*netPen.mat*), where N is the number of text files created by each accelerometer and M is the number of accelerometers. The main script subsequently calls the function *importfileMatrixMHosF.m*, which load one text file at a time, each consisting of approximately 35000 rows (1 hour recording) into MATLAB. These MATLAB scripts can be found in appendix C.0.4 and C.0.4.

Cleaning data - high-pass filters and window functions

After loading is finished, further analyses of the measurements is possible. As stated in section A.4.4, accelerometer data are exposed to noise which can introduce bias and errors in the analyses. Possible sources of noise in the measurements must be filtered out before moving on in analyses. Due to limited prior knowledge about signal processing, effects of applying filters and windows to the data was only studied visually, as seen in figure A.15. Its corresponding script can be found in appendix C.0.4.

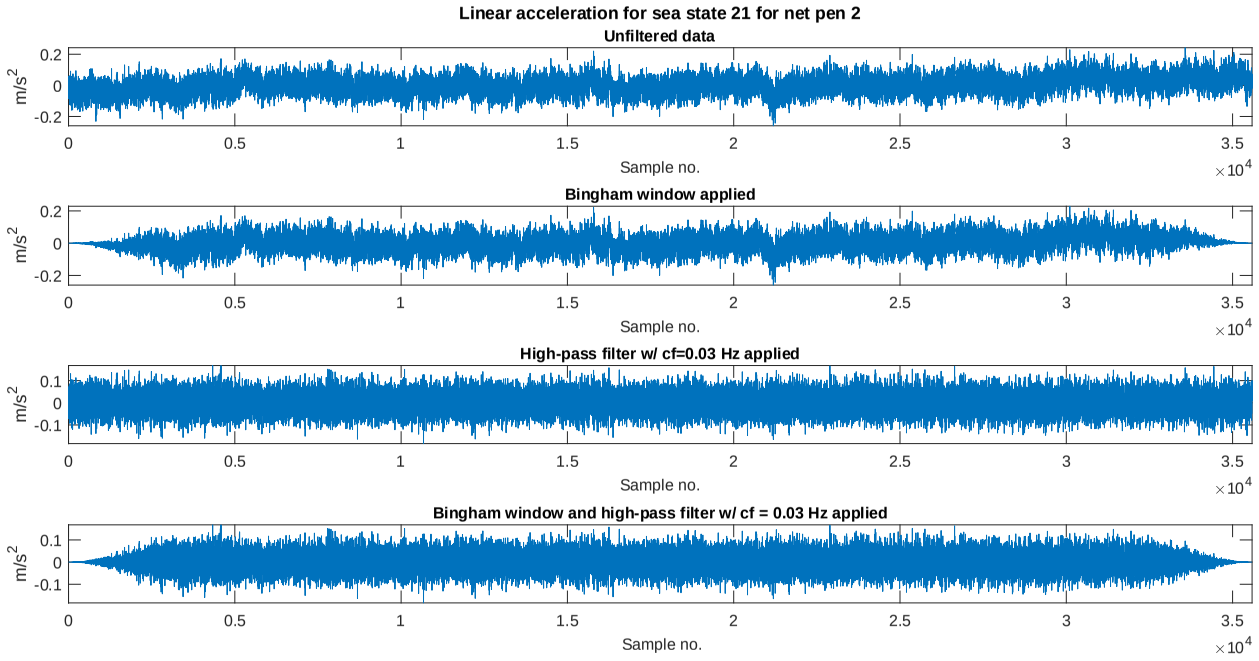

Figure A.15: Example of unfiltered data (uppermost), effects of applying Bingham window function (2nd - see Newland, 2005), high-pass filter (3rd) and both Bingham window and high-pass filter (lowermost).

The linear acceleration is composed of a slowly varying component and as expected, a highly fluctuating component. When applying a high-pass filter, the slowly varying component disappears. Section A.4.4 discuss the requirement of continuous samples when performing a Fourier transform, and it is chosen to apply a Bingham window function (see Newland, 2005). This is not a part of the built-in functions in MATLAB, so the script *BinghamF.m* (appendix) was written. Only Bingham windowing and its associated script is used in further analysis.

Calculating energy content of measurements

Next, all samples of linear acceleration from all floating collars were compared. The main purpose of the analysis was to investigate differences in energy content within the spectrum for each of the net pens. This was done by calculating the zero moment of linear acceleration spectrum for available measurements, by utilizing Parseval's theorem (equation A.43) and applying equation 4.15. The script *loadFilesHosF.m* runs through all columns in the array *netPen.mat* and calculates the zeroth moment for each 1 hour sea state. The script can be found in appendix C.0.5.

A.5.3 Preliminary results - spatial variation in wave energy content within Hosenøyan site

Power spectra for each sea state were calculated for all accelerometers. Figure A.16 shows the development of energy content in spectra for each sea state over time. Only the second half of the data is shown, due to a big leap in magnitude for net pen 9 for the first half of the sea states. Full time history for zeroth moment can be found in figure A.17.

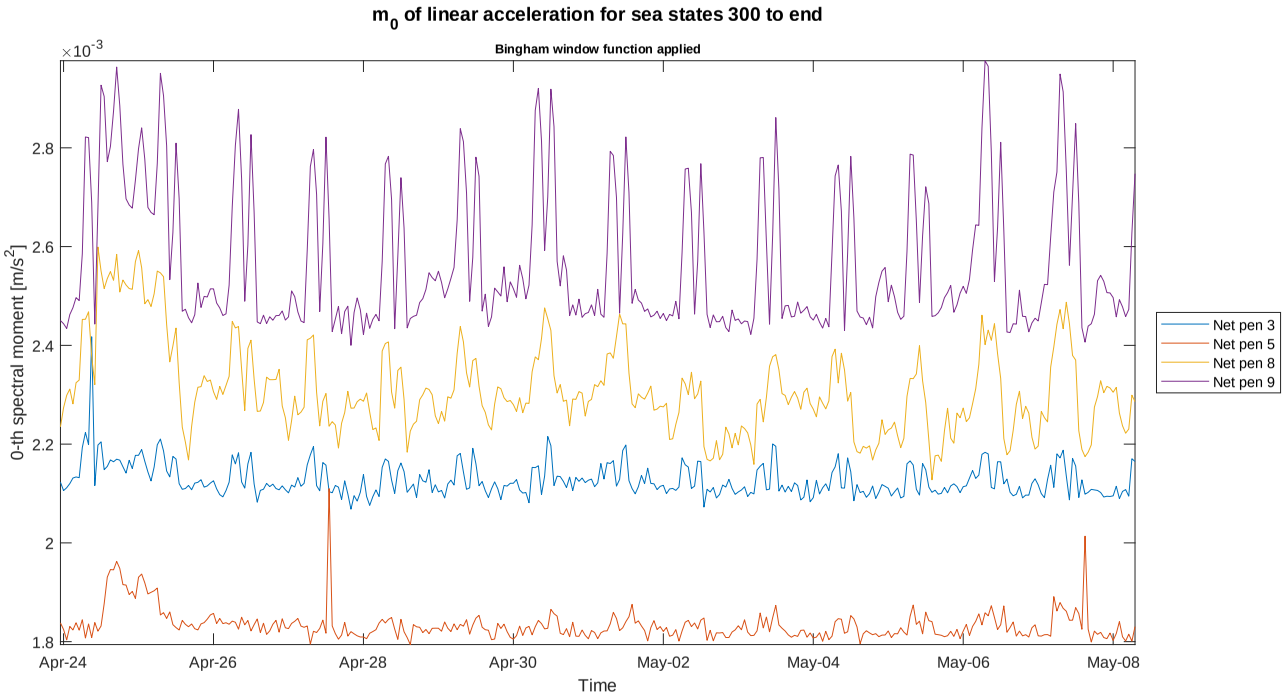

Figure A.16: 0-th spectral moment (energy content) for sea states 300 to 600 of linear acceleration for net pens 3 (blue), 5 (orange), 8 (yellow) and 9 (indigo). Duration of a sea states is one hour.

Despite small scale, three phenomena of deviation between net pens are clearly seen:

- The overall mean energy content in spectra of the net pens are dissimilar
- Net pen 9 has a magnitude of fluctuation deviant from net pen 8, 5 and 3
- Significant periodic peak values are seen for net pens 8 and 9 and smaller periodic peaks are also visible for net pen 3

Wind-wave direction in NYTEK is reported to be 214°, corresponding to waves coming from south-west. This means that waves will hit net pens 3 and 5 first. However, these have spectra with lowest and second lowest energy energy content respectively. Bathymetry is relatively constant along the strait (across the fish farm), implying that wave height should not evolve significantly when waves are propagating from e.g. net pen 3 to 9. The difference in mean energy wave height should be investigated further to reveal possible offsets among accelerometers or other possible sources of errors.

A.5.4 Concluding remarks and recommendations for further work with spatial variations in wave energy contents within aquaculture sites

Due to limited time of analysis, sources of the relatively large offsets and periodic fluctuations in energy content are not known. In further work with full scale measurements the following recommendations should be considered:

- Validity of using dynamic response of floating collars (or other floating structures) to assess wave conditions at a site
  - Investigating the valid ranges of wave frequencies for assuming constant RAO
  - Influences of mooring, bottom weights and other equipment on the RAO of a floating collar
- Reveal sources of the fluctuations in spectral energy
  - Clarify seasonal variations in met-ocean conditions
  - Map out time and duration for operations done at the floating collar the site and how these could influence full scale measurements
- Assess the applicability and reliability of the measurement devices in an oceanic environment

The preliminary study of spatial variation in wave energy content done here does neither reject or confirm any spatial deviation of wave energy content within an aquaculture site. *Nevertheless, the measurements suggest that spatial deviation of wave energy content within an aquaculture site should be investigated further.*

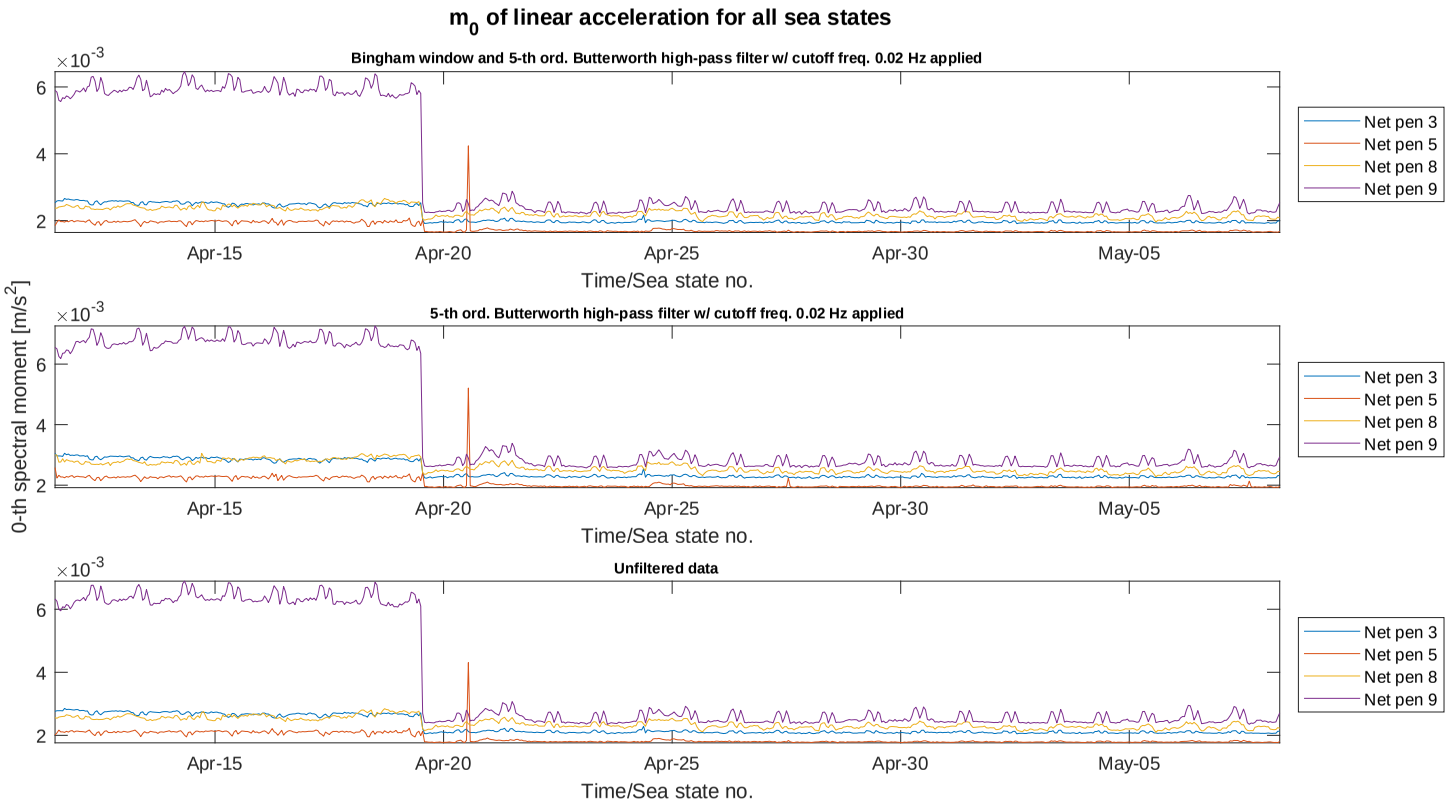

Figure A.17: Effects of high pass filter and window functions on the spectral zero moment of linear acceleration for all sea states. Collars are numbered as in figure A.14.

Appendix B

Additional results from NYTEK data

B.1 Preparing data sets for analyses

Dette arket beskriver kategoriseringen av de manuelt oppgitte alternative målemetoder i NYTEKskjema

Spørsmålet i skjema lyder: "Er vindbølger målt eller beregnet? Hvis annen målemetdode, oppgi hvilken type her:"

SWAN	Fetch length analysis	Aces	STWave	CMSWave	Not available	Empty cells
SWAN	strøklengdeberegning	Aces	ST-Wave	CMS-Wave	HsComp	1077 empty rows, either not stated or "diffraksjonRefraksjon"
Numerisk, SWAN	Effektiv strøklengde metode		StWave	CMS-Wawe	HaComp	
Vindhastighet, n	Vindfart/ strøklengde			CMS-Eave	Vindgenererte bølger beregnes ut fra vinddata	
Numerisk Swan	Strøklengdeberekninger				Vindgenererte bølger beregnes ut fra vinddata fra	
For vindbølger er	Vindfart, effektiv strøklengde				Fastsettelse av vind er basert på referansevindhas	
Strøklengde, Sw	Strøklengde				Saville	
Bølger er beregn	Strøklengde iht NS9415				Se punkt 3 i lok. rapport.	
swan 2006	Effektiv strøklengde				Akustisk bølgemåler AWAC	
Strøklengde og Swan	Effektiv strøklengde beregning.				Berekning av vindfart basert på framgangsmåtar og	

Figure B.1: Categorization of reported methodologies for wind-induced wave estimation in NYTEK schemes. First row indicates label used in further analysis.

B.2 Questionnaire for inspection bodies

The following questions were asked to all inspection bodies whom had done site surveys. Four representatives from four inspection bodies reponded in May 2018.

1. Hvem avgjør i størst grad hvilken metode som skal benyttes til estimering av bølgeforhold?

2. Hvilke kriterier ligger til grunn for deres valg av metode/program for bølgeestimering?

3. Oppgi tidsestimat for ulike analyser

B.3 Comparative studies of wave exposure at identical sites from two different sources of data

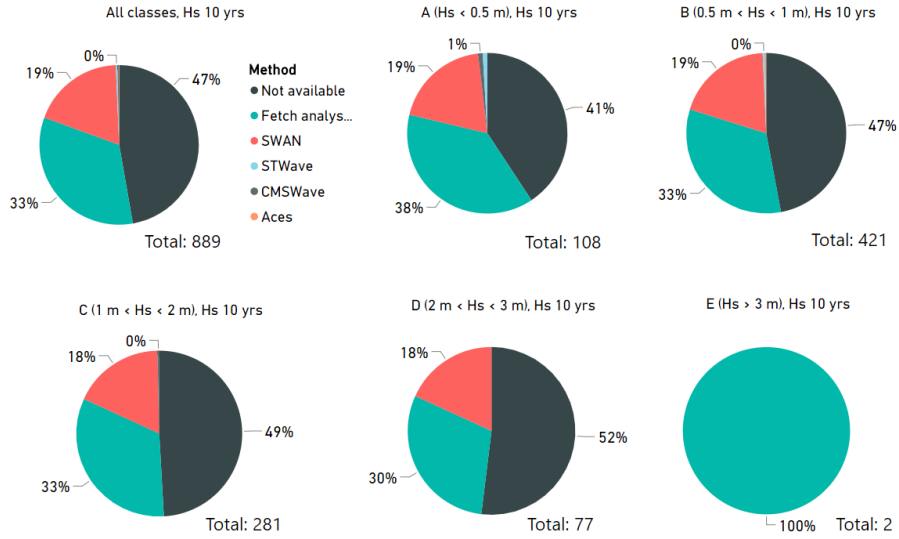

Figure B.2: Share of $H_{s,10yrs}$ for wave classes based exposure. Sites are classified based on results from Lader, Kristiansen, Alver, Bjelland, and Myrhaug, 2017 and wind wave estimation method for sites within the classes are summarized.

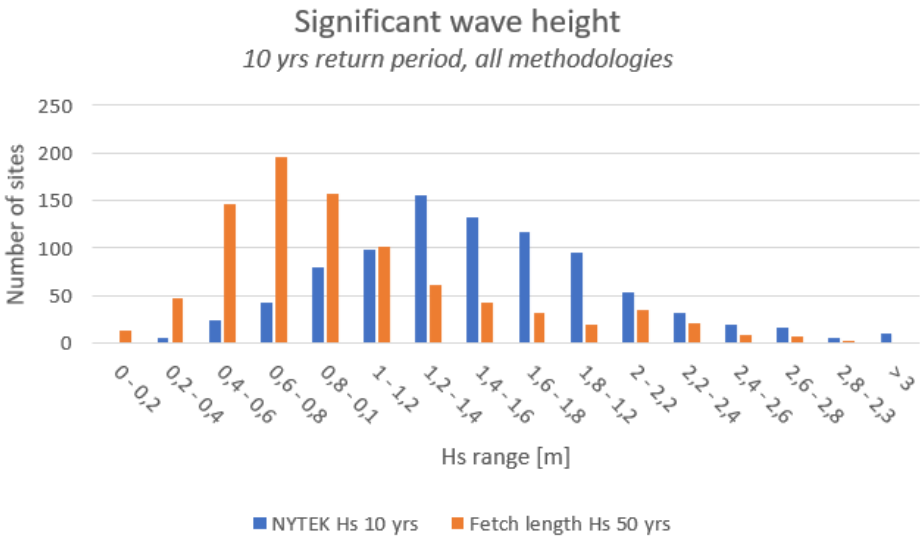

Figure B.3: Comparative analysis of NYTEK and Lader, Kristiansen, Alver, Bjelland, and Myrhaug, 2017: Wind-induced $H_{s_{10yrs}}$ at sites - all methodologies

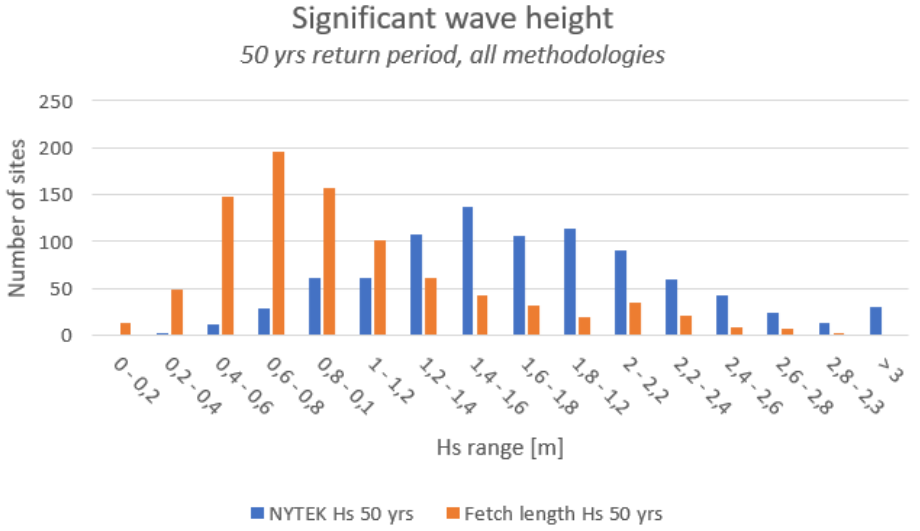

Figure B.4: Comparative analysis of NYTEK and Lader, Kristiansen, Alver, Bjelland, and Myrhaug, 2017: Wind-induced $H_{s_{50yrs}}$ at sites - all methodologies

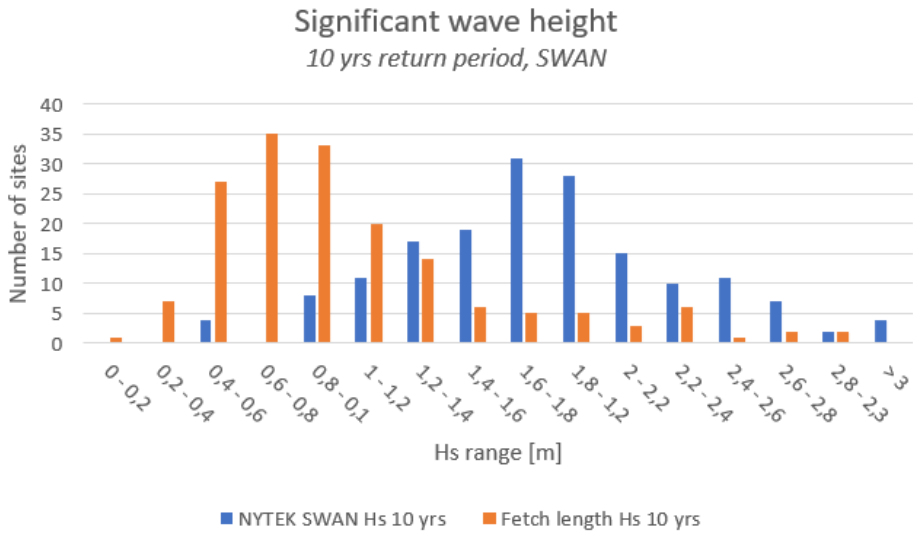

Figure B.5: Comparative analysis of NYTEK and Lader, Kristiansen, Alver, Bjelland, and Myrhaug, 2017: Wind-induced $H_{s_{10yrs}}$ at sites - SWAN

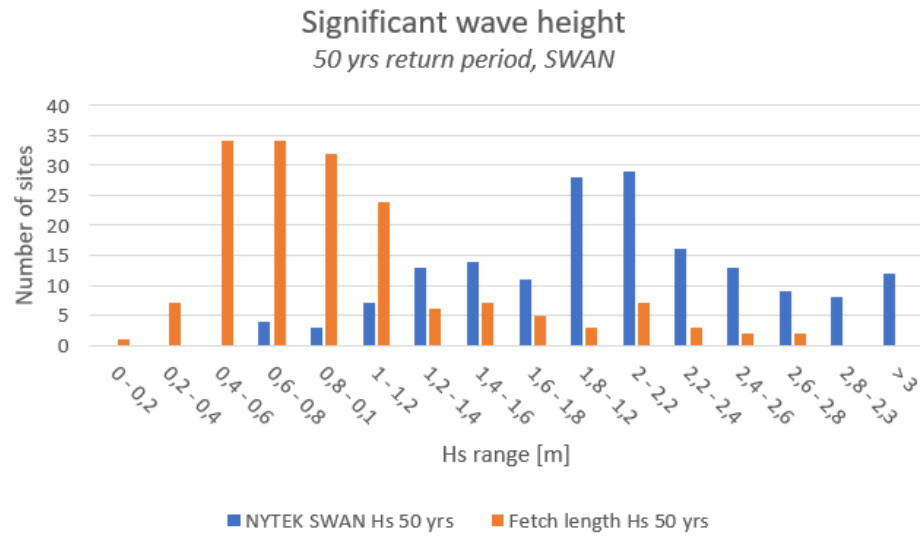

Figure B.6: Comparative analysis of NYTEK and Lader, Kristiansen, Alver, Bjelland, and Myrhaug, 2017: Wind-induced $H_{s_{50yrs}}$ at sites - SWAN

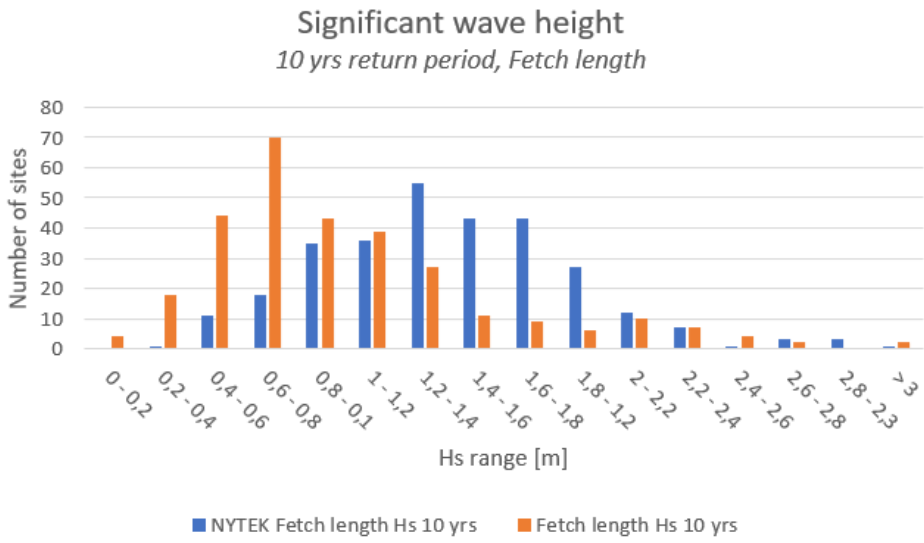

Figure B.7: Comparative analysis of NYTEK and Lader, Kristiansen, Alver, Bjelland, and Myrhaug, 2017: Wind-induced $H_{s_{10yrs}}$ at sites - fetch length analysis as given in NS9415:2009

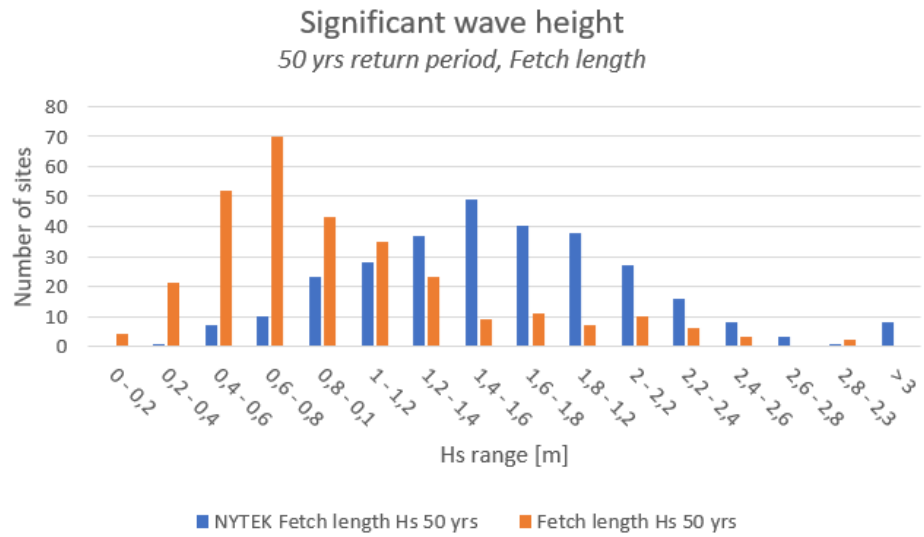

Figure B.8: Comparative analysis of NYTEK and Lader, Kristiansen, Alver, Bjelland, and Myrhaug, 2017: Wind-induced $H_{s_{50yrs}}$ at sites - fetch length analysis as given in NS9415:2009

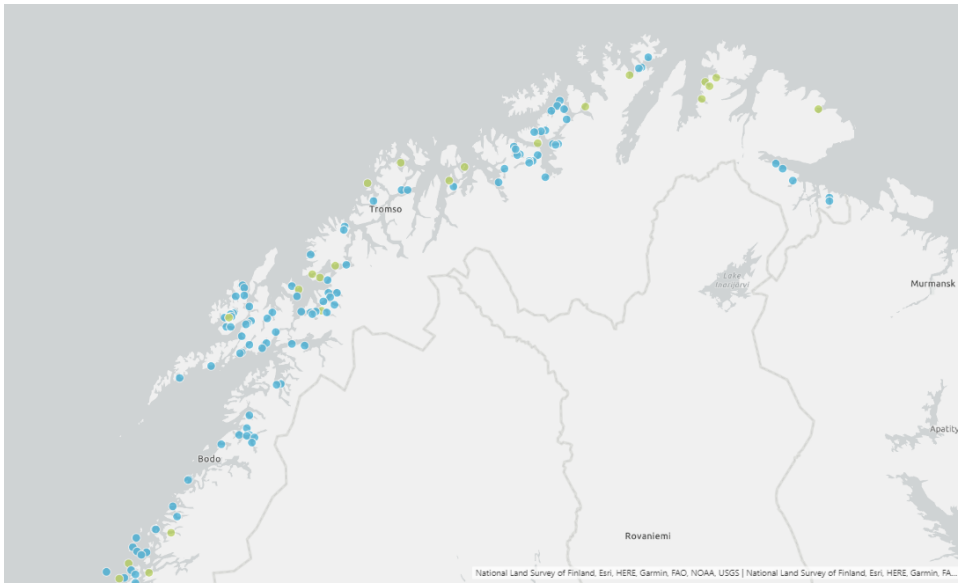

Figure B.9: Locations in Troms and Finnmark where SWAN (green) and fetch length (blue) have been used for wind-induced wave estimation.

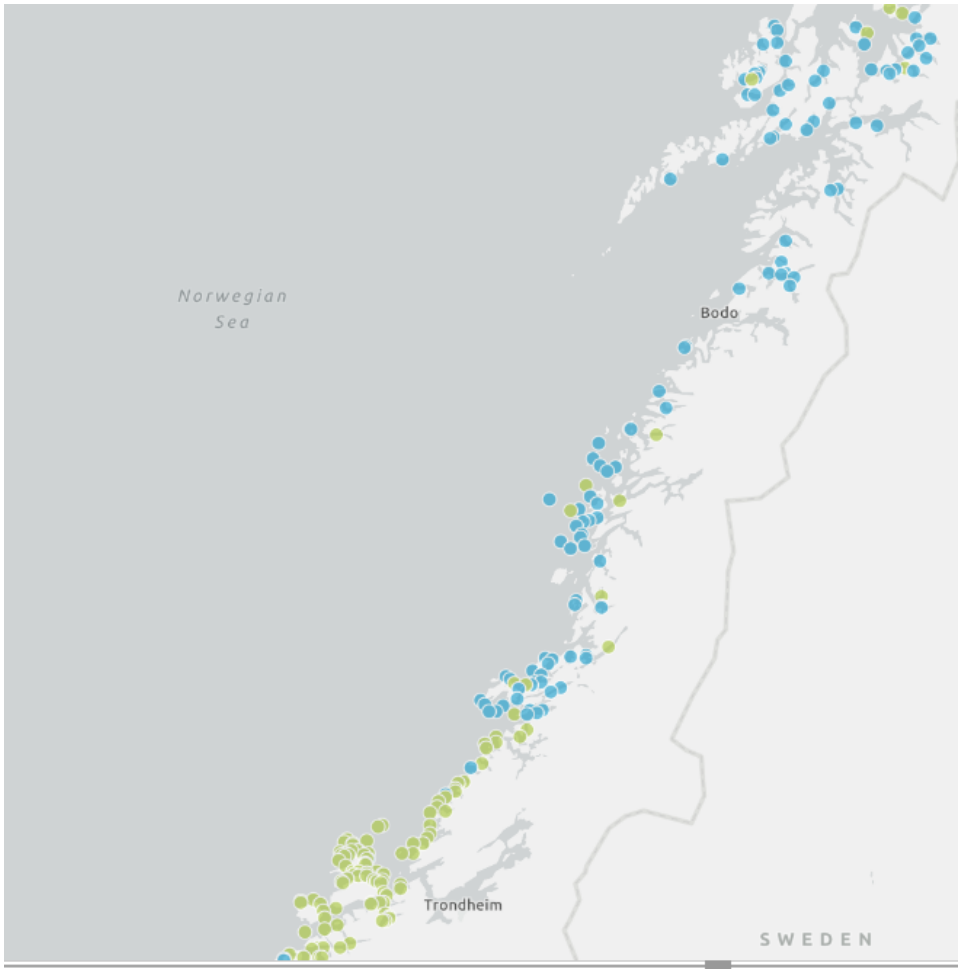

Figure B.10: Locations in Nordland where SWAN (green) and fetch length (blue) have been used for wind-induced wave estimation.

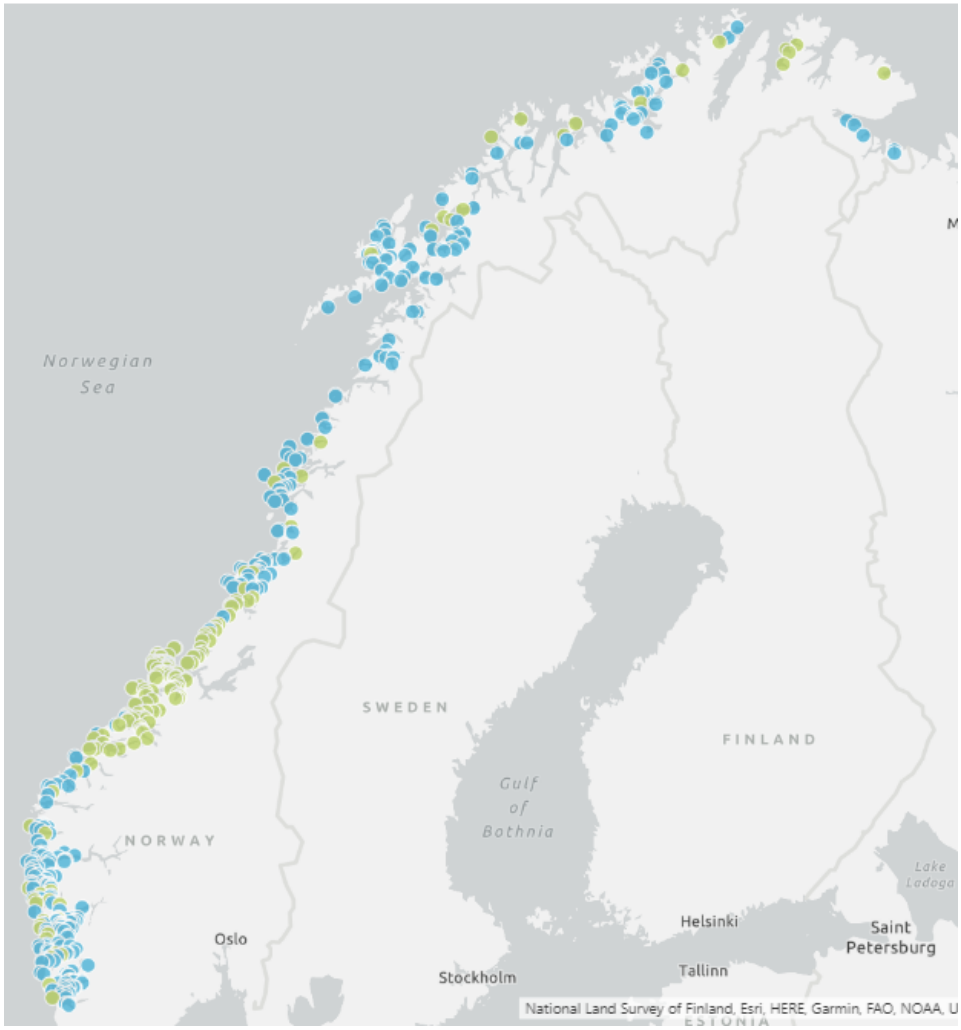

Figure B.11: Overall map showing locations where SWAN and fetch length analysis have been applied.

Presence of swell

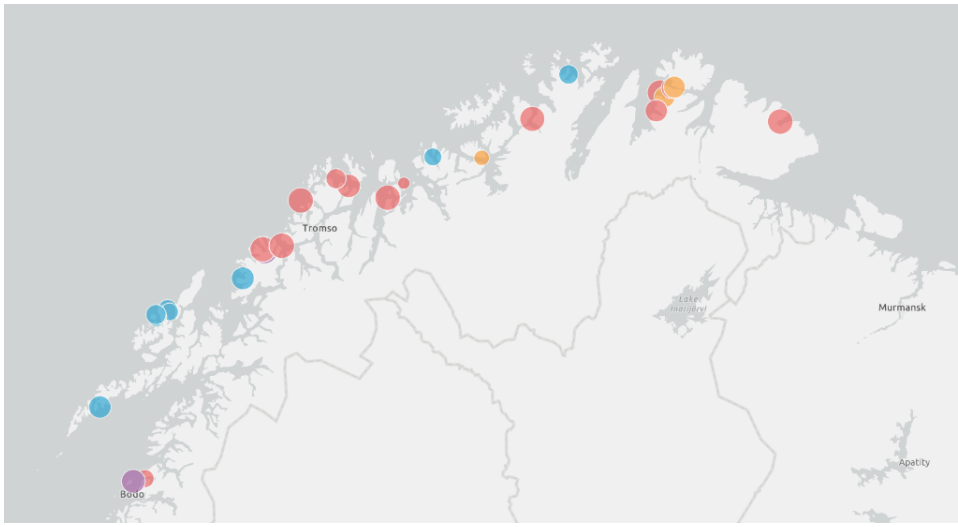

Figure B.12: Methodologies for swell estimation in northern Norway - Yellow: Extreme Value Analysis, blue: STWave, purple: CMSWave, red: SWAN. Size of bubble indicates the magnitude of reported $H_{s50yrscombined}$.

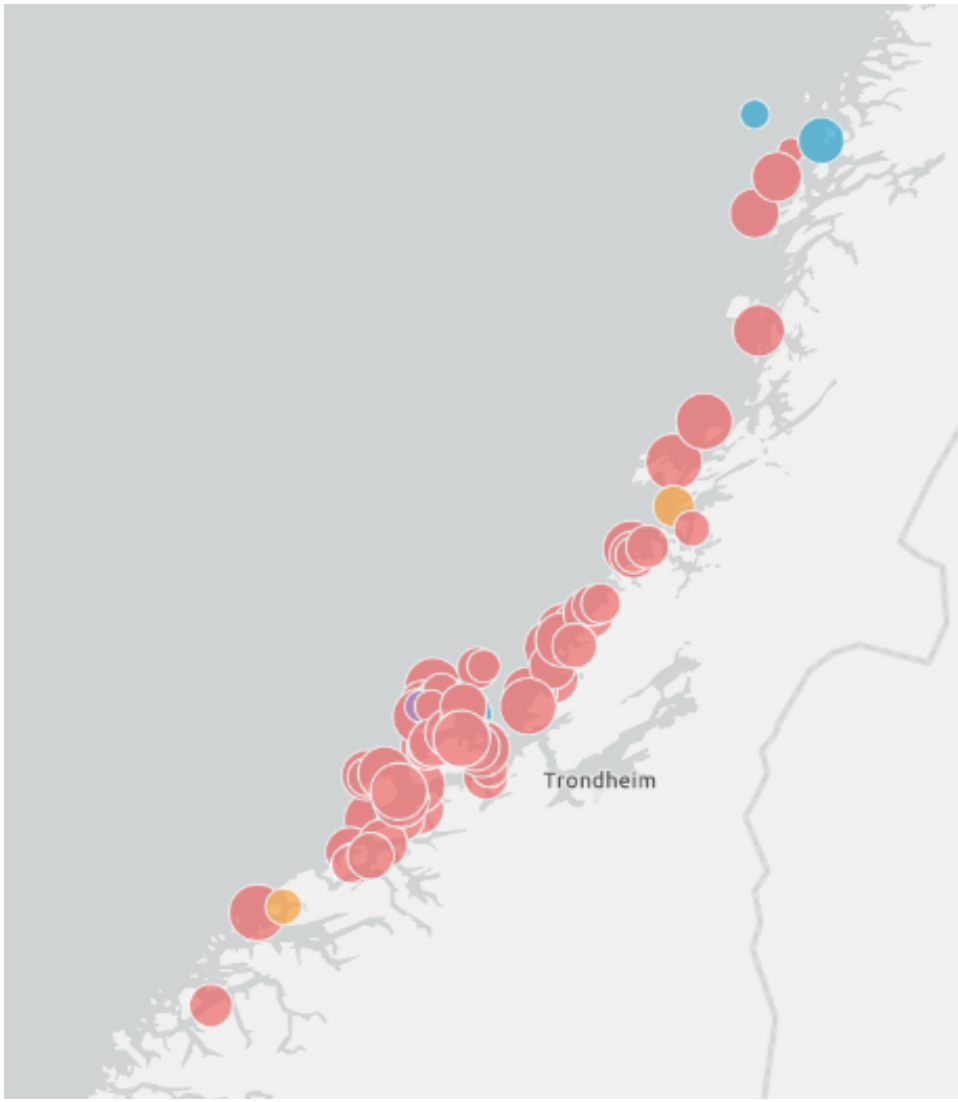

Figure B.13: Methodologies for swell estimation in central Norway - Yellow: Extreme Value Analysis, blue: STWave, purple: CMSWave, red: SWAN. Size of bubble indicates the magnitude of reported $H_{s50yrscombined}$.

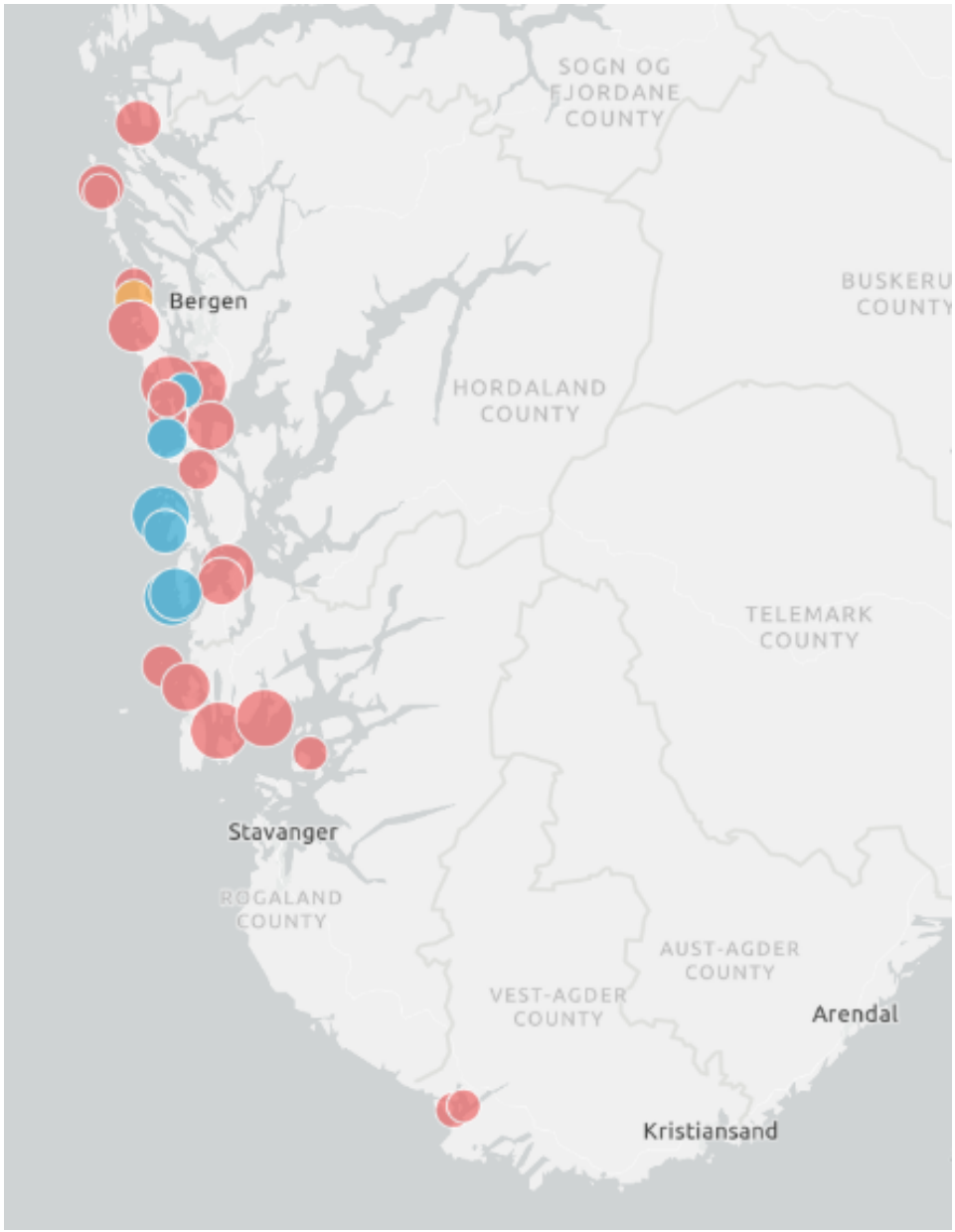

Figure B.14: Methodologies for swell estimation in south-western Norway - Yellow: Extreme Value Analysis, blue: STWave, purple: CMSWave, red: SWAN. Size of bubble indicates the magnitude of reported $H_{s50yrscombined}$.

B.3.1 Corporate size and selection of wave estimation method - additional figures

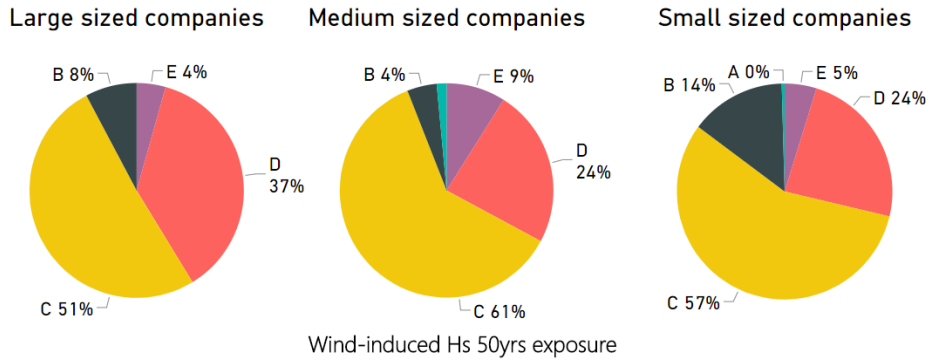

(a) Distribution of exposure level, $Hs_{50yrs \quad wind}$, and company size

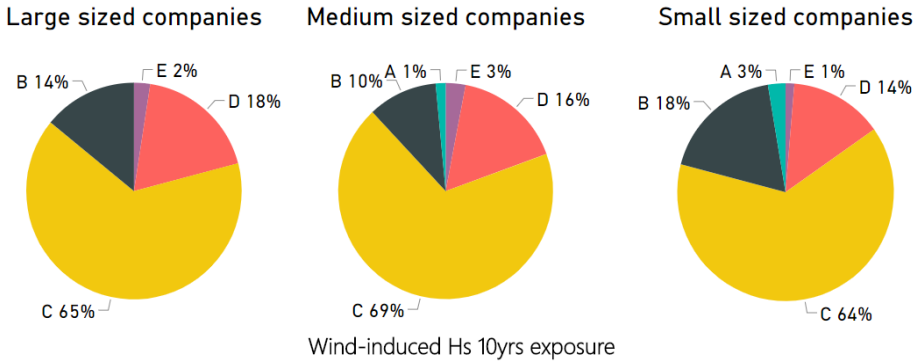

(b) Distribution of exposure level, $Hs_{10yrs \quad wind}$, and company size

Figure B.15: Company sizes and site exposure for wind-induced Hs_{10yrs} and Hs_{50yrs}

Appendix C

MATLAB Codes

C.0.1 NYTEK data

loadNYTEK.m

```
%This script load all variables from NYTEK scheme (NYTEK_hoved1)
%and removes duplicates.
%NB! only valid for waves.
clear all
%Load file
[numbers, strings, NYTEKmain] = xlsread('nytek_hoved1_MATLABF.xlsx','A2:AV2405');
%
% %Assign variable names
 ARCHIVE_REFERENCE = NYTEKmain{:,1};
 LOCALITY_NUMBER = NYTEKmain(:,2);
 LOCALITY_NAME = NYTEKmain(:,3);
 DATE_OF_IMPORT = NYTEKmain(:,4);

LOCALITY_NUMBER = cell2mat(LOCALITY_NUMBER);



%% Remove duplicated rows (i.e. sites) in NYTEKmain.
%Assuming latest date of import is the most recent update in NYTEK scheme
DATES = cell2mat(DATE_OF_IMPORT);
DATES = datenum(DATES,'dd.mm.yyyy HH:MM:SS');
indices = unique(LOCALITY_NUMBER); %One loc. num. for each site
indices2=zeros(length(indices),1);
n=0;

```

```
for i = indices'
    n=n+1;
    k = find(LOCALITY_NUMBER==i); %return site indices
        (ex. row 2 & 14)
     m = max(DATES(k));%return the maximum value of
        the dates
     keep = find(DATES(k)==m);%find site indices of
        newest site certificate
     indices2(n) = k(keep);
end

%Delete all other cells than those indices specified
    by indices2
newNYTEK = NYTEKmain(indices2,:);
NYTEKmain = newNYTEK;
clear newNYTEK %Delete variable
clear START_LAT_N
clear START_LON_O

%Checked 30.3.18, 31.3.18 (Barentswatch, xlsx-files:
    nytek_hoved1-kopi, nytek_strøm2, nytek_strøm2_CSV)
%Lon & lat coordinates added 31.03.18

swan = find(strcmp({NYTEKmain{:,14}},'SWAN'))'; %
    Indices w/ swan
strl = find(strcmp({NYTEKmain{:,14}},'Fetch analysis')
    )';
spec = find(strcmp({NYTEKmain{:,14}},'Spectrum'))';
aces = find(strcmp({NYTEKmain{:,14}},'Aces'))';
stw =  find(strcmp({NYTEKmain{:,14}},'STWave'))';
cms =  find(strcmp({NYTEKmain{:,14}},'CMSWave'))';
div =  find(strcmp({NYTEKmain{:,14}},'Not available'))
    ';

%Write ''cleaned'' data to xlsx-file
filename = 'C:\Users\Synnøve\OneDrive - NTNU\
    Dokumenter\Masteroppgave\Fiskeridirektoratet\
    nytek_hoved1 - Tabulert med kategoriseringer.xlsx';
sheet = 'loadNYTEKres';
xlRange = 'A2';
xlswrite(filename,NYTEKmain,sheet,xlRange)

```

```
SEA_MAX_HS_10A = cell2mat(NYTEKmain(:,34));
SEA_MAX_HS_50A = cell2mat(NYTEKmain(:,35));

%Save workspace variable
save('NYTEKmain','NYTEKmain')
save('SEA_MAX_HS_10A','SEA_MAX_HS_10A')
save('SEA_MAX_HS_50A','SEA_MAX_HS_50A')
```

mapNYTEK.m

```
%% Import NYTEK data into map ... (1.4.18)
... MATLAB Mapping Toolbox is utilized ...
    ...(Feature: Web Browser - Web Map Display)
 clear all
clc
load('NYTEKmain.mat')
% Map latitude and longitude coordinates: LAT & LON are in different
% projection than needed in Google Maps and KML. Correct projections for
% sites are found here: https://www.fiskeridir.no/Akvakultur/Registre-og-skjema/Akvakulturregisteret

%NB: loadNYTEKres must be ordered by site number (lowest first) to match
%values in NYTEKmain.
filename = 'C:\Users\Synnøve\OneDrive - NTNU\Dokumenter\Masteroppgave\Fiskeridirektoratet\nytek_hoved1 - Tabulert med kategoriseringer.xlsx';
[numbers, strings,LAT] = xlsread(filename,'loadNYTEKres','AY2:AY1028');
[numbers, strings,LON] = xlsread(filename,'loadNYTEKres','AZ2:AZ1028');
siteNbX = xlsread(filename,'B2:B1028');

siteNb = cell2mat(NYTEKmain(:,2));

LAT = cell2mat(LAT(:,1));
LON = cell2mat(LON(:,1));

load('SEA_MAX_HS_10A');
load('SEA_MAX_HS_50A');

```

```
%Specify color of geopoint depending on
    WIND_MEASURE_OTHER in data sheet
c= [1 1 0]; %Default color yellow
c = repmat(c,length(siteNb),1); %Color vector

swan = find(strcmp({NYTEKmain{:,14}},'SWAN'))'; %
    Indices w/ swan
strl = find(strcmp({NYTEKmain{:,14}},'Fetch analysis')
    )';
spec = find(strcmp({NYTEKmain{:,14}},'Spectrum'))';
aces = find(strcmp({NYTEKmain{:,14}},'Aces'))';
stw =  find(strcmp({NYTEKmain{:,14}},'STWave'))';
cms =  find(strcmp({NYTEKmain{:,14}},'CMSWave'))';
div =  find(strcmp({NYTEKmain{:,14}},'Not available'))
    ';

%Assign color depending on wind wave measurement
    method
c(swan,1) = 0; c(swan,2) = 0; c(swan,3) = 1; %blue
c(strl,1) = 1; c(strl,2) = 0; c(strl,3) = 1; %magenta
c(spec,1) = 0; c(spec,2) = 0; c(spec,3) = 1; %cyan
c(ns,1) = 1 ;c(ns,2) = 0; c(ns,3) = 0; %red
c(adu,1) = 0.8; c(adu,2) = 0; c(adu,3) = 1;
c(aces,1) = 1; c(aces,2) = 0; c(aces,3) = 0;
c(stw,1) = 1; c(stw,2) = 0.8; c(stw,3) = 0.5;
c(cms,1) = 1; c(cms,2) = 0.4; c(cms,3) = 0.4;
c(div,1) = 0; c(div,2) = 1; c(div,3) = 0; %green
c(tom,1) = 1; c(tom,2) = 0.8; c(tom,3) = 1;

%% Make attributes to each point in map

method = NYTEKmain(:,14);
name = NYTEKmain(:,3);

p=geopoint(LAT,LON,'Site',siteNb(:),'Method',method(:)
    ,'Name',name(:),...
     'HsC10Yr',SEA_MAX_HS_10A(:),'HsC50Yr',
        SEA_MAX_HS_50A(:));%,'FeatureName',name(:),'
        Site',siteNb(:));

webmap('Ocean Basemap')
wmmarker(p,'Color',c(:,:),'OverlayName', 'Aquaculture
```

```
    site')
```

plotWaves.m

```
clear all

load('NYTEKmain.mat')

%% Bivariate histogram/scatter histogram
WindTp10 = cell2mat(NYTEKmain(:,19));
WindTp50 = cell2mat(NYTEKmain(:,20));
Swellp10 = cell2mat(NYTEKmain(:,32));
Swellp50 = cell2mat(NYTEKmain(:,33));

WindHs10 = cell2mat(NYTEKmain(:,17));
WindHs50 = cell2mat(NYTEKmain(:,18));
SwellHs10 = cell2mat(NYTEKmain(:,30));
SwellHs50 = cell2mat(NYTEKmain(:,31));

%Plot respective return periods
figure()
clf

minX = min([WindTp10; Swellp10]);
maxX = max([WindTp10; Swellp10]);
minY = min([WindHs10; SwellHs10]);
maxY = max([WindHs10; SwellHs10]);

resX = 0.25;
resY = 0.25;

nBinsX = ceil((maxX - minX) / resX);
nBinsY = ceil((maxY - minY) / resY);

label = vertcat( ...
              num2cell(repmat('Wind Tp10/Hs10', size(
                  WindTp10)),2), ...
              num2cell(repmat('Swell Tp10/Hs10', size(
                  Swellp10)),2));

Tz = vertcat(WindTp10, Swellp10);
Hs = vertcat(WindHs10, SwellHs10);

```

```
% scatterplot
scatterhist(Tz, Hs, 'Group', label,...
    'Direction','out','LineStyle',{'-','-.',':'},'
       Marker','+*')
hold on
set(gca,'XTick', [0:2:25] )
title('Scatter plot and histogram of $Hs_{10 yrs}$ and
    $Tp_{10 yrs}$ for 1027 sites reported in NYTEK','
   interpreter','latex')
xlabel('Tp [s]')
ylabel('Hs [m]')
hold off

%Plot 50 years return period
figure()
clf

minX = min([WindTp50; Swellp50]);
maxX = max([WindTp50; Swellp50]);
minY = min([WindHs50; SwellHs50]);
maxY = max([WindHs50; SwellHs50]);

resX = 0.25;
resY = 0.25;

nBinsX = ceil((maxX - minX) / resX);
nBinsY = ceil((maxY - minY) / resY);

label = vertcat( ...
            num2cell(repmat('Wind Tp50/Hs50', size(
               WindTp50)),2) ,...
            num2cell(repmat('Swell Tp50/Hs50', size(
               Swellp50)),2));

Tz = vertcat(WindTp50, Swellp50);
Hs = vertcat(WindHs50, SwellHs50);

% scatterplot
scatterhist(Tz, Hs, 'Group', label,...
    'Direction','out','LineStyle',{'-','-.',':'},'
       Marker','+*')
hold on
```

```
74 set(gca,'XTick', [0:2:25] )
75 title('Scatter plot and histogram of $Hs_{50 yrs}$ and
       $Tp_{50 yrs}$ for 1027 sites reported in NYTEK','
       interpreter','latex')
76 xlabel('Tp [s]')
77 ylabel('Hs [m]')
78 hold off
```

C.0.2 createKMLfile.m

```
1 %% Save kml file for exporting geopoints
2
3 mapNYTEKF; %Loading variables & runs loadNYTEK.
4
5  attribspec = makeattribspec(p);
6  attributes = {'Method','Site','HsC10Yr','HsC10Yr'};%'
       Name'
7  attribspec = rmfield(attribspec, attributes);
8  attribspec.HsC10Yr.AttributeLabel = '<b><bold>Hs 
       ;comb. 10: yrs </bold></b>';
9  attribspec.HsC10Yr.Format = '%.1f meters';
10 attribspec.HsC50Yr.AttributeLabel = '<b><bold>Hs 
       ;comb. 50: yrs </bold></b>';
11 attribspec.HsC50Yr.Format = '%.1f meters';
12 attribspec.Site.AttributeLabel = '<b><bold>Site 
       number: <bold></b>';
13 attribspec.Site.Format = '%.0f';
14 attribspec.Method.AttributeLabel = '<b><bold>Method&
       nbsp;for estimation:</bold></b>';
15 filename = 'AquacultureSites.kml';
16 kmlwrite(filename,p,'Description',attribspec,'Name',
       name,'Color',c);
17
18 %% Simple kml file
19 %This kml file displays methods and name only
20
21 site = num2str(siteNb);
22 filename = 'AquacultureSitesMethodsOnly.kml';
23 kmlwritepoint(filename,LAT,LON,'Description',method,'
       Name',name,'Color',c);
```

C.0.3 Fetch length and NYTEK comparative study

FetchLengthNYTEKScatterF.m

```
%% Plot and compare NYTEK and fetch length analysis
clc
clear all

NYTEK_Hs10 = xlsread('C:\Users\Synnøve\OneDrive - NTNU
    \Dokumenter\Masteroppgave\Fiskeridirektoratet\
    StroklengdeHsAlleLok','NYTEK & StrLen Ferdig','D2:
    D890');
NYTEK_Hs50 = xlsread('C:\Users\Synnøve\OneDrive - NTNU
    \Dokumenter\Masteroppgave\Fiskeridirektoratet\
    StroklengdeHsAlleLok','NYTEK & StrLen Ferdig','E2:
    E890');

FetLen_Hs10 = xlsread('C:\Users\Synnøve\OneDrive -
    NTNU\Dokumenter\Masteroppgave\Fiskeridirektoratet\
    StroklengdeHsAlleLok','NYTEK & StrLen Ferdig','L2:
    L890');
FetLen_Hs50 = xlsread('C:\Users\Synnøve\OneDrive -
    NTNU\Dokumenter\Masteroppgave\Fiskeridirektoratet\
    StroklengdeHsAlleLok','NYTEK & StrLen Ferdig','M2:
    M890');

%% Compare deviation between NYTEK and Fetch length
    for 10 and 50 years
%% return periods
x=0:max(FetLen_Hs10);
y = x;

figure()
clf

NYTEK_Hs10 = NYTEK_Hs10(:);
FetLen_Hs10 = FetLen_Hs10(:);
NYTEK_Hs50 = NYTEK_Hs50(:);
FetLen_Hs50 = FetLen_Hs50(:);

% scatterplot
scatter(NYTEK_Hs10,FetLen_Hs10,'Marker','+')
hold on
```

```
scatter(NYTEK_Hs50,FetLen_Hs50,'Marker','.')
hold on
plot(x,y,'Linewidth',1,'Color','k')
hold on
axis([0 5 0 3.5])
title({['Scatter plot of estimates of wind-induced
    waves for ' num2str(length(NYTEK_Hs50)), ' sites'
    ]})
legend('Hs_{10yrs} NYTEK/FL',...
     'Hs_{50yrs} NYTEK/FL','One-to-one relationship')
xlabel('Hs_{NYTEK}')
ylabel('Hs_{Fetch length}')
hold off
```

C.0.4 Hosenøyan measurements

importfileForMHosF.m

```
%% This script imports numeric data from a large
    number of txt-files.
clear all
clc


txtFiles = dir('*.txt');
numfiles = length(txtFiles);
mydata = cell(1, numfiles);

numFiles = 645; %Number of txt-files to import.
startRow = 2; %Exclude column headings
endRow = inf; %Include all rows
myData = cell(1,numFiles);

for fileNum = 1:numFiles
     fileName = sprintf('data%01d.txt',fileNum);
     myData{fileNum} = importfileMatrixM(fileName,
         startRow,endRow);
     %Excludes time and date and an array of floats:
     %formatSpec = '%*q%*q%*q%*q%*q%*q%*q%*q%*q%*q%*q%f
         %f%f%[^\n\r]';
end
%
M3= myData;
```

```
23 save('netPen.mat','M3','-append')
```

importfileMatrixMHosF.m

```
1  function data1 = importfileMatrixM(filename, startRow,
       endRow)
2  %IMPORTFILE Import numeric data from a text file as a
       matrix.
3  %    DATA1 = IMPORTFILE(FILENAME) Reads data from text
       file FILENAME for the
4  %    default selection.
5  %
6  %    DATA1 = IMPORTFILE(FILENAME, STARTROW, ENDROW)
       Reads data from rows
7  %    STARTROW through ENDROW of text file FILENAME.
8  %
9  % Example:
10 %    data1 = importfile('data1.txt', 2, 35539);
11 %
12 %    See also TEXTSCAN.
13
14 % Auto-generated by MATLAB on 2018/05/10 12:58:47
15
16 %% Initialize variables.
17 delimiter = {',',' '};
18 if nargin<=2
19     startRow = 2;
20     endRow = inf;
21 end
22
23 %% Format for each line of text:
24 %    column18: double (%f)
25 %        column19: double (%f)
26 %    column20: double (%f)
27 % For more information, see the TEXTSCAN documentation
       .
28 formatSpec = '%*q%*q%*q%*q%*q%*q%*q%*q%*q%*q%*q%*q%*q%*q
       %*q%*q%*q%*q%f%f%f%[^\n\r]';
29
30 %% Open the text file.
31 fileID = fopen(filename,'r');
32
33 %% Read columns of data according to the format.
```

```
% This call is based on the structure of the file used to generate this
% code. If an error occurs for a different file, try regenerating the code
% from the Import Tool.
dataArray = textscan(fileID, formatSpec, endRow(1)-startRow(1)+1, 'Delimiter', delimiter, 'MultipleDelimsAsOne', true, 'TextType', 'string', 'EmptyValue', NaN, 'HeaderLines', startRow(1)-1, 'ReturnOnError', false, 'EndOfLine', '\r\n');
for block=2:length(startRow)
    frewind(fileID);
    dataArrayBlock = textscan(fileID, formatSpec, endRow(block)-startRow(block)+1, 'Delimiter', delimiter, 'MultipleDelimsAsOne', true, 'TextType', 'string', 'EmptyValue', NaN, 'HeaderLines', startRow(block)-1, 'ReturnOnError', false, 'EndOfLine', '\r\n');
    for col=1:length(dataArray)
        dataArray{col} = [dataArray{col}; dataArrayBlock{col}];
    end
end

%% Close the text file.
fclose(fileID);

%% Post processing for unimportable data.
% No unimportable data rules were applied during the import, so no post
% processing code is included. To generate code which works for
% unimportable data, select unimportable cells in a file and regenerate the
% script.

%% Create output variable
data1 = [dataArray{1:end-1}];
```

compareFiltersSpectraF.m

```
%% Test window functions
%Compares and presents effects of various window
```

```
    fucntions
clear all
clc

%Load data
x=randi(645); %Select a random sea state
load('netPen.mat')
data = M3{1,x}(:,2);
%Convert to m/s^2
data = data.*9.81;
%Remove offset
data = data-mean(data);

%% Hanning
dataHanning = data.*hanning(length(data));

%% Hamming
dataHamming = data.*hamming(length(data));

%% Modified Bartlett-Hann window
dataBH = data.*barthannwin(length(data));

% Plot figure for comparison
figure()
subplot(2,2,1)
plot(1:length(dataHanning),dataHanning,'r');
legend('Hanning window')
xlabel(['All samples in sea state ',num2str(x),' for
    collar 3'])
ylabel('Linear acceleration [m/s^2]')
axis([0 length(data) -inf inf])

subplot(2,2,2)
plot(1:length(dataHamming),dataHamming,'b');
legend('Hamming window')
xlabel(['All samples in sea state ',num2str(x),' for
    collar 3'])
ylabel('Linear acceleration [m/s^2]')
axis([0 length(data) -inf inf])

subplot(2,2,3)
plot(1:length(dataBH),dataBH,'m');
```

```
42 legend('Bartlett-Hann window')
43 xlabel(['All samples in sea state ',num2str(x),' for
       collar 3'])
44 ylabel('Linear acceleration [m/s^2]')
45 axis([0 length(data) -inf inf])
46
47 subplot(2,2,4)
48 plot(1:length(data),data,'Color',[0.8500 0.3250
       0.0980])
49 legend('Signal without windowing')
50 xlabel(['All samples in sea state ',num2str(x),' for
       collar 3'])
51 ylabel('Linear acceleration [m/s^2]')
52 axis([0 length(data) -inf inf])
53
54 %% _-_-_-_-_-_-_Comparisation of applying windowing and
       not _-_-_-_-_-_
55
56 %% High pass Butterworth filter to attenuate low-freq.
       noise
57 dt = 0.1;
58 Fs = 1/dt;
59 nyq = Fs/2;  % Nyquist frequency
60 [filtb,filta]=butter(5,0.1/nyq,'high');
61
62 %Filter out low freq. noise
63 dataHanning=filtfilt(filtb,filta,dataHanning);
64
65 %% Fouirer transform
66 Yh = fft(dataHanning); %Fast Fourier transform of
       linear acceleration
67 Lh = length(dataHanning);
68 P2h = abs(Yh/Lh);
69 P1h = P2h(1:Lh/2+1);
70 P1h(2:end-1) = 2*P1h(2:end-1); %One sided spectrum
71
72 fvh = Fs*(0:(Lh/2))/Lh;
73 Tvh=1./fvh;
74 %Filter out low freq. noise
75 dataF=filtfilt(filtb,filta,data);
76
77 %% FFT - found here:
```

```
78 %https://se.mathworks.com/help/matlab/ref/fft.html
79
80 Y = fft(dataF); %Discrete Fourier Transform of linear
       acceleration
81 L = length(dataF);
82 P2 = abs(Y/L); %Even-valued signal length L.
83 P1 = P2(1:L/2+1); %Compute the single-sided spectrum
       P1 based on P2.
84 P1(2:end-1) = 2*P1(2:end-1); %Single-sided spectrum
85
86 fv = Fs*(0:(L/2))/L;
87 Tv=1./fv;
88
89 figure()
90 subplot(2,1,1)
91 plot(fv,P1h);
92 xlabel('Frequency [Hz]')
93 ylabel('Spectral density amplitude [m/s^2/Hz]')
94 title('Single sided amplitude spectrum of linear
       acceleration in sea state ',num2str(x))
95 legend({['High pass filter applied', newline, 'Hanning
       window applied']})
96 subplot(2,1,2)
97 plot(fv,P1)
98 legend({['High pass filter applied', newline, 'No
       window applied']})
99 xlabel('Frequency [Hz]')
100 ylabel('Spectral density amplitude [m/s^2/Hz]')
101 hold off
```

BinghamF.m

```
1 % Functions
2 %% Bingham window (Newland)
3 %% Test window functions
4
5 % clear all
6 % clc
7 % Compare various window functions
8
9 N = length(data);
10
11 N101 = round(N*0.1); %Up to 10% of the recording will
```

```
    be attenuated
N901 = round(N*0.9); %The last 10% of the recording
    will be attenuated

N10 = 1:N101;
N90 = N901:N;

D10 = 0.5*(1-cos((10*pi.*N10)./N)); %for 0<i<N/10
D = ones(1,round(N*0.8));
D90 = 0.5*(1+cos((10*pi*(N90-0.9*N))/N)); %for 0.9N <
    i < N

DW = [D10, D, D90]';

if length(data)< length(DW)
   DW(length(data)+1:end)=[]; %remove last index if
       size does not match
    dataW = data.*DW;
elseif length(data)> length(DW)
     DW(numel(data)) = 0;
     dataW = data.*DW;
else
     dataW = data.*DW;
end

% dataW = zeros(length(data),1);

clear N; clear N101; clear N901; clear N10; clear N90;
clear D10; clear D; clear D90
```

C.0.5 loadFilesHosF.m

```
%% This script presents measured linear acceleration
    from Hosenøyan site
% The script plots mean linear acceleration in time
    domain for net pens 3,...
%5, 8 and 9 and calculates the zero-th moment for all
    sea states.
% It further compare various combinations of high-pass
     filtered, Hanning
% windowed and unfiltered data.
clear all
clc
```

```
8
9  %Load data
10 load('netPen.mat')
11 LA.M3 = M3;
12 LA.M5 = M5;
13 LA.M8 = M8;
14 LA.M9 = M9;
15
16 clear M9; clear M8; clear M5; clear M3
17
18 %% _____FREQUENCY DOMAIN
       ANALYSIS_____
19 %% Find the energy within spectrum for all signals
       within a frequency band
20 %% for each sea state. This corresponds to one txt-
       file/one cell in myData
21 dt = 0.1;
22 Fs = 1/dt;
23
24 MomentLA = zeros(646,4);
25 MomentLAF = MomentLA;
26 MomentLAHP = MomentLA;
27 MomentLAW = MomentLA;
28
29 fields = fieldnames(LA);
30
31  for k=1:length(fields)
32     categoryname=fields{k};
33
34  for m = 1:length(LA.(categoryname))
35     %Load data
36     data = LA.(categoryname){1,m}(:,2);
37     %Convert to m/s^2
38     data = data.*9.81;
39     %Remove offset
40     data = data-mean(data);
41
42     %% Bingham filtering to attenuate tails/make tails
           continous for FFT
43     BinghamF;
44 %% High pass Butterworth filter to attenuate low-freq.
       noise
```

```
dt = 0.1;
Fs = 1/dt;
nyq = Fs/2;  % Nyquist frequency
[filtb,filta]=butter(5,0.1/nyq,'high');
dataF=filtfilt(filtb,filta,dataW); %Filter signal
    after Hanning window

%% Frequency domain analysis - window + high-passed
    filter
YF = fft(dataF); %Fast Fourier transform of linear
    acceleration
LF = length(dataF);
P2F = abs(YF/LF);
P1F = P2F(1:LF/2+1);
P1F(2:end-1) = 2*P1F(2:end-1); %One sided spectrum

fvF = Fs*(0:(LF/2))/LF;

%% Frequency domain analysis - window only
YW = fft(dataW); %Fast Fourier transform of linear
    acceleration
LW = length(dataW);
P2W = abs(YW/LW);
P1W = P2W(1:LW/2+1);
P1W(2:end-1) = 2*P1W(2:end-1); %One sided spectrum

fvW = Fs*(0:(LW/2))/LW;

%% Frequency domain analysis - unfiltered data
Y = fft(data); %Fast Fourier transform of linear
    acceleration
L = length(data);
P2 = abs(Y/L);
P1 = P2(1:L/2+1);
P1(2:end-1) = 2*P1(2:end-1); %One sided spectrum

fv = Fs*(0:(L/2))/L;

%% Frequency domain analysis - high-pass filtered data
dataHP=filtfilt(filtb,filta,data); %Filter signal
    after Hanning window
%filtData.(categoryname) = dataHP;
```

```
81  YHP= fft(dataHP); %Fast Fourier transform of linear
        acceleration
82  LHP = length(dataHP);
83  P2HP= abs(YHP/LHP);
84  P1HP = P2HP(1:LHP/2+1);
85  P1HP(2:end-1) = 2*P1HP(2:end-1); %One sided spectrum
86
87  fvHP = Fs*(0:(LHP/2))/LHP;
88
89  %% Calculate spectral moment
90  % Given as m_{n} = \int{0}{\infty}\omega^{n}S^{+}(\
        omega)d\omega;
91  % n=0,1,2....
92
93  %Windowed + filtered
94  SwHP = zeros(((length(fvHP)-1)),1);
95  for r = 1:(length(fvHP)-1)
96       dwHP = fvHP(r+1)-fvHP(r);
97       SwHP=P1HP(r)*dwHP;
98       MomentLAHP(m,k) = MomentLAHP(m,k)+SwHP;
99       clear SwHP
100 end
101
102 clear r
103
104 %Unfiltered
105 Sw = zeros(((length(fv)-1)),1);
106 for r = 1:(length(fv)-1)
107      dw = fv(r+1)-fv(r);
108      Sw=P1(r)*dw;
109      MomentLA(m,k) = MomentLA(m,k) + Sw;
110      clear Sw
111 end
112
113 clear r
114
115 %High pass filtered only
116 SwF = zeros(((length(fvF)-1)),1);
117 for r = 1:(length(fvF)-1)
118      dwF = fvF(r+1)-fvF(r);
119      SwF =P1F(r)*dwF;
120      MomentLAF(m,k) = MomentLAF(m,k) +SwF;
```

```
121 clear SwF
122 end
123
124 clear r
125
126 %Windowed only
127 SwW = zeros(((length(fvW)-1)),1);
128 for r = 1:(length(fvW)-1)
129     dwW = fvW(r+1)-fvW(r);
130     SwW =P1W(r)*dwF;
131     MomentLAW(m,k) = MomentLAW(m,k) +SwW;
132 clear SwW
133 end
134
135 clear r
136 %% Clear all variables
137 clear data; clear dataF; clear dataW; clear Y; clear
      YW; clear YF; clear LF;
138 clear L; clear LW; clear P1; clear P2; clear fv; clear
      P1W; clear P2W;
139 clear fvW; clear rF; clear P1F; clear P2F; clear fvF;
      clear dw; clear dwHP;
140 clear P1HP; clear P2HP; clear fvHP; clear dwF; clear
      LHP; clear YHP
141  end
142  end
143
144 %% ------------------------Plot data in frequency domain
      -------------------------------
145
146 L = 1:644; %Do not include any end effects
147 % t1 = datetime(2018,4,11,11,0,0);
148 % t2 = datetime(2018,5,8,6,0,0);
149 % time = (t1:hours(1):t2)';
150 time = datestr((datetime(2018,4,11,11,0,0)+hours
      (1:644)));
151 time = datenum(time,'dd-mm-yyyy HH:MM:SS');
152 figure()
153 subplot(3,1,1)
154 plot(time,MomentLAF(L,1))
155 datetick('x','mmm-dd','keepticks','keeplimits')
156 hold on
```

```
157 plot(time,MomentLAF(L,2))
158 datetick('x','mmm-dd','keepticks','keeplimits')
159 hold on
160 plot(time,MomentLAF(L,3))
161 datetick('x','mmm-dd','keepticks','keeplimits')
162 hold on
163 plot(time,MomentLAF(L,4))
164 datetick('x','mmm-dd','keepticks','keeplimits')
165 hold on
166 legend('Net pen 3','Net pen 5','Net pen 8','Net pen 9'
    ,'location','eastoutside')
167 title({['\fontsize{12} m_0 of linear acceleration for
    all sea states',newline,...
168     '\fontsize{8}Bingham window and 5-th ord.
        Butterworth high-pass filter w/ cutoff freq.
        0.02 Hz applied']})
169 xlabel('Time/Sea state no.')
170 axis([time(1) time(end) -inf inf])
171
172 subplot(3,1,2)
173 plot(time,MomentLA(L,1))
174 datetick('x','mmm-dd','keepticks','keeplimits')
175 hold on
176 plot(time,MomentLA(L,2))
177 datetick('x','mmm-dd','keepticks','keeplimits')
178 hold on
179 plot(time,MomentLA(L,3))
180 datetick('x','mmm-dd','keepticks','keeplimits')
181 hold on
182 plot(time,MomentLA(L,4))
183 datetick('x','mmm-dd','keepticks','keeplimits')
184 hold on
185 legend('Net pen 3','Net pen 5','Net pen 8','Net pen 9'
    ,'location','eastoutside')
186 title({'\fontsize{8}5-th ord. Butterworth high-pass
    filter w/ cutoff freq. 0.02 Hz applied'})
187 xlabel('Time/Sea state no.')
188 ylabel('0-th spectral moment [m/s^2]')
189 axis([time(1) time(end) -inf inf])
190
191 subplot(3,1,3)
192 plot(time,MomentLAHP(L,1))
```

```
193 datetick('x','mmm-dd','keepticks','keeplimits')
194 hold on
195 plot(time,MomentLAHP(L,2))
196 datetick('x','mmm-dd','keepticks','keeplimits')
197 hold on
198 plot(time,MomentLAHP(L,3))
199 datetick('x','mmm-dd','keepticks','keeplimits')
200 hold on
201 plot(time,MomentLAHP(L,4))
202 datetick('x','mmm-dd','keepticks','keeplimits')
203 hold on
204 legend('Net pen 3','Net pen 5','Net pen 8','Net pen 9'
    ,'location','eastoutside')
205 title({'\fontsize{8}Unfiltered data'})
206 xlabel('Time/Sea state no.')
207 axis([time(1) time(end) -inf inf])
208 hold off
209
210 %Plot only windowed data from sea state 300 (due to
    disturbances in data
211 %before sea state 300)
212 figure()
213 plot(time(300:end),MomentLAW(L(300):L(end),1))
214 datetick('x','mmm-dd','keepticks','keeplimits')
215 hold on
216 plot(time(300:end),MomentLAW(L(300):L(end),2))
217 datetick('x','mmm-dd','keepticks','keeplimits')
218 hold on
219 plot(time(300:end),MomentLAW(L(300):L(end),3))
220 datetick('x','mmm-dd','keepticks','keeplimits')
221 hold on
222 plot(time(300:end),MomentLAW(L(300):L(end),4))
223 datetick('x','mmm-dd','keepticks','keeplimits')
224 hold on
225 legend('Net pen 3','Net pen 5','Net pen 8','Net pen 9'
    ,'location','eastoutside')
226 title({['\fontsize{12}m_{0} of linear acceleration for
     sea states 300 to end',newline,...
227     '\fontsize{8}Bingham window function applied']})
228 xlabel('Time')
229 ylabel('0-th spectral moment [m/s^2]')
230 axis([time(300) time(end) -inf inf])
```

```
231
232 %Plot Bingham window function
233 figure()
234 plot(DW)
235 axis([0 length(DW) -inf inf])
236 xlabel('Time')
237 ylabel('Magnitude')
238 title('Bingham window function')
```